Report No.
UCB/SEMM-2017/02

Structural Engineering
Mechanics and Materials

Member Capacity Factors for Seismic Isolators to Limit Collapse Risks of Seismically Isolated Structure to ASCE 7 Stipulated Limits

By

Benshun Shao
Stephen A. Mahin
Victor Zayas

November 2017

Department of Civil and Environmental Engineering
University of California, Berkeley

MEMBER CAPACITY FACTORS FOR SEISMIC ISOLATORS TO LIMIT COLLAPSE RISKS OF SEISMICALLY ISOLATED STRUCTURE TO ASCE 7 STIPULATED LIMITS

Benshun Shao [1], Stephen A. Mahin [2], Victor Zayas [3]

Abstract

Current seismic design code (ASCE 7-16) indicates that structures should not collapse, with a high degree of confidence, when subjected to risk-targeted maximum considered earthquake (MCE_R) intense ground shaking. The report explores the minimum seismic isolator displacement and shear capacities needed for seismically isolated structures to achieve the target reliability specified in ASCE 7-16 chapter 1. Probabilistic interpretation of seismic responses using FEMA P695 methodology indicates providing isolator capacities equal to the MCE_R demand from ASCE 7 Chapter 17 does not achieve the targeted levels of reliability. To achieve the target reliability, three isolation systems are considered to provide enough isolator capacities beyond MCE_R demand from ASCE 7. These isolation systems include: (I) Providing isolators with sufficient displacement capacity without any additional displacement restraining mechanism; (II) Augmenting isolators with a physical, hard stopping mechanism, such as a moat wall; and (III) Providing isolators having a built-in, soft stopping mechanism. The investigations focus on the seismic performance of a three story, base isolated archetype structure having lateral resistance above the base provided by concentrically brace steel frames.

Results indicate isolator displacement capacities ranging from 1.5 to 2.45 times the ASCE 7 MCE_R demands and isolation system shear capacities ranging from 2.1 to 5.0 times MCE_R demands are required, depending on seismic risk categories and isolation system types. Use of isolator with internal stiffening behavior is an efficient option to provide required capacities for achieving reliability goals.

Keywords: Seismic isolation, isolator failure, FEMA P695, collapse probability

1) Structural Analyst, Arup. shaobenshun@berkeley.edu
2) Professor emeritus, Department of Civil and Environmental Engineering, University of California at Berkeley. mahin@berkeley.edu. Deceased 2018
3) President, Earthquake Protection Systems. victor@earthquakeprotection.com

ACKNOWLEDGEMENT

The authors appreciate Earthquake Protection Systems' financial support, development of the isolator system types studied, isolator test data, and prior work on the development of isolator capacity factors as required to satisfy the ASCE 7-10 Collapse Risk Limits specified. However, the findings and conclusions in this paper are those of the authors, do not necessarily reflect the views of the sponsor.

The work described in this report was carried out by the three authors acknowledged on the title page. The second author, Professor Mahin, became ill during the final stages of preparing this report and passed away before it was completed. Professor Jack Moehle, a current member of the SEMM program, kindly approved the publication of this report in accordance with requirements of the SEMM publications policy

1 INTRODUCTION

Seismic isolation is an effective and reasonably economical means for minimizing earthquake damage and enhancing seismic performance of structures. It has thus been widely used, especially for cases where continued post-earthquake functionality is desired. The concepts underlying seismic isolation have been extensively studied (e.g., Zayas et al. 1987, 1989, Kelly et al. 1990, 1997, Naeim, et al. 1999, Mokha et al. 1990, Constantinou et al. 1990, Tajirian, et al. 1990, Aiken et al. 1993, Clark et al. 1997, Kikuchi, et al. 1997, Fenz. et al. 2008 [a] [b], Morgan et al. 2010, Yang, et al. 2010). The classical idea underlying seismic isolation is that the horizontal movement of the structure is uncoupled from that of the ground by a plane of high quality manufactured devices typically having low horizontal and high vertical stiffness. This generally lowers the forces developed in the super-structure and concentrates horizontal deformations within the isolation plane. Recent studies have developed design criteria that reduce structural, nonstructural, and content damage for seismically isolated structures sufficient to maintain continued functionality (Zayas et al. 2010, 2013). However, a critical safety issue in the design and construction of seismically isolated structures is to determine the required isolator displacement and shear capacities which provide the ASCE 7 (ASCE 2017) specified targeted reliabilities (Iiba et al. 2008, Zayas 2017, Shao et al. 2016, 2017).

This report firstly examines the ability of design based on demand specified in ASCE 7 Chapter 17 (Seismic design requirements for seismically isolated structures) to achieve ASCE 7-16 targeted level of reliability when subjected to the maximum considered earthquake demand. Then three isolation systems providing capacities beyond MCE_R demand are investigated considering the seismic performance of a three-story seismically isolated case study structure, which has lateral resistance above the base provided by Ordinary Concentrically Braced Steel Frames (OCBFs).

1.1. TARGET RELIABILITY FOR SEISMIC DESIGN

With development of performance-based earthquake engineering concept and framework as well as higher seismic performance requirement, significant attentions are paid into minimizing damage and achieving seismic resiliency under frequent and moderate earthquake events in seismic design. However, reliability or "safety" under rare and extreme earthquake event should always be the fundamental performance objective for seismic design.

Due to different characteristics of ground motion records used in time history analysis as well as other sources of uncertainty regarding structural modeling, design procedure, structural response is not a deterministic value under a certain level seismic event. Which means seismic design should meet a target requirement represented as a probability value rather than a single deterministic value.

Therefore, in current seismic design regulation ASCE 7-16 (ASCE 2017), "Reliability" is used to describe how reliable a structure will be under extreme seismic event. Reliability is represented quantitively in terms of conditional failure probability on the occurrence of MCE_R shaking hazard based on current seismic design regulation (ASCE 2017). Which means when considering seismic design of structure, the resulted design should have a certain probability of failure under MCE_R shaking hazard. The exact probability requirement depends on the importance of designed structure. For this purpose, risk category is used to demonstrate the functional importance. The target reliability in seismic design for structures belonging to different risk categories are summarized in Table 1. For example, if a hospital is designed which belongs to risk category IV, one needs to demonstrate that the resulted design will have less than 2.5% probability of failure when a MCE_R level shaking happens.

In additional, these targets should be satisfied by all critical structural components of all types of structural systems. No matter when a traditional fixed base structure is considered, or seismic isolated structural system, viscous damped structural system or other innovative structural systems are used, the resulted design should always satisfy the requirement in Table 1. However, seismically isolated structures are new types of structural systems for which prescriptive structure details and component standards have not been established as adequate based on historical performance.

Table 1. Target reliability for structural stability caused by earthquake (Adapted from ASCE 7-16, Table 1.3-2)

Risk Category	Basic Use or Occupancy	Conditional Probability of Failure Caused by the MCE_R Shaking Hazard (%)
I	Low occupancy	10
II	Normal Occupancy	10
III	Substantial economic impact, disruption or risk to life	5
IV	Essential facilities	2.5

1.2. CURRENT DESIGN PRACTICE FOR SEISMICALLY ISOLATED STRUCTURE

"Structural reliability" target shown in Table 1 above refers to reliability of all critical components of structural system. For a general fixed-base building, it refers to the upper structure itself. For a seismically isolated structure, it includes the reliability of upper structure and isolators. Because not only upper structure can collapse, the isolator can fail when the displacement and shear force capacities provided are exceeded. Failure of seismic isolators might result into failure of the entire structural system because they are served as the primary gravity supporting component for the upper structure. Reliability of entire seismically isolated system depends on the lower reliability of the two critical components.

Following current seismic design regulation for seismically isolated structure (ASCE 7 Chapter 17), upper structure is designed based on force developed in the isolator at maximum considered level seismic event (MCE_R). A force reduction factor R_I around 1-2 is commonly used. Considering the over strength factor and low horizontal stiffness of isolator, reliability target of upper structure will typically be satisfied. Which means the upper structure itself will have a small enough probability of failure.

According to ASCE 7-16, the maximum isolator displacement demand (D_M) is taken as the average peak displacement demand for the MCE_R excitations. Because of economic and practical considerations, construction specifications have previously required isolators to remain stable for just slightly larger than the MCE_R displacement demand, without directly accounting for the resulting probability of collapse. As such, a significant portion of MCE_R excitations would drive isolators to displacements exceeding their stability limits.

. When determining the displacement capacity of isolator, different design methods are allowed. Typical design methods considered are: Equivalent Lateral Force Procedure (ELP) and Dynamic Response History Method.

1.2.1. Equivalent Lateral Force Method

If the Equivalent Lateral Force Design Procedure (ELP) is used, the maximum bearing displacement demand is calculated as

$$D_{Max} = \frac{gS_{M1}T_M}{4\pi^2 B_M} \quad (1)$$

This calculation is based on a simplified MCE_R level displacement response spectrum ($gS_{M1}T_M/(4\pi^2)$ accounting for the effective period (T_M) and equivalent damping ratio (B_M) for a linearized model of the bearing. If additional torsional effect is considered, the D_M obtained will need to be amplified to get D_{TM}. This approach simplifies the isolation system behavior into an equivalent linear system, based on the equivalent linear period, the maximum displacement demand is obtained directly from linear displacement spectrum corresponding to MCE_R level event.

1.2.2. Dynamic Method (Response History Method)

The response history design approach obtains isolator displacement capacity based on time history analysis results of the isolated structure. Ground motion time records are selected and scaled based on the MCE_R target spectrum. Then, D_{Max} is selected based on either (1) the largest demand predicted using dynamic analyses considering at least 3 ground motions, or (2) the average maximum displacement demand computed considering 7 or more ground motions. The maximum estimated bearing demand (D_{Max}) estimated in this manner are then adjusted to consider torsional and other effects to obtain the maximum total displacement demand (D_{TM}) for design.

It is clear that no matter what method is used, the isolator displacement capacity determined based on current design regulations should correspond to an average value when MCE_R level seismic event happens, we use the terminology D_M in this report to represent this demand specified by ASCE 7. Another important thing to notice, for all different risk categories, the design requirement is the same. This is different from design requirement for fixed-based building. Based on ASCE 7, when determining the design base shear for a fixed based building

using equivalent lateral force method, the design force obtained from design spectrum and required R value need to be amplified by an importance factor Ie. For higher risk category, Ie will be larger which means larger design base shear is required. However, for isolator, a risk category I and risk category IV structure would have the same isolator displacement capacity based on code minimum requirement (ASCE 7). This is not consistent with the target reliability requirement since as shown in Table 1, for different risk categories, different reliability targets are needed.

1.3. RELIABILITY OF CASE STUDY BUILDING HAVING ISOLATOR CAPACITY EQUAL TO MCE_R DEMAND

Does the current design regulation for seismically isolated structure satisfy the target reliability as shown in Table 1? In this section, a brief evaluation will be conducted using probabilistic approach. Archetype seismically isolated structure based on the dynamic response history design procedure is designed. The numerical modal of the structure used will be discussed later in the report. Then, using probabilistic failure assessment method introduced in FEMA-P695 (FEMA 2009), which will be discussed in detail in the following section, the failure risk of this archetype seismically isolated structure designed based on ASCE 7 demand will be evaluated. The calculated reliabilities for the archetype structure with isolator capacity equal to the demand specified by ASCE 7 are summarized in Table 2 below for different risk categories consideration.

Table 2. Resulted reliabilities of system with isolator capacity equal to ASCE 7 demand. Results are calculated based on FEMA-P695 approach

Risk Category	Calculated probability of failure of upper structure (%)	Calculated probability of failure of Isolator (%) [Lower bound /Nominal property]	Combined probability of failure (%) [Lower bound /Nominal property]	Target Reliability (%)
I&II	<0.1	45/32	45/32	10
III	<0.1	45/32	45/32	5
IV	<0.1	45/32	45/32	2.5

Upper structure designed based on force requirement at MCE_R event according to ASCE 7-16 has negligible probability of failure, since no lateral restraint is requirement, the resulted reliability of entire isolated system is controlled by the probability of isolator losing stability.

Based on the analysis results, the resulted design will have a failure probability larger than 40% on the occurrence of MCE_R event for all risk categories, if lower bound property of isolator is used in the evaluation procedure. However, if nominal property of isolator is used, a smaller probability of failure around 30% is expected under MCE_R event since the isolator is sized considering lower bound property based on code design requirement, which leads to certain levels of conservative results. However, this is still much larger comparing to the target reliability. Note, here we assume the manufactured bearing has high quality and can provide displacement capacity specified. If bearings with poor or uncertain quality are used, even higher failure risk will be expected. As discussed, we use D_M from response history analysis as minimum code required capacity in the evaluation. If equivalent lateral force design method is used or additional torsional effect is considered for isolator design, a larger total code design displacement D_{TM} comparing to D_M might be considered, the resulted failure probability might be slightly different as indicated in Table 2, however, it will still be significantly larger than the target reliability.

1.4. MOTIVATION OF THE STUDY

From above discussion, design for seismically isolated structure with isolator capacity equal to the ASCE 7 MCE_R demand (D_M) will result into a reliability much larger comparing to the target. Especially for high risk category cases, the design will end up with more than 10 times allowable probability of failure. Isolator capacity beyond the MCE_R demand specified by ASCE 7 is needed. Recall for seismic design of fixed base structure, design base shear is amplified using importance factor (Ie) to account for different risk categories since higher reliability target is needed for higher risk category as shown in Table 1. Design of isolator is based on displacement demand rather than force demand. Current regulation requires a displacement capacity based on average demand under MCE_R level motions regardless of risk categories. This minimum design requirement is far from adequate even for the lowest risk categories as indicated in Table 2.

To solve this problem, similar “importance factor” concept should be used for isolator capacity determination in design since the reliability of upper structure and isolator are equally essential for the entire reliability of seismically isolated structure. Minimum code required isolator displacement and force capacity determined based on MCE_R demand need to be

amplified using an "importance factor" in order to meet the target reliability. We use the isolator capacity factor (α_D for displacement, $\alpha_V$for shear capacity) in the study to represent the ratio between required capacity ($Dcapacity$ and $Vcapacity$) and MCE_R demand specified by ASCE 7 (D_M and V_M). If we define the member capacity factor of isolator as:

$$\alpha_D = \text{Dcapacity}/D_M \quad (2a)$$

$$\alpha_V = \text{Vcapacity}/V_M \quad (2b)$$

Then the fundamental problem remaining is to determine what α_D and α_v values are needed for different risk categories in design of seismically isolated structure.

Through numerical analysis of archetype seismically isolated building and statistical framework developed, the required α_D and α_v values are quantitively investigated in the study considering three isolation systems to provide the additional capacity beyond code demand. Response history analyses are performed in OpenSees (McKenna et al. 2000) to obtain α_D and α_v corresponds to the target reliability. The three isolation systems considered are: I Provide additional isolator displacement capacity without displacement restrained mechanism; II Provide physical isolator movement stopping mechanism using moat wall; III Provide additional isolator displacement and shear force capacity using stiffening isolator. Required design parameters as well as effectiveness for each method are investigated separately and then compared. The most efficient and practical solution to achieve target reliability in design of seismically isolated structure is proposed together with recommended α_D and α_v value for isolator design.

2 STUDY BACKGROUND

In this section, the numerical analysis model, ground motion record selection considered in the study will be discussed.

2.1. UPPER STRUCTURAL MODEL

The study considers an archetype seismically isolated structure designed based on current code regulation (ASCE 2017) with force reduction factor R_I=1 at MCE_R level seismic event for a target design spectrum of seismic category Dmax.

The upper structure is a three-story conventional braced frame. A 2-D nonlinear numerical model is established in OpenSees as shown in Figure 1. In order to capture possible highly nonlinear behavior when physical stopping mechanism is considered in the study, nonlinear force-based distributed elasticity elements are used with fiber sections (Neuenhofer et al. 1997). For each brace member, multiple elements are used to capture buckling behavior and fracture due to low cycle fatigue (Uriz et al. 2008). A section damage identifier is programed and triggered at each analysis time step to automatically identify brace section fatigue damage and remove fracture brace member to maintain the robustness of numerical solver. Leaning columns are used to consider addition P-Delta effects associated with axial loads acting on gravity resisting columns which is not modeled on the perimeter braced frame plane.

Some key features for the numerical model are summarized as below:

- Concentrically braced frame system
- Fully nonlinear 2D model in OpenSees. (Both material and geometry nonlinearity are captured)
- Multiple elements each brace with corotational geometric transformation to capture buckling behavior and post buckling behavior
- Fatigue material wrapper to account for material failure due to low cycle fatigue
- Section damage identifier is programmed and triggered at each time step to remove fractured brace member
- Additional P-delta effect of gravity columns are considered by leaning column

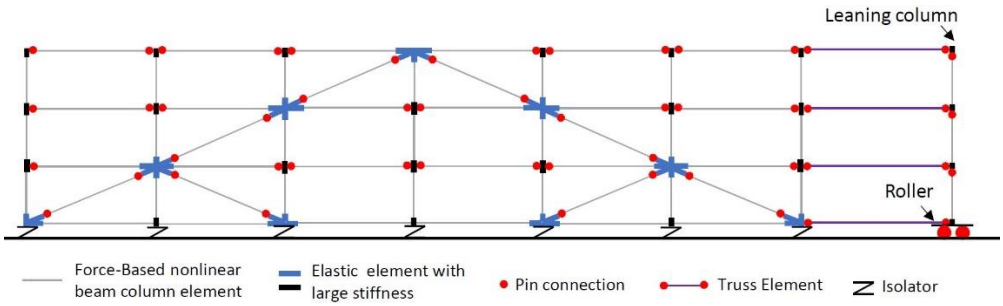

Figure 1. Scheme of Architype building 2D model considered in the study

2.2. ISOLATOR MODEL

Triple Friction Pendulum (TFP) Bearing is used for the archetype building in the study with hysteresis behavior shown in Figure 2. This TFP bearing used for the study is a newly developed type of TFP bearing, which has different stiffening and unloading behavior comparing to the traditional TFP bearing as shown in Figure 2. Stiffening happens when displacement exceeds a controllable point D_h. When shear force reaches a prescribed shear capacity Vcapacity, a plastic yielding stage will follow. Hysteresis shape are controlled and determined by radius of sliding concaves and friction coefficients of different sliding surfaces. An 2D numerical model is constructed in OpenSees. The design parameters for the TFP bearing used in the study are obtained from manufacture and are summarized below in Table 3.

Table 3. Design parameters of TFP used for the architype structure

Friction Coefficients				Radius of sliding concaves [inch]	MCE_R Level	
	Lower bound	Nominal	Upper bound			
mu_1	1%	2%	3%	30	Dm [in]	27
mu_2	3%	4%	5%	156	Teff [sec]	4.55
mu_3	6%	7%	8%	156	Damping	17%

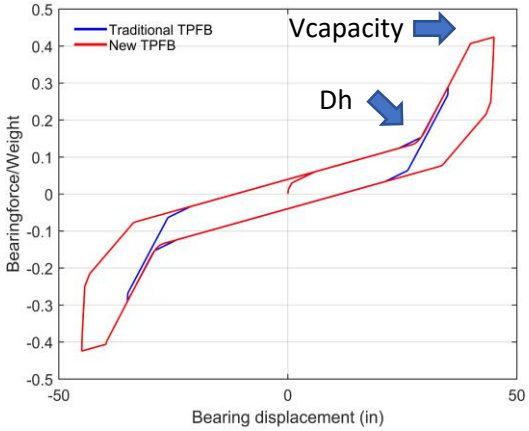

Figure 2. Hysteresis of TPFB used in the study. Dh corresponds to the point stiffening starts, Vcapacity refers to the shear force capacity for bearing.

Besides the TFP bearing used as one of the enhanced design method as indicated in previous section, to investigate the design procedure using bearing without stiffening, the stiffening starting displacement (D_h) is put at an infinite large point. To mimic the behavior of moat wall impact when physical stopping mechanism is introduced, parallel nonlinear spring models are constructed in OpenSees with gap material. The impact will be engaged when the defined seismic gap size is exceeded.

2.3. GROUND MOTION RECORD CONSIDERED

To investigate probability of failure under MCE_R level seismic event, a target MCE_R design spectrum is needed. In the study a generic site corresponds to seismic category Dmax is used. This target MCE_R level spectrum does not correspond to a specific site. The value used to construct the MCE_R spectrum for seismic category Dmax is obtained from ASCE 7-16. The seismic category Dmax spectrum represents a site which will have high seismic intensity. The use of this general design spectrum rather than a specific site spectrum will result into a more general result. However, since we are investigating the isolator member capacity factor, which is defined as the ratio between enhanced design requirement and the minimum code requirement, the results should not be directly related to the target spectrum intensity.

In order to be consistent with FEMA P695 (FEMA 2009) approach, the far field motion set containing 22 ground motion records as selected to quantify building performance factor in FEMA P695 is used. The ground motion records are scaled so that elastic response spectrum at

effective period of the architype isolated structure for individual ground motion record matches the target value. The 5% damping SDC Dmax MCE_R target design spectrum as well as the individual ground motion spectra selected are shown in Figure 3 below. Since the numerical model is a 2D model, we input two horizontal components of each ground motion records individually which results into 44 individual time histories for the response history analysis.

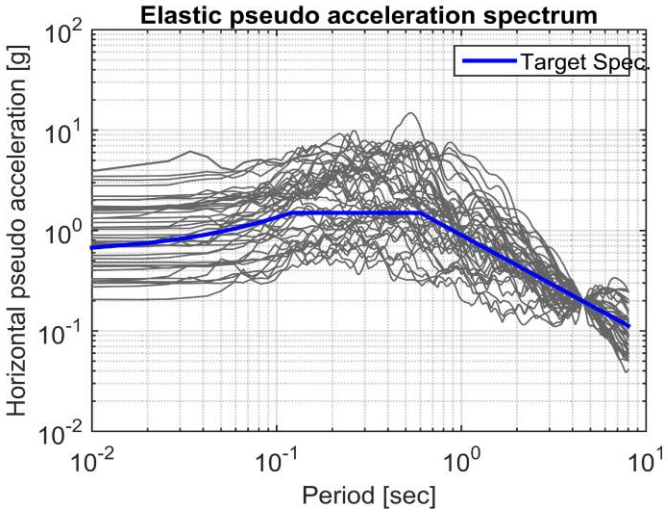

Figure 3. Target MCE_R spectrum considered in this study and the seed ground motion records matched to the fundamental effective period of the isolation system.

3 STATISTICAL FRAMEWORK USED TO OBTAIN ISOLATOR CAPACITY FACTOR

Probabilistic approach to quantify seismic performance has been widely used in performance based design (FEMA 2009, 2012, PEER 2010). For the purpose of this study, using probabilistic framework originally developed in FEMA P695 (FEMA 2009), failure probability of isolator under MCE_R level seismic event can be assessed given a certain bearing design capacity. In this approach, an incremental dynamic analysis will be conducted first. Then a failure fragility curve will be constructed based on the Incremental Dynamic Analysis (IDA) results as shown in Figure 4. Then based on the fragility curve, one can obtain the probability of failure under a given seismic hazard.

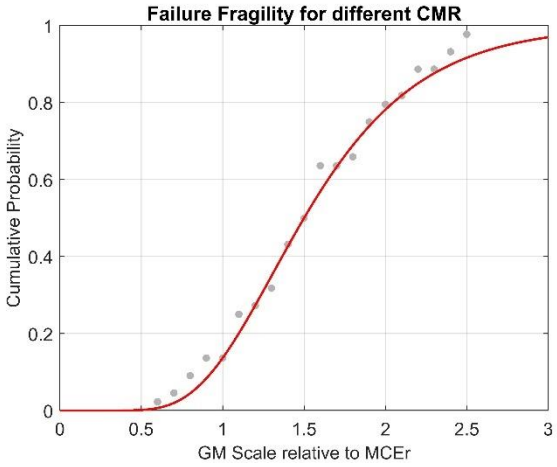

Figure 4. A simple demonstration of failure fragility curve from incremental dynamic analysis.

3.1. INTORDUCTION OF STATISTICAL FRAMEWORK USED

However, in the study, our task is not to evaluate an existing design but to establish the required design requirement (Isolator capacity factor) to achieve a certain design target. This is a slightly different problem than simply evaluating and quantifying failure risk. Because bearing capacity is not known and remains to be find at the beginning, if using the traditional probabilistic approach to quantify the failure probability, iterative process might be needed as shown in Figure 5 (a). Isolator capacity is firstly selected, reliability based on the selected capacity will be evaluated and compared to the target. Then the design capacity might be modified and the evaluation process would be conducted again until an optimized bearing design parameter are obtained satisfying the target reliability.

Instead of updating failure fragility by changing bearing capacity at each iterative step, in this study we directly start with a target fragility based on required reliability and back calculate the required bearing design capacity as shown in Figure 5 (b) below. The steps involved in this statistical framework is shown in Figure 6 below. Target reliability in terms of conditional probability of failure under MCE_R level shaking as well as fragility dispersion β_{TOT} need to be obtained at beginning of the framework. Based on the log-normal distribution assumption, the fragility curve can be determined mathematically with the target point and dispersion value β_{TOT}. This fragility curve is the target curve which will result into required reliability. Then target collapse margin ratio (CMR) which is defined as the ground motion intensity causing 50% probability of failure can be calculated mathematically. Therefore, instead of finding the required design capacity which will result into a lower probability of failure under MCE_R event, using this statistical framework, we end up finding design capacity which will result into 50% of failure under an enhanced intensity level beyond MCE_R. And these two probability levels are equivalent and related by fragility curve.

Then the remaining problem is to find the capacity of isolator so that 50% probability of failure under the enhanced ground motion intensity determined by the CMR target calculated will happen.

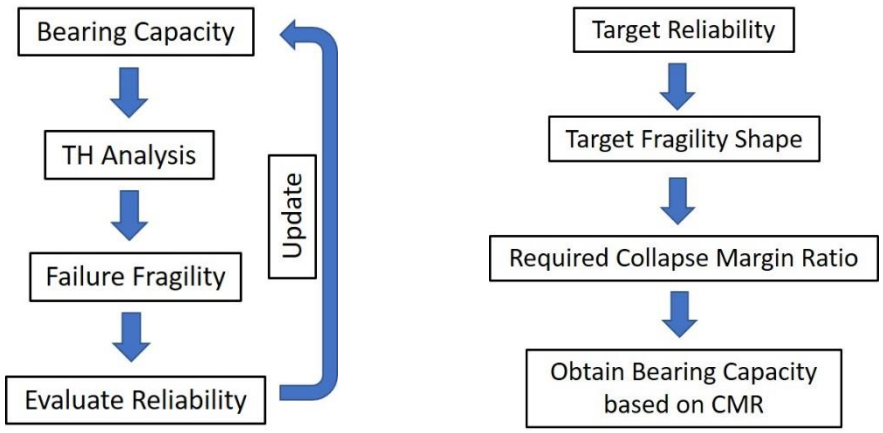

Figure 5. Probability framework for designing of seismically isolated structure based on target reliability. (a) Traditional approach involving iterative process (b) Approach used in this study

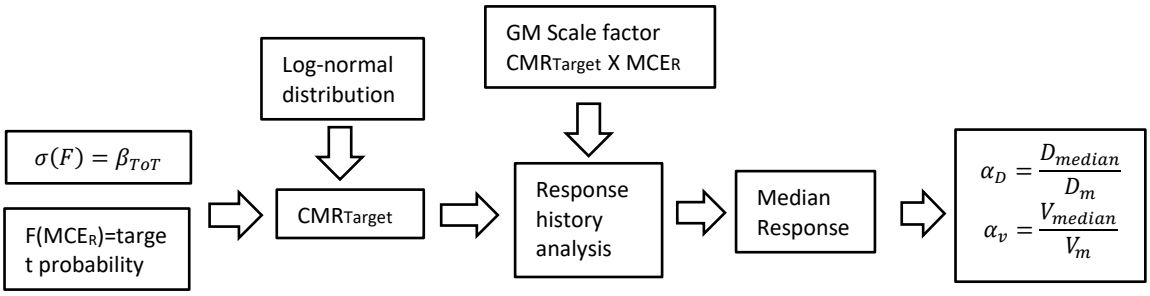

Figure 6. Original statistical framework used to calculate required capacity factor in this study.

Seed ground motion records selected based on MCE_R target spectrum will be scaled by target CMR calculated. Required bearing capacity factor can be determined by taking median response from response history analysis results. The selected bearing displacement and force capacity will thus satisfy the required collapse margin ratio and result into target fragility shape. The approach does not involve any iteration process and is potentially applicable for a general design case of seismically isolated structure.

The reason for using this statistical framework is to establish a relation between ground motion record used for response history analysis and the target reliability. The ground motion records are selected based on the MCE_R target spectrum, the target reliability is represented by a conditional probability of failure under MCE_R seismic event. Therefore, modification of the original ground motion record intensity will be needed to make sure the results obtained from response history analysis using modified records will result into the required reliability. The statistical framework proposed in this section will calculate the modification factor needed (Target CMR) directly.

3.2. ASSUMPTION IN THE STATISTICAL FRAMEWORK

Determination of fragility uncertainty value β_{TOT} serves as the basis when constructing the target failure fragility curve for the statistical framework introduced above. Different β_{TOT} values will require different fragility curve shapes for same target reliability thus affect the final design results significantly.

As shown in Figure 7 (a), to achieve the same 10% failure probability under MCE_R level event, because different β_{TOT} are considered, different fragility curve shapes are needed. The scale factor needed to scale up the seed ground motions (CMR_{Target}) will be different. Therefore,

as shown in Figure 7 (b), the required isolator displacement capacity needed to achieve same target reliability are much different. For example, to achieve 10% failure under MCE_R level event, if a dispersion of 0.1 is assumed, the required displacement capacity of bearing is around 35 inches, however, if β_{TOT} of 0.4 is used, a bearing with displacement capacity of almost 55 inches will be needed for the same target reliability. Therefore, correct assumption of β_{TOT} is essential to get correct bearing capacity in design.

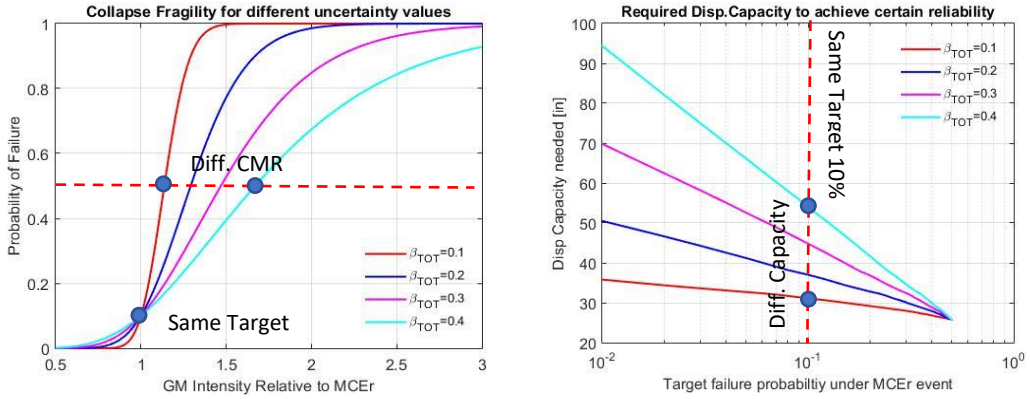

(a) (b)

Figure 7. Effect of different fragility uncertainty β_{TOT} on fragility curve shapes and resulted isolator capacity needed to achieve same reliability. (a) Different target failure fragility under different β_{TOT} to achieve same reliability. (b) Different isolator displacement capacity needed for different β_{TOT} to achieve same reliability. Result are based on a representative GM Record

The collapse uncertainty β_{TOT} is derived from different sources as indicated in equation 3 below. β_{TD} is uncertainty associated with test data, β_{MDL} is the uncertainty associated with design requirement, β_{DR} is the uncertainty associated with structural model. Values of these three sources are determined based on archetype structural model information. β_{RTR} is determined based on empirical relation in FEMA P695 from period ductility (μ_T). Quality rating of test data, case structure model and design requirement are determined as (B) Good, (A) superior and (A) superior respectively based on Table 3-1, Table 3-2 and Table 5-3 in FEMA-P695, which lead to uncertainty values of β_{TD}, β_{MDL} and β_{DR} as 0.2, 0.1 and 0.1. Total system uncertainty β_{TOT} of 0.35 is calculated based on equation (2) in this case.

$$\beta_{TOT} = \sqrt{{\beta_{TD}}^2 + {\beta_{MDL}}^2 + {\beta_{DR}}^2 + {\beta_{RTR}}^2} \quad (3)$$

However, for the design approach using physical stopping mechanism like moat wall, quality rating of structure model is identified as (B) good instead of (A) superior where system failure is governed by "collapse" of upper structure. This leads to model uncertainty (β_{MDL}) value of 0.2 and total system uncertainty (β_{TOT}) of 0.39, which are consistent with similar investigations conducted by Kircher and Masroor (FEMA 2009, Masroor and Mosqueda 2015). Spectral Shape Factor (SSF) is used to correct median collapse capacity considering spectral shape quantified by $\varepsilon(T)$ value. The imperical relation to obtain SSF in FEMA-P695 is developed based on 0.5% 50 years hazard level and target ε at 1 secs period for concrete moment frame (Haselton and Baker 2011). For seismically isolated steel OCBF considered in the study, SSF value of 1.13 would be obtained. However, considering fundamental period (4.5 secs) and structural system (Steel OCBF) of case study structure, the use of original relation is not justified. Therefore, SSF value of 1.0 is assumed herein, which will conservatively estimate the isolator capacity needed. Target collapse margin ratio values for different reliability levels (10%, 5% and 2.5%) are calculated based on lognormal distribution with dispersion (β_{TOT}) as shown in Table 4.

Table 4. Parameters and their values of FEMA P695 approach used in the study

	β_{RTR}	β_{TD}	β_{MDL}	β_{DR}	β_{TOT}	10% Failure CMR_{Target}	5% Failure CMR_{Target}	2.5%Failure CMR_{Target}	μ_t	SSF
"Moat Wall" case	0.25	0.2	0.2	0.1	0.39	1.64	1.90	2.15	1.43	1.0
Other cases	0.25	0.2	0.1	0.1	0.35	1.56	1.78	1.99	1.43	1.0

4 ANALYSES RESULTS

In this study, capacity factors required for isolation systems to meet target reliability are investigated. Three different isolation systems are considered: I Using bearing without displacement restraint mechanism; II Using a physical stopping mechanism like a moat wall; III Using isolator with stiffening behavior (using TFP bearing as an example in this study). The capacity requirements for isolation systems are represented by member capacity factors as defined as below:

$$Isolator\ Disp.Capacity\ Factor\ \alpha_D = \frac{Disp\ Capacity\ needed}{Dm}$$

$$Isolator\ Shear\ Capacity\ Factor\ \alpha_V = \frac{Shear\ Capacity\ needed}{Vm}$$

At the same time, upper structure responses are also investigated besides the member capacity for isolator. Peak story drift ratio is calculated for upper structures to investigate the possible damage in upper structures when using these three isolation systems.

4.1. USING ISOLATOR WITHOUT DISPLACEMENT RESTRAINT

Firstly, the study investigates required capacity factor of isolation system beyond minimum code demand if a larger bearing with no displacement constraint is used in design. For different risk categories, the requirement is different. Based on the method discussed in previous section, the bearing displacement and force capacity factor are summarized in Table 5 below:

Table 5. Required capacity factors and upper structure drift demands for achieving target reliability levels when isolator without displacement restraint is used

Risk Category	Target Reliability [%]	Isolator Design Requirement		Upper Structure Responses (R_I=1)	
		Disp. capacity factor α_D	Force capacity factor α_V	Drift Demand at isolator failure δ_c[%]	Damage of upper structure before isolator failure
I & II	10	1.65	1.53	0.13	negligible
III	5	2.08	1.84	0.16	negligible
IV	2.5	2.45	2.09	0.19	negligible

From numerical analysis results, a bearing with 1.65 times code MCE demand is needed in order to achieve the target reliability for risk category I&II structure. If higher risk categories are considered in design, a bearing capacity with even 2.45 times MCE demand will be needed. Besides the extra displacement capacity, bearing needs to have corresponding shear capacity determined by the hysteresis shape of isolator. Hysteresis comparison under an individual representative ground motion record is shown in Figure 8. Bearing size needed to achieve target reliability is much larger than MCE demand from ASCE 7.

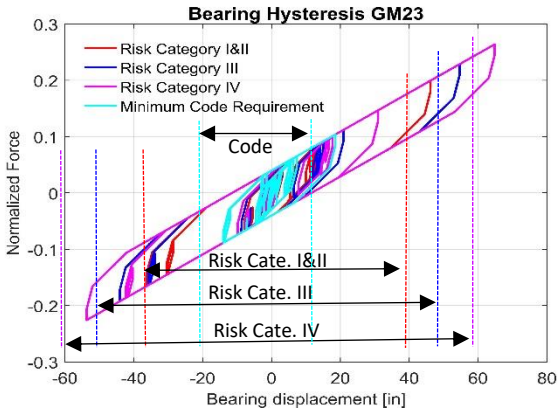

Figure 8. Isolator hysteresis comparison to achieve target reliability for different risk categories under a representative ground motion.

As shown in Table 5, no additional requirement on upper structure is needed. Although intuitively, larger bearing force might result into larger force demand on upper structure, considering over strength effect, the upper structure strength is more than adequate to accommodate larger bearing force developed. The resulted story drift demand as well as peak floor acceleration responses are shown in Figure 9. As one can expect, following this procedure, the upper structure will remain almost elastic and negligible damage would be expected before the entire system fails when isolator loses stability.

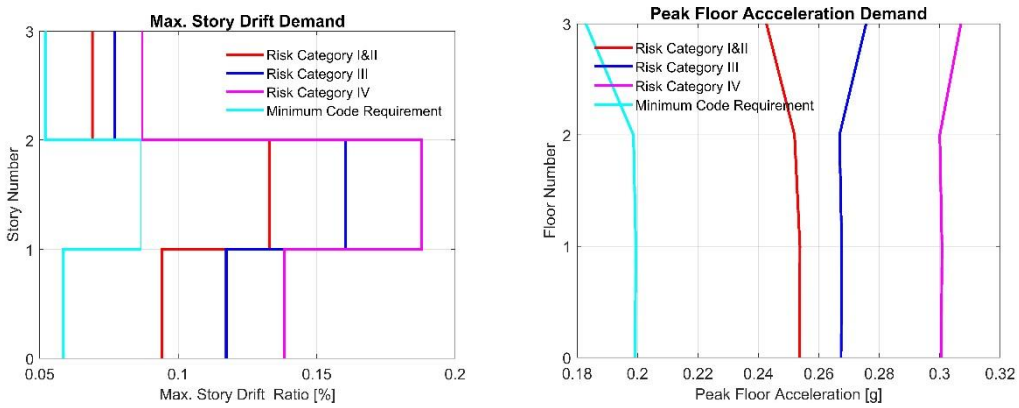

(a) (b)

Figure 9. Peak story drift response as well as peak floor acceleration response using bearing without displacement restraint to design for target reliability

In summary, if isolator without displacement restraint mechanism is used, a large isolator member capacity factor needs to be provided in order to achieve the target reliability. The resulted upper structure will remain elastic and damage free under frequent to moderate earthquake even under very rare earthquake before the isolators lose stability and the entire system fails. A bearing displacement capacity factor around 1.65-2.45 will be needed based on design risk categories.

4.2. USING PHYSICAL STOPPING MECHANISM: MOAT WALL

As discussed above, increasing isolator capacity is the most straightforward way to provide enough isolator capacity for achieving target reliability. Another commonly considered procedure is to provide a physical displacement restraint to protect the bearing so that isolator will not loss stability. Moat wall or retaining wall around isolation plane is typically used in practice to provide such a restraint despite this approach may not be feasible for varies architectural or practical reasons. (e.g. the isolation plane is above grade). The target reliability for isolator is achieved, however, whether the upper structure will achieve the target reliability at the same time need to be carefully investigated in this case since impact load from moat wall will introduce large demand into upper structure because of dynamic amplification effect (Masroor et al. 2012 and 2015, Shao et al. 2017). Reliability of entire seismically isolated structure is controlled by the upper structure failure risk instead of the probability of isolator losing stability since the isolator is protected by the stopping mechanism.

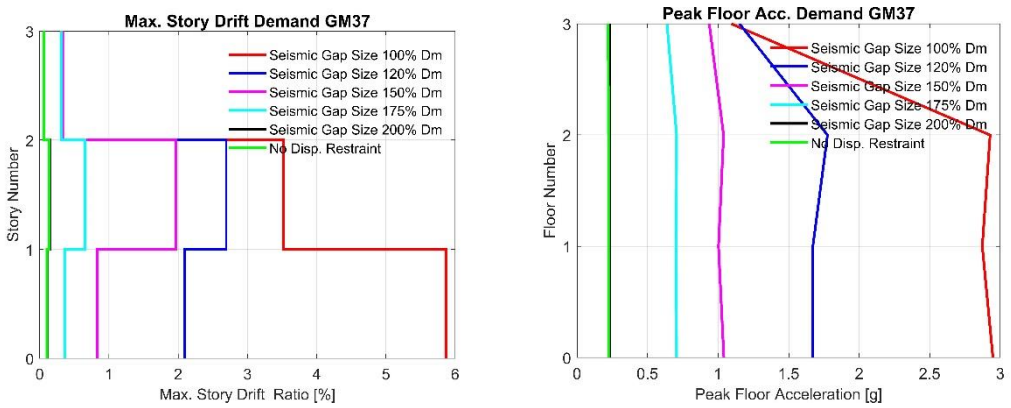

(a) (b)

Figure 7. Peak story drift response as well as peak floor acceleration response using physical stopping mechanism for different seismic gap sizes (moat wall clearance distances). Responses compared are under the same ground motion record (GM 37) which has a beyond MCE_R intensity

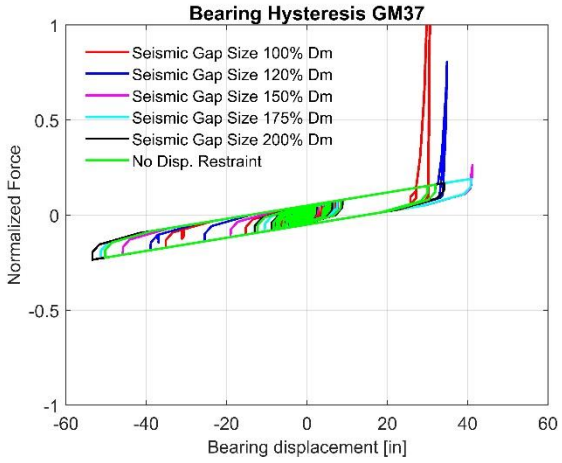

Figure 8. Combined forces resisted by isolator and moat wall for different seismic gap sizes (moat wall clearance distances). Responses compared are under the same ground motion record (GM 37) which has a beyond MCE_R intensity.

Therefore, for this enhanced design procedure, it is important to investigate what is the additional design requirement on upper structure and what is the appropriate seismic gap sizes to provide. Through numerical simulation of our archetype structure, if most wall is used, drift and acceleration responses of upper structure as well as bearing hysteresis are shown in Figure 7 and Figure 8 for different seismic gap sizes. One can see that significantly larger responses will be introduced into upper structure, for a conventional braced frame, the large drift response will possibly result into severe structural damage or even global collapse of upper structure. If larger seismic gap sizes are used in design, less damage will be introduced since the impact will be

engaged with a lower velocity as shown in Figure 9. The acceptable seismic gap sizes depend on the upper structure deformation capacity. As shown from the trend in Figure 9, the larger deformation capacity upper structure has, the smaller seismic gap sizes are needed to achieve a certain risk target, vice versa. For example, if we assume archetype structure will not have global collapse mechanism until maximum story drift ratio reaches around 2.5%, then for risk category I&II structure, a seismic gap size around 110% D_M would be enough. However, to achieve higher reliability for risk category III and IV structures, a seismic gap size of 175% D_M and 225% D_M are needed respectively. In addition, upper structure will experience severe damage despite the total reliability target is achieved.

Table 6. Required seismic gap sizes (moat wall clearance distances), isolator capacity factors and upper structure drift demand to achieve target reliability when moat wall is used to provide physical stopping mechanism

Seismic Risk Category	Target Reliability [%]	Required Seismic Gap Size	Isolator Design Requirement		Upper Structure Response (R_I=1)	
			Disp. capacity factor α_D	Force capacity factor α_V	Maximum drift ratio developed δ_c[%]	Damage in the upper structure
I & II	10	1.10Dm	1.10	1.07	2.50	Severe
III	5	1.75Dm	1.75	1.53	2.46	Severe
IV	2.5	2.25Dm	2.25	1.88	2.52	Severe

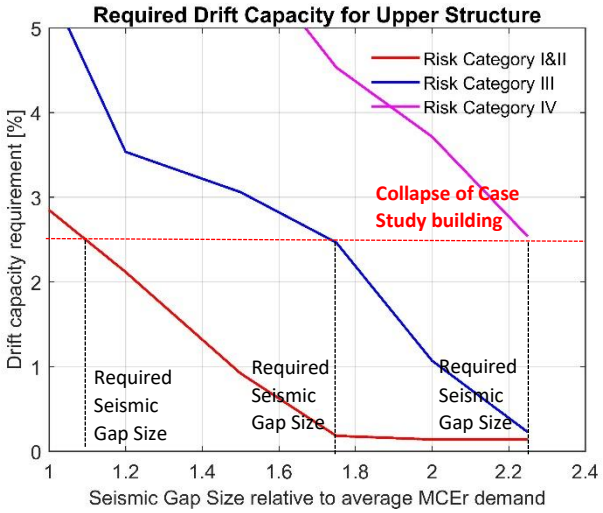

Figure 9. Relation between upper structure collapse limit (story drift capacity) and minimum seismic gap sizes (moat wall clearance distances) requirement for different risk categories

In summary, if external stopping mechanism is introduced, isolator will achieve target reliability as long as bearing displacement capacity is larger than seismic gap size. However, upper structure might have large risk of failure. In order to limit the collapse risk of upper structure due to impact loading and to achieve target reliability for upper structure, high deformation capacity requirement is needed together with large enough seismic gap size This will lead to large capacity factor for isolator for high risk category design. At the same time, the moat wall needs to demonstrate enough strength. From analysis, a shear strength capacity of 5.0 times the MCE_R isolator shear demand (Vm) is needed for moat wall.

4.3. USING BEARING WITH INTERNAL STIFFENING MECHANISM

As discussed for the first two isolation systems, to achieve the target reliability, if no displacement restraint mechanism is used for the bearing, upper structure will have negligible small risk of failure while a significantly larger bearing capacity factor will be needed in design; If a physical “hard stop” mechanism is considered such as using moat wall, the isolator will have negligible small risk of failure as long as it has larger capacity than the seismic gap size. However, the upper structure will need to accommodate large deformation demand and will develop severe damage before “collapsing”.

To reduce the effects of sudden impact loading on upper structure and to reduce the uneconomical large bearing capacity demand, a “soft stop” bearing displacement restraint mechanism is desired. This can be achieved by increasing stiffness of isolator gradually at certain displacement. The ideal isolator will have relative low horizontal stiffness and damping under moderate displacement demand for minimizing damage of upper structure. Then stiffness and damping ratio starts to increase to provide additional safety margin beyond the minimum code requirement.

As shown in Figure 10 and 11, because bearing shear force increases due to stiffening behavior, upper structure responses will be amplified comparing to bearing without any displacement restraint. However, comparing the responses to the case with moat wall as indicated by black line in Figure 10 and Figure 11, yielding and damage of upper structure using stiffening bearing is much smaller. The amount of yielding and damage depends on the shear force capacity of bearing. Larger shear force capacity will result into larger responses. In Figure

10 and 11, the isolator force capacity is fixed at several discretized values based on commonly available shear capacities of TPFB.

For other types of bearing with stiffening behavior, a different design for stiffening portion might be used based on manufacturing property. A combination of shear force capacity factor α_V and displacement capacity factor α_d will be needed for determining enhanced design requirement using stiffening bearing. The combination needs to be achieved with specific bearing design rather than the prescribed stiffening hysteresis behavior considered in this study.

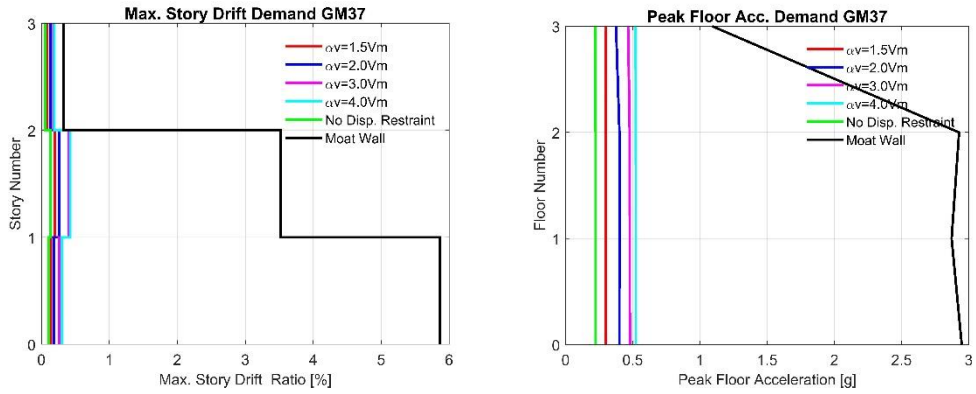

(a) (b)

Figure 10. Peak story drift response as well as peak floor acceleration response using TFPs with different Vcapacity (α_V) under a ground motion with beyond MCE_R intensity. Responses of using isolator without displacement restraint and moat wall are shown together for comparison under the same motion (GM 37)

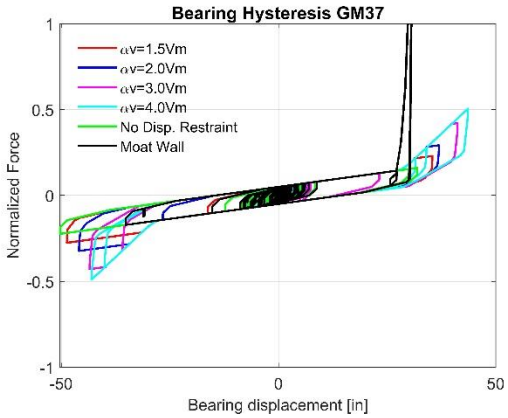

Figure 11. Hysteresis behavior of TFPs with different Vcapacity (α_V) under a ground motion with beyond MCE_R intensity. Combined forces resisted by isolator and moat wall as well as isolator hysteresis when displacement restraint is not provided are shown for comparison under same ground motion (GM 37).

The required capacity for isolator and upper structure responses using stiffening bearing are summarized in Figure 12. The required displacement capacities of bearing are different for different isolators with varied shear force capacities. Using stiffening bearing with larger shear force capacity, the required displacement capacity can be reduced while the upper structure deformation will increase. Considering a hardening TFP bearing design with manufactured shear capacity of 3.0 Vm, the required isolator displacement capacities are summarized in Table 7.

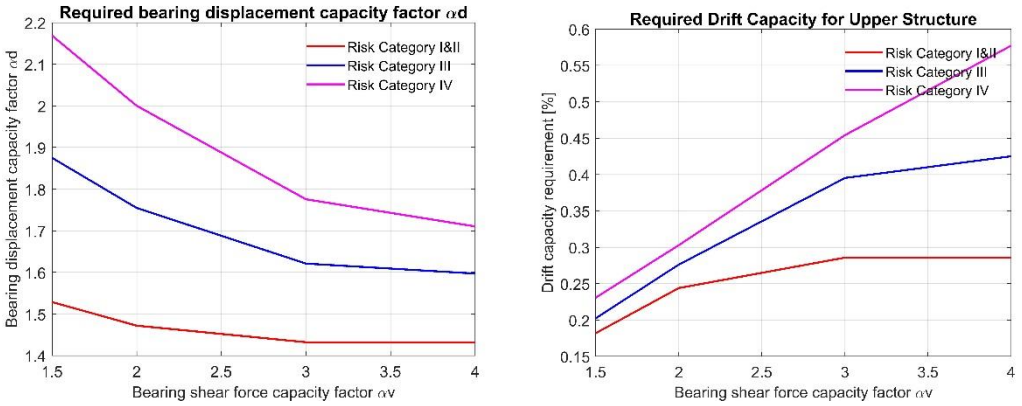

(a) (b)

Figure 12. (a) Required isolator displacement capacity factors when TFPs with different Vcapacity (αV) are used for different risk categories. (b) Maximum story drift ratio developed in upper structure when the required isolator displacement capacity is provided for TFPs with different Vcapacity (αV) for different risk categories

Table 7. Required isolator capacity factors and responses of upper structure to achieve target reliability using stiffening isolator

Risk Category	Target Reliability [%]	Isolator Design Requirement		Upper Structure Requirement (R_I=1)	
		Disp. capacity factor α_D	Prescribed shear capacity factor α_V	Drift Demand at isolator failure δ_c[%]	Damage of upper structure before isolator failure
I&II	10	1.43	3.0	0.29	minor
III	5	1.62	3.0	0.40	minor
IV	2.5	1.76	3.0	0.45	minor

4.4. COMPARISON OF THREE ENHANCED ISOLATION SYSTEMS

As discussed above, three isolation system types to provide enough capacities for seismically isolated structure meeting target reliability are discussed in detail. The required member capacity

factors for isolator are quantified using capacity factor α_d and α_V defined in Equation 2. Detailed design requirements for each of the three design procedures are investigated based on response history analysis and statistical framework, results are summarized in Table 5, Table 6 and Table 7.

To further compare these three systems, suppose a risk category III structure is considered in design, and sufficient isolator capacity and moat wall clearance are assumed to achieve reliability target using the three approaches. Upper structure as well as isolator responses under a beyond MCE_R ground motion are shown and compared in Figure 13 for each case. Yielding of beam and column are indicated at the end of each element with red dot while brace buckling is indicated using a blue dot.

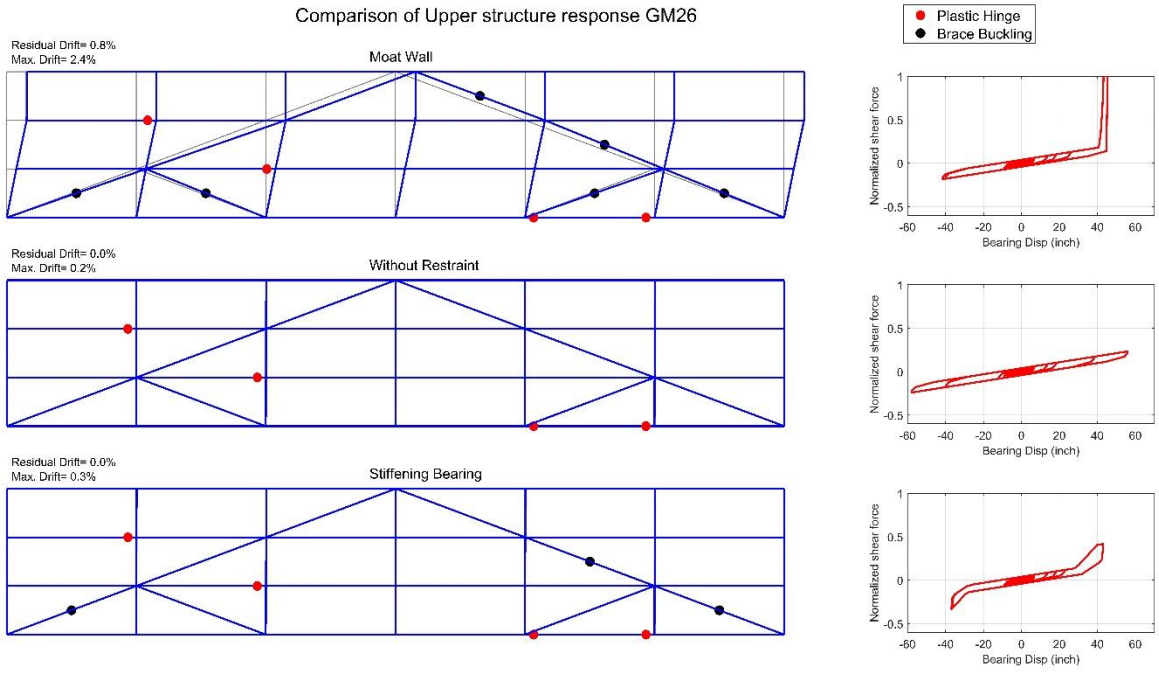

Figure 13. Residual deformation shape and yielding mechanism of upper structure considering three enhanced design procedures as well as hysteresis for combination of restraining system (if any) and isolator. Responses shown are under the same ground motion (GM 26) which has a beyond MCE_R intensity. The systems are designed assuming to achieve reliability target of risk category III.

Firstly, using physical stopping mechanism with all design requirement discussed satisfied, upper structure will have severe damage and large residual drift. Plastic hinges form at both column and beams. Although the entire isolated structure might satisfy target reliability, resulted structure after the rare event may not stand through an aftershock and might be unrepairable.

If bearing without displacement restraint is used, minor yielding is expected in upper structure and it will remain almost elastic. However, bearing will undergo a large horizontal displacement. Besides the huge displacement capacity needed, this procedure might not be an efficient solution conceptually. Recall the ground motions we are looking at might be 1.5 or even 2 times larger comparing to an average maximum considered earthquake shaking. Minimizing damage of upper structure with bearing without displacement restraint under such rare event might not be the most appropriate performance objective one likes to achieve.

Finally, use of stiffening bearing falls in between the two approaches discussed above. Minor yielding and damage will be expected in the upper structure depending on the bearing shear force capacity. At the same time, a moderately larger bearing displacement and force capacity will be needed relative to MCE demand from ASCE 7.

The required design parameters for the three isolation systems are summarized in Table 8. There are different combinations of acceptable capacities for each method to achieve the same target reliability. The most economical combination is shown for each isolation system in the table. We assume archetype conventional braced frame upper structure will collapse at a maximum drift ratio around 2.5 %.

Among three enhanced design procedures considered, use of stiffening bearing results into most economical design. No moat wall construction is needed and the upper structure will only develop minor damage. Ductility detailing of the upper structure is not strictly required comparing to the case when moat wall is used. For the isolator design, additional displacement and force capacity beyond MCE_R demand are needed, but the additional capacities are much smaller comparing to using isolator without any displacement restraint mechanism. This is a lower cost solution compared to moat walls or an unrestraint isolation system.

Table 8. Required design capacity factor for bearing and ductility demand for upper structure

Risk Category	Isolation systems considered	Target reliability	α_D	α_v	Upper Structure damage	Moat Wall	Initial Cost
Risk Category I&II	Bearing without disp. restraint	10%	1.65	1.55	negligible	N	Bearing Size: 1.65Dm
	Bearing with Moat Wall	10%	1.10	1.10	Severe	Y	Bearing Size: 1.1Dm Moat wall construction
	Stiffening bearing	***10%***	***1.50***	***2.0***	***Minor***	***N***	***Bearing Size: 1.0Dm+0.5Dm Stiffening***
Risk Category III	Bearing without disp. restraint	5%	2.10	1.85	negligible	N	Bearing Size: 2.10Dm
	Bearing with Moat Wall	5%	1.75	1.50	Severe	Y	Bearing Size: 1.75Dm Moat wall construction
	Stiffening bearing	***5%***	***1.60***	***3.0***	***Minor***	***N***	***Bearing Size: 1.0Dm+0.6Dm Stiffening***
Risk Category IV	Bearing without disp. restraint	2.5%	2.45	2.10	negligible	N	Bearing Size: 2.45Dm
	Bearing with Moat Wall	2.5%	2.25	1.90	Severe	Y	Bearing Size: 2.25Dm Moat wall construction
	Stiffening bearing	***2.5%***	***1.75***	***3.0***	***Minor***	***N***	***Bearing Size: 1.0Dm+0.75Dm Stiffening***

5 MEMBER CAPACITY FACTORS USING STIFFENING BEARING

Based on the evaluation of archetype seismically isolated structure and established statistical framework used in this study, the required member capacity factors for isolator using TPF considered in this study are summarized in Table 9 below. For different risk categories, the required capacity factors will be different. In additional, if TPF isolators with different manufactured shear strengths are used, the required displacement capacity factors will be different. For each risk category, different combinations of displacement and shear capacity factor of bearing are available and will result into the same target reliability.

Overall, for risk category I and II structure, bearing displacement capacity factor of 1.50 and shear capacity factor of 2.0 can result into a target reliability of 10% failure under MCE_R level shaking. For risk category III structure, bearing displacement capacity factor of 1.60 and shear capacity factor of 3.0 can result into a target reliability of 5% failure under MCE_R level shaking. For risk category III structure, bearing displacement capacity factor of 1.75 and shear capacity factor of 3.0 can result into a target reliability of 2.5% failure under MCE_R level shaking.

These recommended member capacity factors are derived considering a specific archetype upper structure and a specific stiffening isolator design. For a general design case using stiffening bearing, a specific evaluation is recommended to obtain most accurate and optimized member capacity factors for isolator.

Table 9a. Isolator Capacity Factor needed for Risk Category I&II structure (10% collapse under MCE_R earthquake shaking)

α_V	α_D	CMR	δ_C(%)	Ductility Demand
1.5	1.53	1.57	0.18	1.0
2.0	**1.47**	1.57	0.24	1.0
3.0	1.43	1.57	0.29	1.1
4.0	1.43	1.57	0.29	1.1

Table 9b. Isolator Capacity Factor needed for Risk Category III structure (5% collapse under MCE_R earthquake shaking)

α_V	α_D	CMR	δ_C(%)	Ductility Demand
1.5	1.88	1.80	0.20	1.0
2.0	1.75	1.80	0.28	1.1
3.0	**1.62**	1.80	0.40	1.6
4.0	1.60	1.80	0.43	1.7

Table 9c. Isolator Capacity Factor needed for Risk Category IV structure (2.5% collapse under MCE_R earthquake shaking)

α_V	α_D	CMR	δ_C(%)	Ductility Demand
1.5	2.17	2.00	0.23	1.0
2.0	2.00	2.00	0.30	1.2
3.0	**1.76**	2.00	0.45	1.8
4.0	1.71	2.00	0.58	2.3

6 SUMMARY AND DISCUSSION

6.1. SUMMARY OF KEY CONCLUSIONS

The study investigates the required isolator capacities beyond MCE demand specified in ASCE 7 to achieve target reliability for design of seismically isolated structure. Three isolation systems are discussed to provide enough capacities. Results are compared quantitively through numerical response history analysis. Main findings and conclusions are summarized below:

The results clearly demonstrate that for seismically isolated structures, providing isolator design capacity equal to the MCE_R demand from ASCE 7-16 Chapter 17 does not satisfy the minimum reliability targets. Furthermore, it is found that the capacities for isolator displacement and shear strength should increase with Risk Category, which depends on the use or occupancy of the structure.

This study investigated the ability of three different isolator system types for seismically isolated buildings to satisfy collapse prevention limit state, with satisfactory reliability, under risk-targeted maximum considered earthquake excitations.

If isolators without any added displacement restraint are used, to satisfy the reliability targets in ASCE 7-16, the displacement capacity of isolators needs to be increased by factors of 1.65, 2.10 and 2.45 for Risk Categories I & II, II and IV, respectively relative to the MCE_R demand (D_M). For these designs, the superstructures remain essentially elastic, have very limited and localized yielding, and sustain low story drifts and peak floor accelerations.

When a moat wall restraint is utilized, the reliability targets are satisfied by using a moat with seismic gap (and isolators with displacement capacities) equal to 1.10, 1.75 and 2.25 times the MCE_R demand (D_M) for risk category I & II, III and IV, respectively. While the isolator displacements can be reduced in these cases, damage in the superstructure is severe for motions where moat impact occurs.

The last case considered uses a special hardening TFP where the internal displacement restraining rims and sliders are modified to provide a stronger stopping mechanism and larger displacement capacity after the primary sliding capacity is reached. For the case considered herein, the stopping mechanism is initiated at the MCE_R displacement (D_M). If the rim strength for TFP is 3 times the value of MCE_R demand (V_M), the isolator displacement capacity needs to

be 1.45, 1.60 and 1.75 times V_M for RC I & II, III, and IV occupancies. In this case the damage to the superstructure was found to be far more moderate than in the case where displacement restraint is provided by the moat wall when a beyond MCE_R event occurs.

It appears that to achieve targeted reliability, the use of the hardening TFP results in lower construction costs than the other two options, since the reduced isolator displacement capacity (12%, 30%, 40% for RC I&II, III and IV) would result in a more economical isolator, and construction will be cheaper than the incremental cost of constructing a properly detailed moat wall capable of developing the forces needed to restrain displacements. In addition, much more moderate damage and yielding will be expected in upper structure comparing to use of moat. However, future cost studies are recommended.

. In order to achieve the targeted reliability for a seismically isolated structure, besides providing required isolator capacity factors in design as discussed in this report, other requirements should also be addressed, which are beyond the topic of this study. These include: isolator prototype tests to determine the minimum member capacities; isolator qualification tests for long term reliability of properties and capacities; manufacturer qualifications and responsibilities; and analysis of the isolated structure to correctly represent the isolator properties as determined by the specified component tests. All of which are important to achieve the ASCE specified target reliabilities for isolated structures.

6.2. FURTHER DISCUSSION

6.2.1. The reference value for member capacity factor

The number shown in above result tables are member capacity factor needed to achieve certain probability of collapse under MCE_R level seismic shaking. The member capacity factors for isolators are the ratio between required capacity and the minimum code requirement (Average MCE_R demand). In this study, the minimum code demand used to normalize our calculated bearing capacity factor are calculated from dynamic response history analysis. However, if other method like equivalent lateral force method is used to obtain the demand from ASCE 7, the results will be different. Since using equivalent lateral force method will give us slightly larger estimation of isolator displacement demand than using dynamic approach. Which means the required member capacity factor calculated in the study might be smaller when the minimum code requirement is obtained using equivalent lateral force method.

In summary, the specific value of member capacity factors for isolator depends on how the average MCE_R displacement is obtained at the first place. If the recommended value in this study is used, the minimum code demand should be obtained using dynamic response history approach.

6.2.2. Assumption on record to record uncertainty

The collapse fragility standard deviation or total collapse uncertainty β_{TOT} determines the shape of failure fragility curve which affects member capacity factor needed. The uncertainty is contributed from different sources. In FEMA P695 framework, four different uncertainties are accounted for the calculation of collapse fragility. The structural model, design as well as test data uncertainty are determined by judgement. Several quality levels are listed with corresponding recommended uncertainty values in FEMA P695. The selection of these quality depends on the judgement and will affect the final results. The most important part of this uncertainty is coming from ground motion uncertainty also called record to record uncertainty. Which describes the dispersion of responses under a set of ground motions scaled to the same level shaking. This part of dispersion depends on the individual ground motion record used in response history analysis as well as specific bearing design. The most accurate way to estimate this source of uncertainty should be performing incremental dynamic analysis.

In this study, we do not use incremental dynamic analysis to calculate the record to record uncertainty. Instead we estimate this source of uncertainty using recommended relation in FEMA P695 based on system period-based ductility.

6.2.3. Different stiffening starting displacement (Dh)

In this study, the stiffening isolator used has a specific design when stiffening starts at MCE displacement demand D_M. However, for most types of isolator bearing which demonstrates a stiffening behavior when displacement is large, the stiffening can start at different displacement points. Based on specific manufacture, the design of stiffening portion will be different. If different D_h is used, the resulted member capacity factor might be different as shown in Figure 10. If stiffening starts at a later displacement point, larger displacement capacity factor of bearing will be needed to achieve the same target reliability in design.

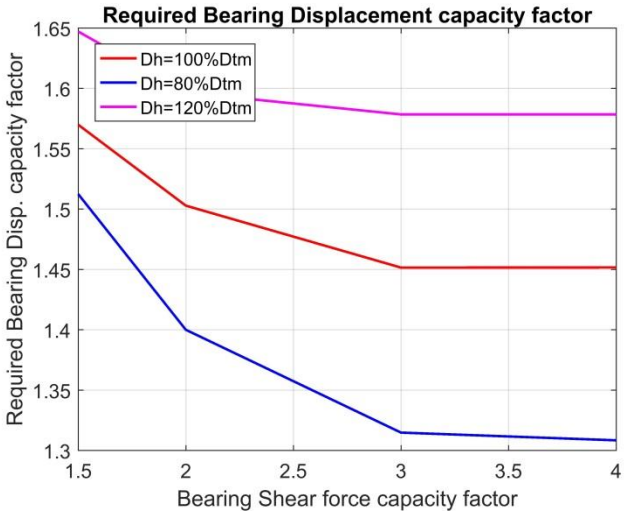

Figure 10. Required bearing displacement capacity in terms of bearing shear capacity selected under different stiffening starting displacements. The results are for 10% probability of collapse under MCE level event.

Therefore, it is important to use the correct member capacity factor based on specific design of stiffening portion of isolator. The member capacity factor established in this study assumes a stiffening starts at 100% D_M.

REFERNECES

Aiken, I.D., Nims, D.K., Whittaker A.S. et al., 1993. Testing of Passive Energy Dissipation Systems, *Earthquake Spectra* **9**,335-370.

American Institute of Steel Construction (AISC), 2016. Seismic Provisions for Structural Steel Buildings, *ANSI/AISC 341-16*, AISC, Chicago, Illinois.

American Institute of Steel Construction (AISC), 2016. Prequalified Connections for Special and Intermediate Steel Moment Frames for Seismic Applications, *ANSI/AISC 358-16*, AISC, Chicago, Illinois.

American Society of Civil Engineers (ASCE), 2017. *Minimum Design Loads for Buildings and Other structures. ASCE Standard ASCE/SEI 7-16*, American Society of Civil Engineer, Reston, US.

Clark, P.W., Aiken, I. D., and Kelly, M.J., 1997, *Experimental studies of the ultimate behavior of seismically isolated structures, Report No. UCB/EERC-97/18,* Earthquake Engineering Research Center, University of California, Berkeley, CA.

Constantinou M., Mokha, A., and Reinhorn, A., 1990. Teflon Bearings in Base Isolation. II: Modeling, *Journal of Structural Engineering* **116**, 455–474.

Federal Emergency Management Agency (FEMA), 2006. *Next-Generation Performance-Based Seismic Design Guidelines, Tech. Rep. FEMA-445*, Washington, D.C.

Federal Emergency Management Agency (FEMA), 2009. *Quantification of Building Seismic Performance Factors, Tech. Rep. FEMA-P695*, Washington, D.C.

Fenz, D., Constantinou M., 2008a. Spherical sliding isolation bearings with adaptive behavior: Theory. *Earthquake Engineering and Structural Dynamics* **37,** 163-283.

Fenz, D., Constantinou M., 2008b. Spherical sliding isolation bearings with adaptive behavior: Experimental verification. *Earthquake Engineering and Structural Dynamics* **37**, 185-205.

Filippou F.C., Popov, E.P., and Bertero, V.V., 1983. Effects of Bond Deterioration on Hysteretic Behavior of Reinforced Concrete Joints, *Report EERC 83-19*, Earthquake Engineering Research Center, University of California, Berkeley.

Haselton, C.B., and Deierlein, G., 2007. *Assessing seismic collapse safety of modern reinforced concrete moment frame buildings*. Pacific Earthquake Engineering Research Center Technical Report 2007/08, Berkeley, CA.

Haselton, B.C., Baker, J., Liel, A., and Deierlein, G., 2011. Accounting for Ground-Motion Spectral Shape Characteristics in Structural Collapse Assessment through an Adjustment for Epsilon, *Journal of Structural Engineering* 137, 332-344.

Iiba, M., Hanai, T., Midorikawa, M., Azuhata, T. and Inoue, N. Safety evaluation of seismically isolated houses with displacement restraint devices under severe earthquake motions, in *Proceedings, 14th World Conference on Earthquake Engineering*, 12-17 October, 2008, Beijing, China.

Kelly, M.J., 1990. Base Isolation: Linear Theory and Design, *Earthquake Spectra* **6**, 223-244.

Kelly, M. J., 1997. *Earthquake-Resistant Design with Rubber*, Springer, London, UK.

Kikuchi, M. and Aiken, I.D., 1997, An Analytical hysteresis model for elastomeric seismic isolation bearings. *Earthquake Engineering and Structural Dynamics* **26,** 215-231.

Lakhani, M., Soni, D., 2017. Comparative Study of Smart Base-Isolation Using Fuzzy Control and Neural Network, *Procedia Engineering* **173**, 1825-1832.

Masroor, A., and Mosqueda, G., 2012. Experimental simulation of base-isolated buildings pounding against moat wall and effects on super structure response, *Earthquake Engineering and Structural Dynamics* **41,** 2093-2109.

Masroor, A., and Mosqueda, G., 2013. Impact model for simulation of base isolated buildings impacting flexible moat walls, *Earthquake Engineering and Structural Dynamics* **42,** 357-376.

Masroor, A., and Mosqueda, G., 2013. *Seismic Response of Base Isolated Buildings Considering Pounding to Moat Walls*, Technical Report MCEER-13-0003.

Masroor, A., and Mosqueda, G., 2015. Assessing the Collapse Probability of Base-Isolated Buildings Considering Pounding to Moat Walls Using the FEMA P695 Methodology, *Earthquake Spectra* **31**, 2069-2086.

Mckenna, F., Fenves, G.L., 2000. *Open system for earthquake engineering simulation*. University of California, Berkeley, CA.

Moehle, J., and Deierlein, G., 2004. A framework methodology for performance-based earthquake engineering, in *Proceedings, 13rd World Conference on Earthquake Engineering*, 1–6 August, 2004, Vancouver, Canada.

Mokha, A., Constantinou M., and Reinhorn, A., 1990. Teflon Bearings in Base Isolation. I: Testing, *Journal of Structural Engineering* **116**, 438–454.

Morgan, A., and Mahin, S., 2010. Achieving reliable seismic performance enhancement using multi-stage friction pendulum isolators, *Earthquake Engineering and Structural Dynamics* **39**, 1443-1461

Naeim, F., Kelly, M.J., 1999. *Design of seismic Isolated structures*, John Wiley, New York, US

Neuenhofer, A., Filippou, C.F., 1997 Evaluation of Nonlinear Frame Finite Element Models. Journal of Structural Engineering, *American Society of Civil Engineers*, **123**, 958-966.

Shao, B., and Mahin, S., 2016. *Design of Safe Base Isolated Structures Using Hardening of Bearing* in *Proceedings, 85th SEAOC convention*, 12–15 October, 2016, Maui, Hawaii, US.

Sabelli, R., Roeder, C.W., Hajjar, J.F., 2013. Seismic Design of Steel Special Concentrically Braced Frame Systems, *NEHRP Seismic Design Technical Brief No.8*, National Institute of Standards and Technology.

Shafei, B., Zareian, F., and Lignos, D. G., 2011. A simplified method for collapse capacity assessment of moment-resisting frame and shear wall structural systems, *Engineering Structures* **33**, 1107–1116.

Shao, B., and Mahin, S., 2017. *Understanding and Design of seismically isolated structure using hardening of bearing*, in *Proceedings, 16th World Conference on Earthquake Engineering*, 9–13 January, 2017, Santiago, Chile.

Simpson, B. and Mahin, S. 2015. An Introductory Guide for Modeling a "Basic" Braced Frames in OpenSees, Berkeley, CA, 2015.

Tajirian, F.F., Kelly, M.J., and Aiken, I.D., 1990.Seismic Isolation for Advanced Nuclear Power Stations, *Earthquake Spectra* **6**, 223-244.

Uriz, P., Mahin, S., 2008. *Toward earthquake-resistant design of concentrically braced steel-frame structures*, University of California, Berkeley, USA.

Vamvatsikos, D., and Cornell, C. A., 2002. Incremental dynamic analysis, *Earthquake Engineering & Structural Dynamics* **31**, 491–514.

Yang, T.Y., Konstantinidis, D., and Kelly, M.J., 2010. The influence of isolator hysteresis on equipment performance in seismic isolated buildings, *Earthquake Spectra* 2**6**, 275-293.

Zareian, F., and Krawinkler, H., 2007. Assessment of probability of collapse and design for collapse safety, *Earthquake Engineering & Structural Dynamics* **36**, 1901–1914.

Zargar, H., Ryan, K.L. and Marshall, J.D., 2013. Feasibility study of a gap damper to control seismic isolator displacements in extreme earthquakes, Structural control and health monitoring 20, 1159-1175.

Zayas, V., Low, S., and Mahin, S., 1987. The FPS Earthquake Resisting System, Experimental Report. Report No. UCB/EERC-8701, June 1987.

Zayas, V., Low, S., Bozzo, L., and Mahin, S. 1989. Feasibility and Performance Studies on Improving

the Earthquake Resistance of New and Existing Buildings Using the Friction Pendulum System. Report No. UCB/EERC-89/09, September 1989.

Zayas, V., Low, S., and Mahin, S., 1990. A Simple Pendulum Technique for Achieving Seismic Isolation, *Earthquake Spectra* **6**, 317–333.

Zayas, V. and Mahin, S., 2010. Seismic Design Methodology to Avoid Damage to Structures, Non-Structural Components and Contents, 13th US-Japan Workshop, Applied Technology, Council, 2010.

Zayas, V., 2013. Seismic Isolation Design Criteria for Continued Functionality, in *Proceedings, 82nd SEAOC convention*, 18–21 September, 2013, San Diego, CA, US.

Zayas, V., 2017. *Saving Lives Building Hospitals That Function After Earthquakes, Article.* Earthquake Protection Systems, Vallejo California.

Zhou, X., Han, M., and Yang, L., 2003. Study on protection measures for seismic isolation rubber bearings, *ISET Journal of Earthquake Technology* **40**, 137-160.

APPENDIX A

Selected results of response history analysis under individual ground motion input will be shown in the appendix. (The figures are not numbered in this appendix).

STIFFENING BEARINGS WITH DIFFERENT SHEAR FORCE CAPACITIES.

The results of stiffening bearing hysteresis for individual ground motion under different shear force capacity factors are shown in this section. Stiffening starts at a displacement corresponds to minimum code requirement. For comparison, cases with moat wall starts at 100% D_M and bearing without displacement restraint are shown together in the plot.

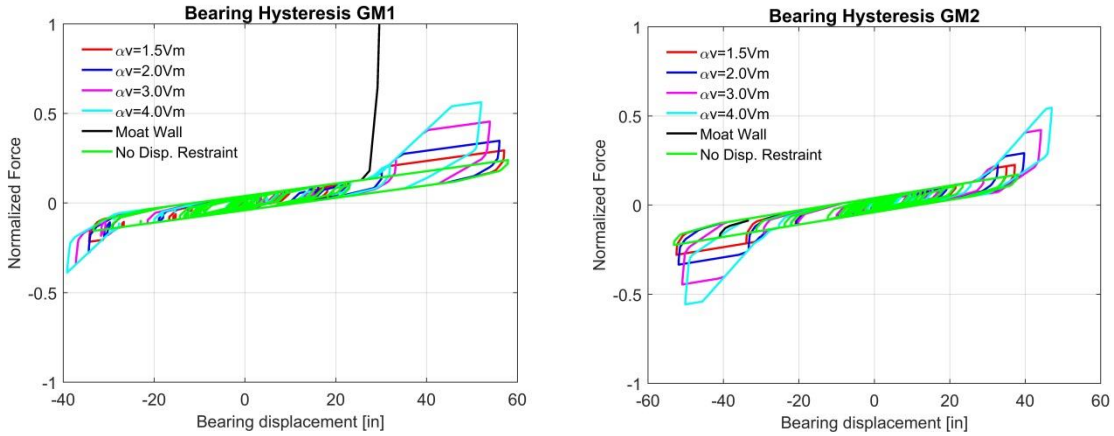

Figure. Bearing hysteresis responses comparison among stiffening bearing with different shear force capacities. (a) GM1 (b) GM2

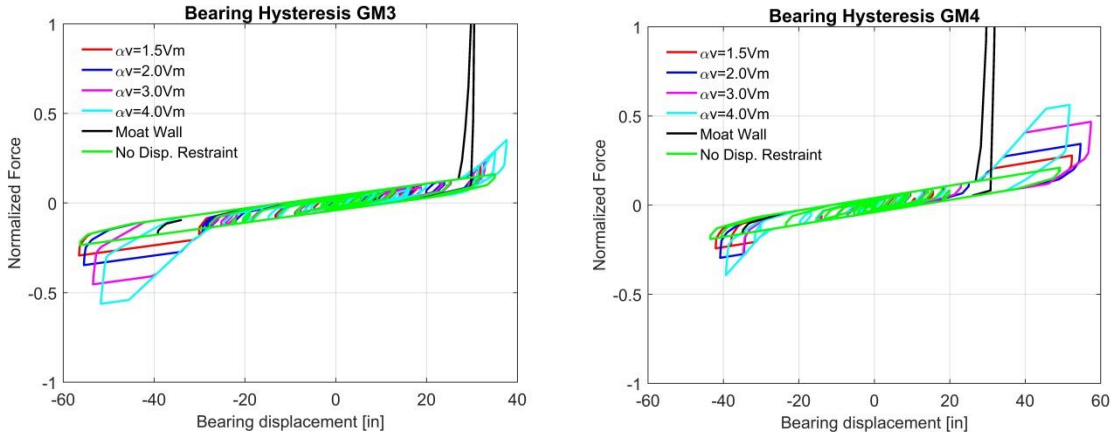

Figure. Bearing hysteresis responses comparison among stiffening bearing with different shear force capacities. (a) GM3 (b) GM4

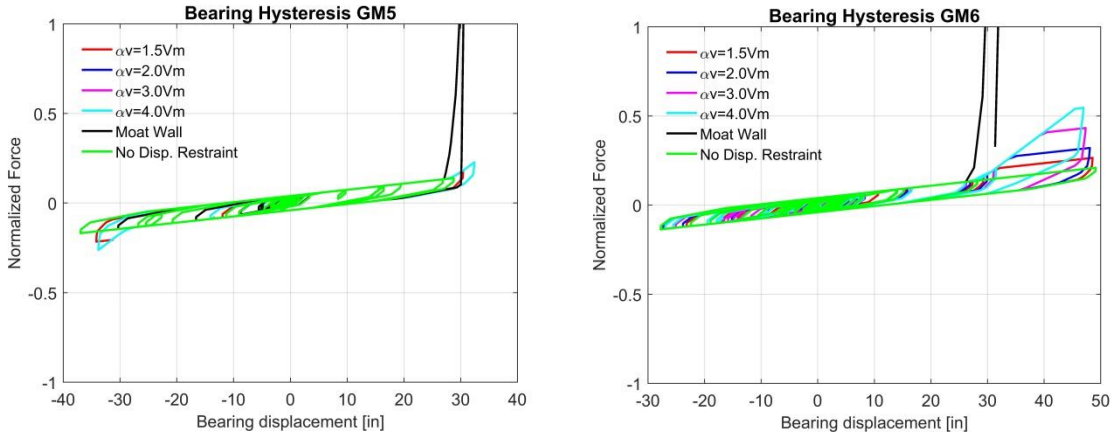

Figure. Bearing hysteresis responses comparison among stiffening bearing with different shear force capacities. (a) GM5 (b) GM6

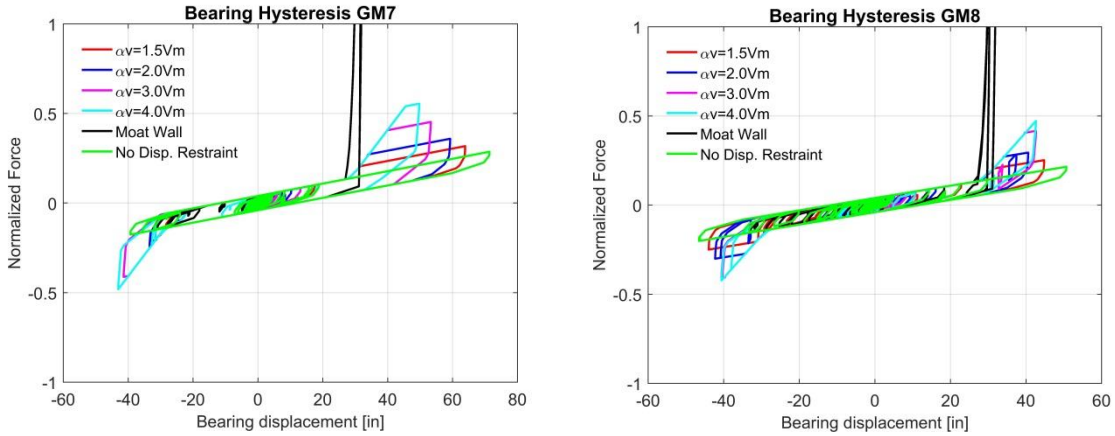

Figure. Bearing hysteresis responses comparison among stiffening bearing with different shear force capacities. (a) GM7 (b) GM8

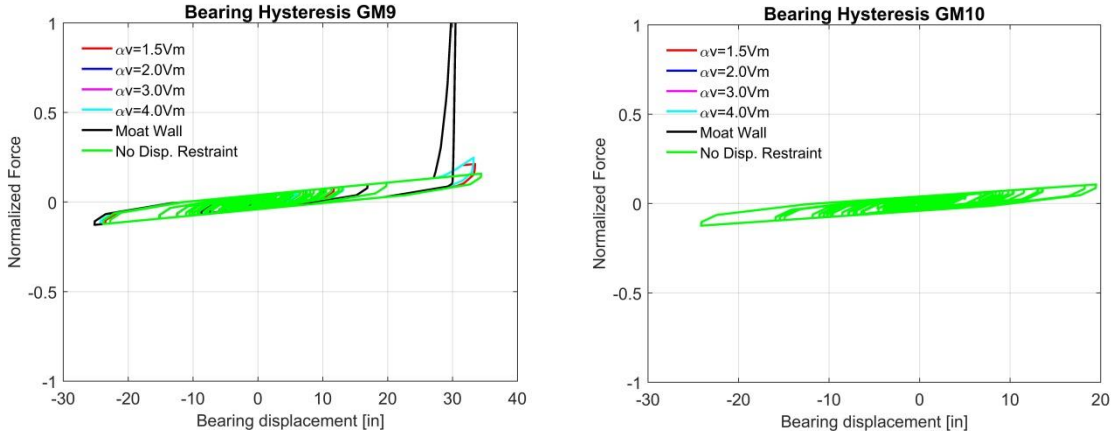

Figure. Bearing hysteresis responses comparison among stiffening bearing with different shear force capacities. (a) GM9 (b) GM10

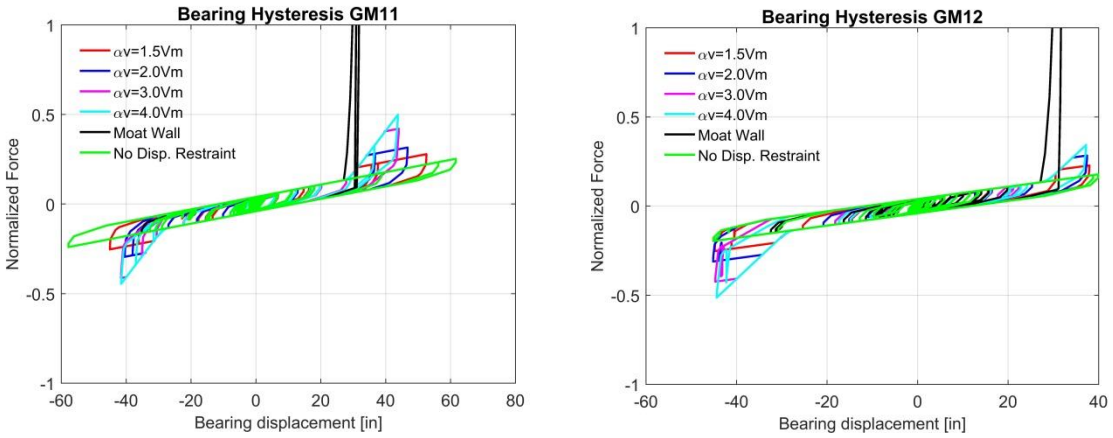

Figure. Bearing hysteresis responses comparison among stiffening bearing with different shear force capacities. (a) GM11 (b) GM12

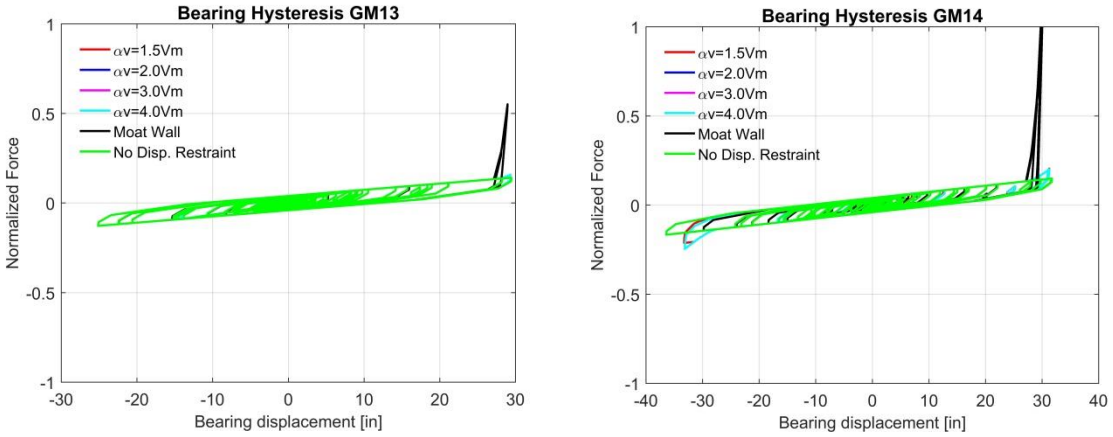

Figure. Bearing hysteresis responses comparison among stiffening bearing with different shear force capacities. (a) GM13 (b) GM14

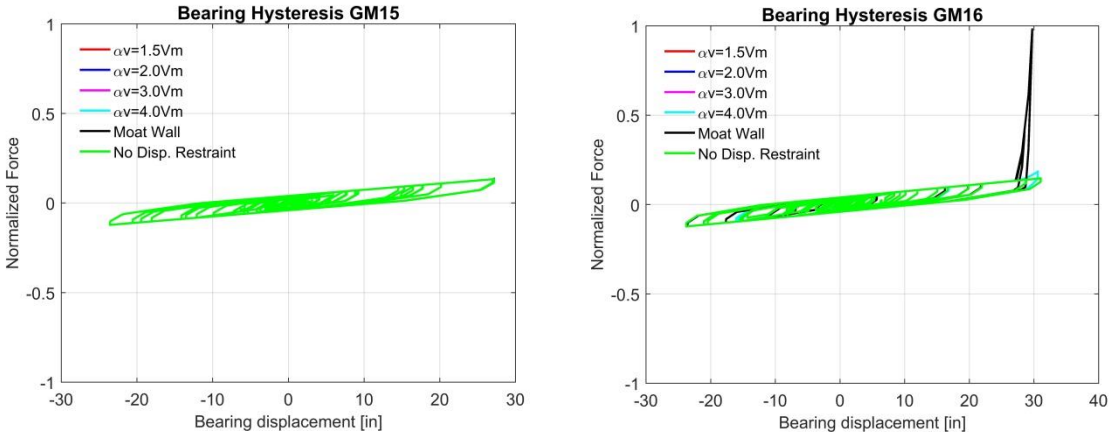

Figure. Bearing hysteresis responses comparison among stiffening bearing with different shear force capacities. (a) GM15 (b) GM16

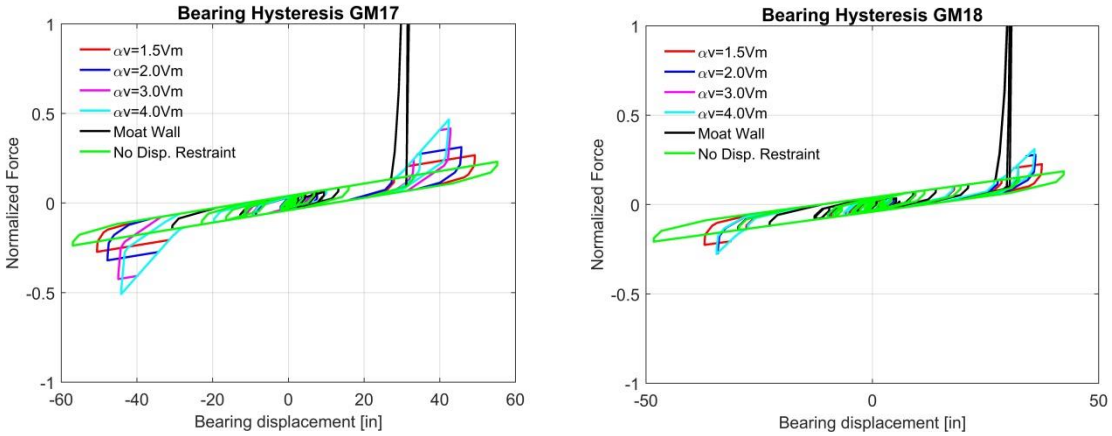

Figure. Bearing hysteresis responses comparison among stiffening bearing with different shear force capacities. (a) GM17 (b) GM18

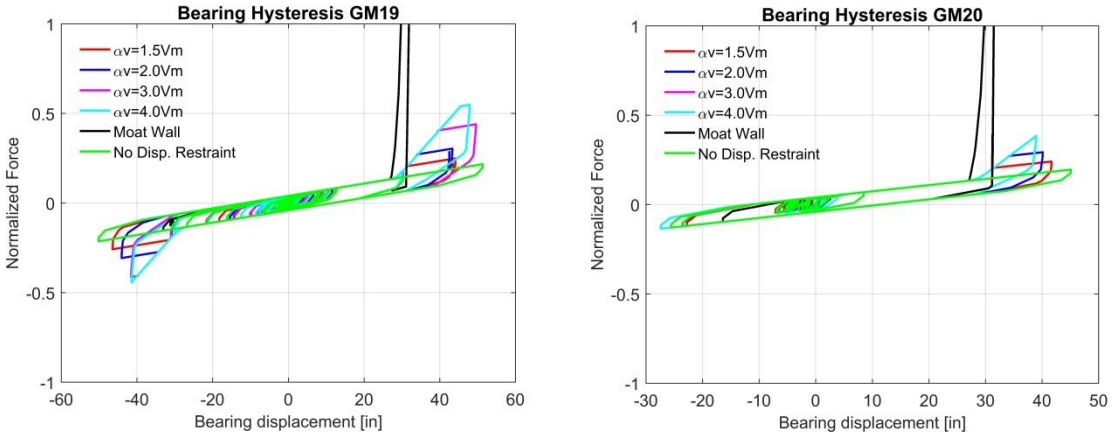

Figure. Bearing hysteresis responses comparison among stiffening bearing with different shear force capacities. (a) GM19 (b) GM20

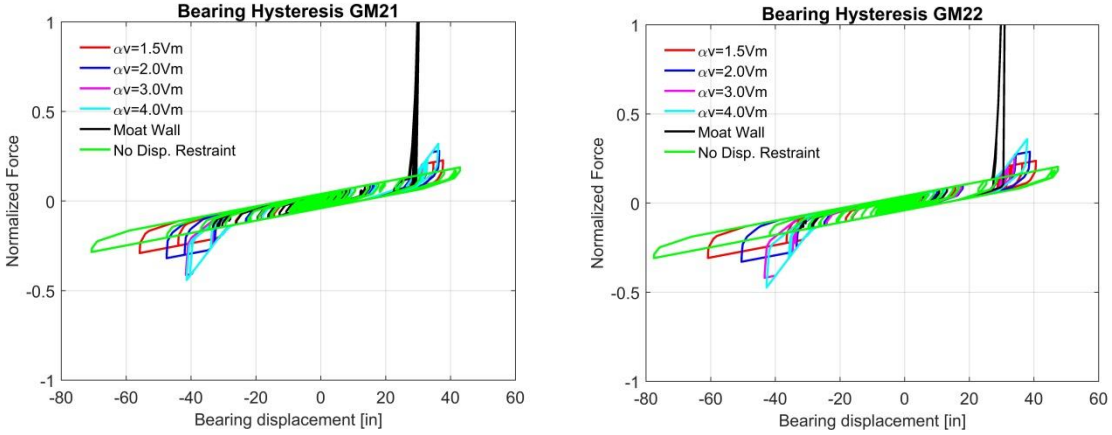

Figure. Bearing hysteresis responses comparison among stiffening bearing with different shear force capacities. (a) GM21 (b) GM22

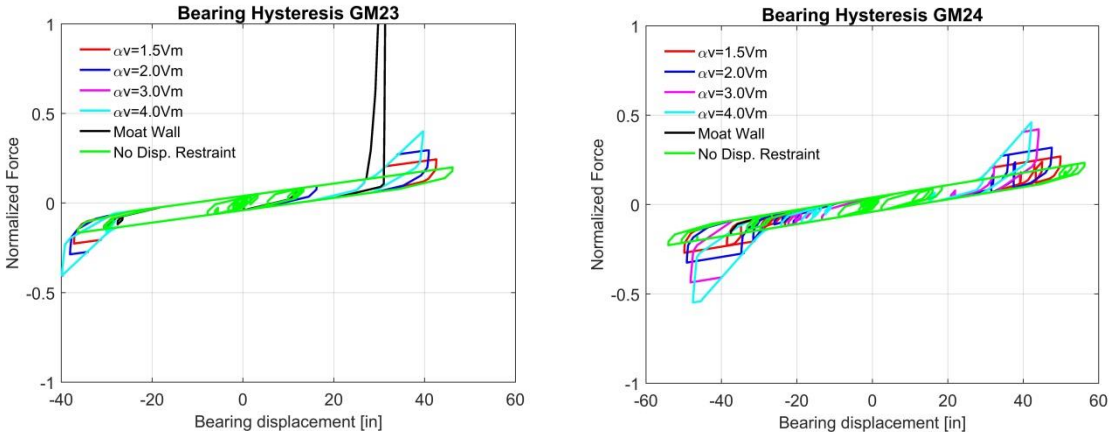

Figure. Bearing hysteresis responses comparison among stiffening bearing with different shear force capacities. (a) GM23 (b) GM24

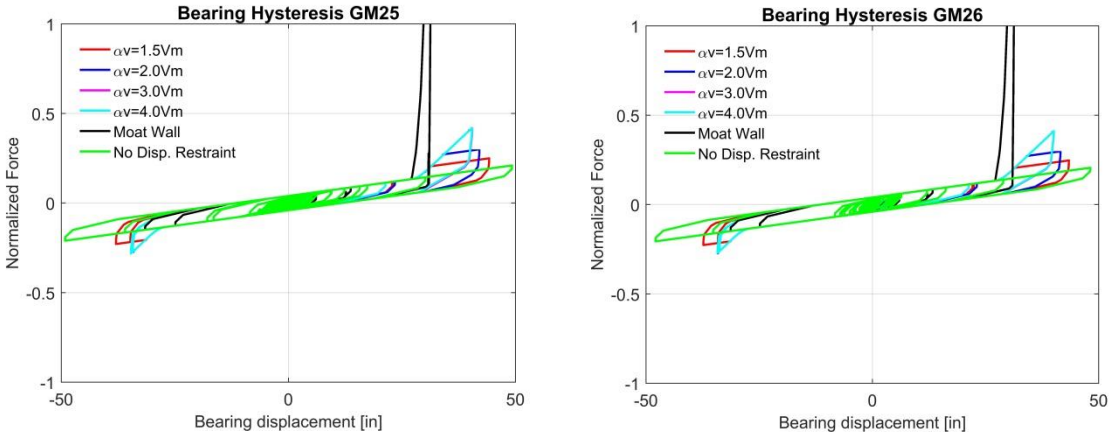

Figure. Bearing hysteresis responses comparison among stiffening bearing with different shear force capacities. (a) GM25 (b) GM26

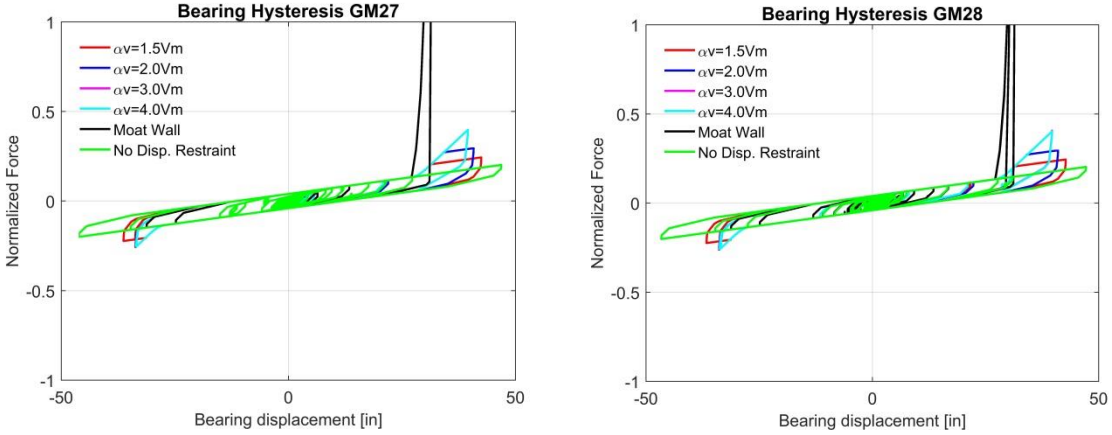

Figure. Bearing hysteresis responses comparison among stiffening bearing with different shear force capacities. (a) GM27 (b) GM28

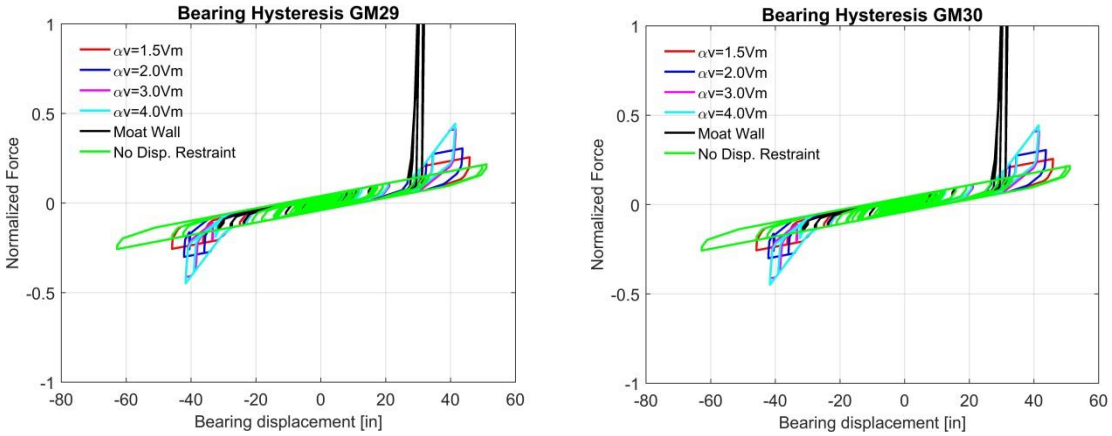

Figure. Bearing hysteresis responses comparison among stiffening bearing with different shear force capacities. (a) GM29 (b) GM30

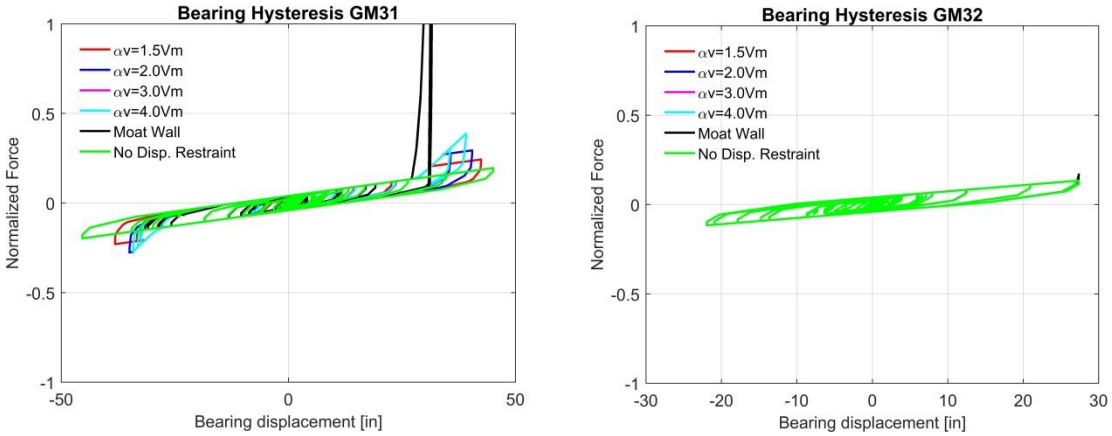

Figure. Bearing hysteresis responses comparison among stiffening bearing with different shear force capacities. (a) GM31 (b) GM32

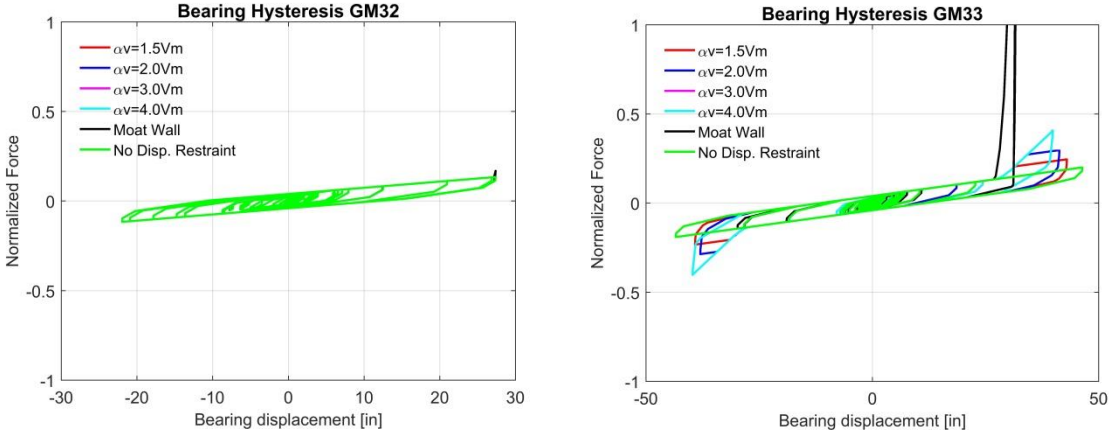

Figure. Bearing hysteresis responses comparison among stiffening bearing with different shear force capacities. (a) GM33 (b) GM34

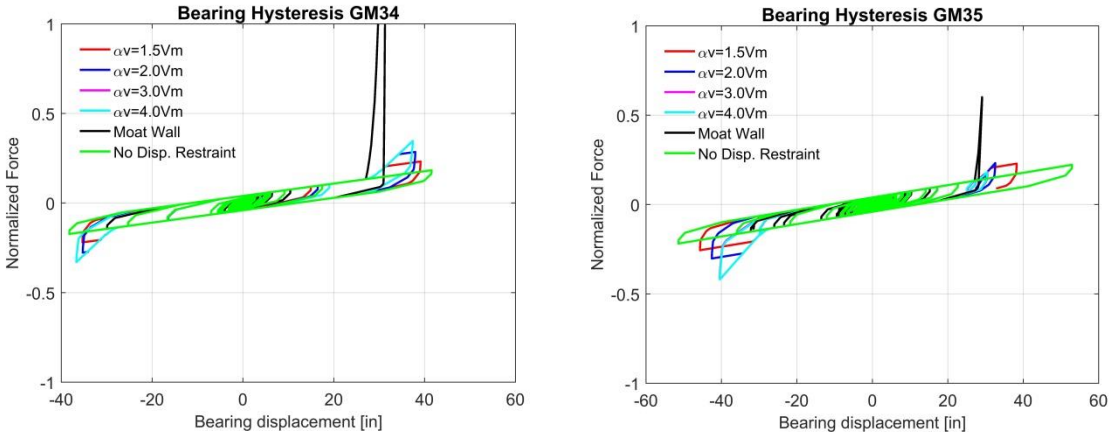

Figure. Bearing hysteresis responses comparison among stiffening bearing with different shear force capacities. (a) GM35 (b) GM36

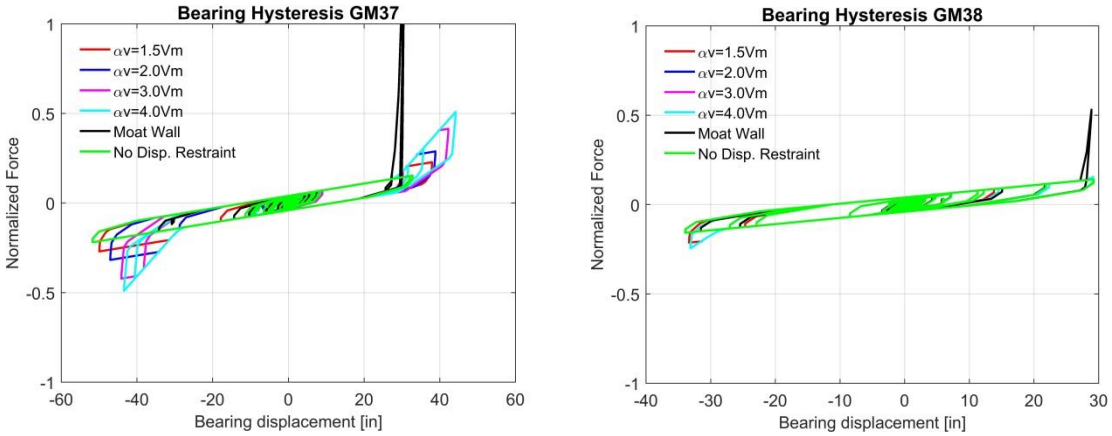

Figure. Bearing hysteresis responses comparison among stiffening bearing with different shear force capacities. (a) GM37 (b) GM38

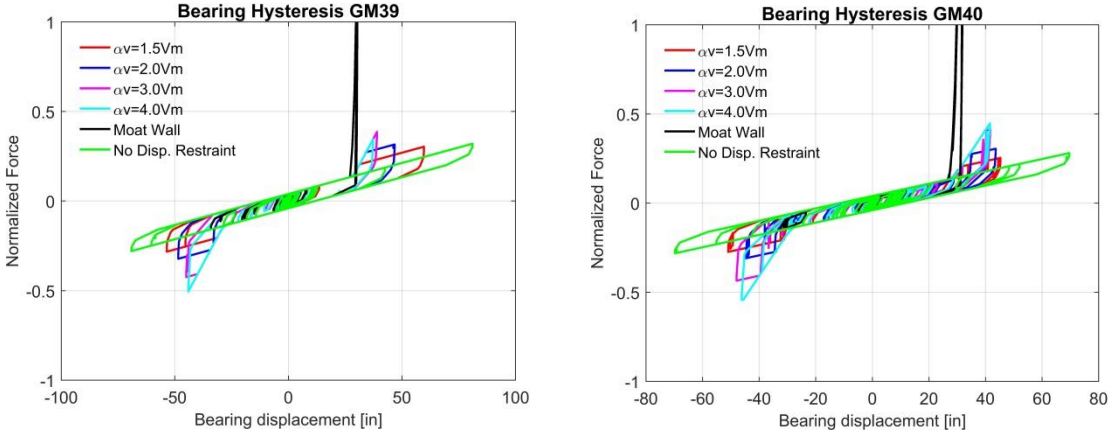

Figure. Bearing hysteresis responses comparison among stiffening bearing with different shear force capacities. (a) GM39 (b) GM40

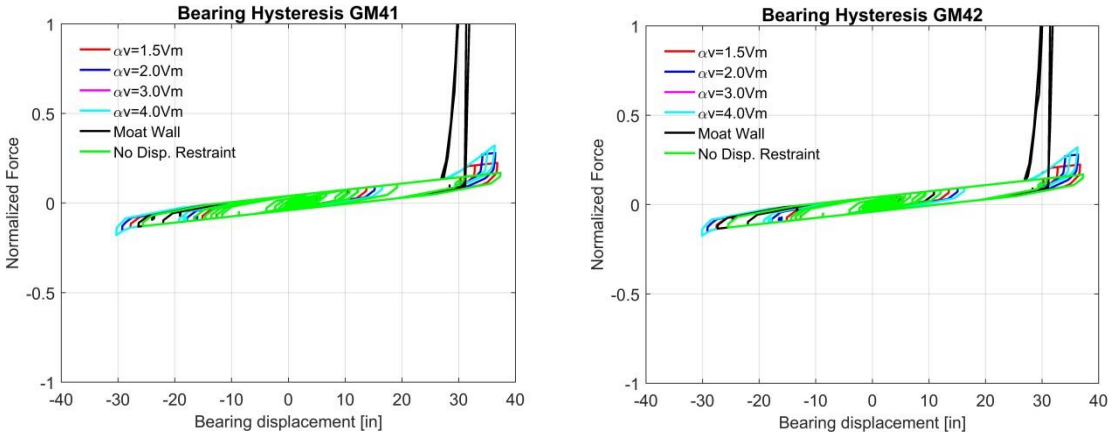

Figure. Bearing hysteresis responses comparison among stiffening bearing with different shear force capacities. (a) GM41 (b) GM42

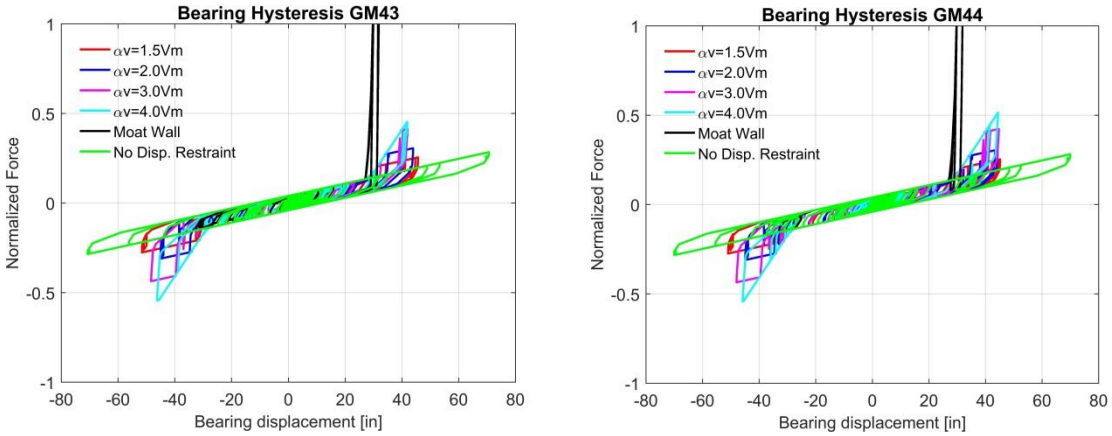

Figure. Bearing hysteresis responses comparison among stiffening bearing with different shear force capacities. (a) GM43 (b) GM44

MOAT WALL SOLUTION WITH DIFFERENT SEISMIC GAP SIZES.

In this section, the isolator hysteresis as well as impact force for the case when moat wall is used are shown. The hysteresis shown in the following figure is the combination of isolator hysteresis and the impact force. Note the impact force does not occur on the isolator but on the moat wall. Cases with different seismic gap sizes are shown together.

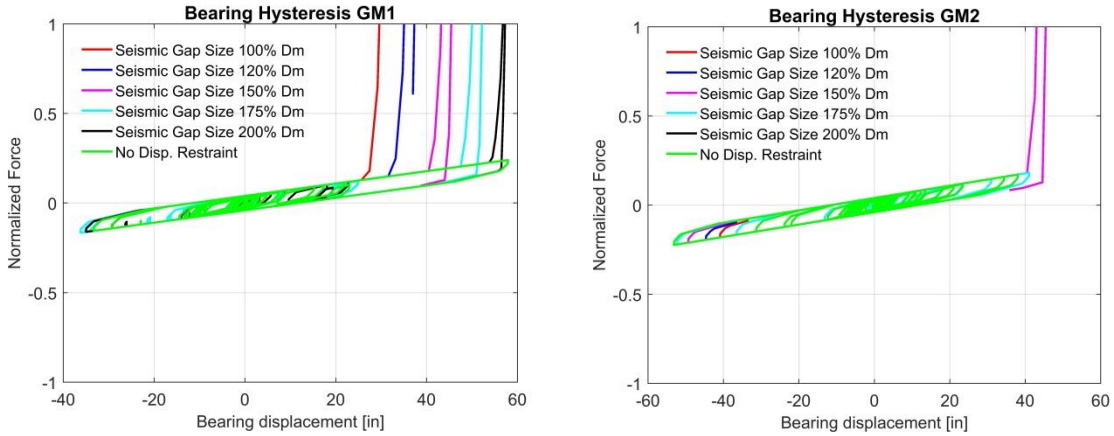

Figure. Bearing hysteresis and impact responses for use of moat wall with different seismic gap sizes. (a) GM1 (b) GM2

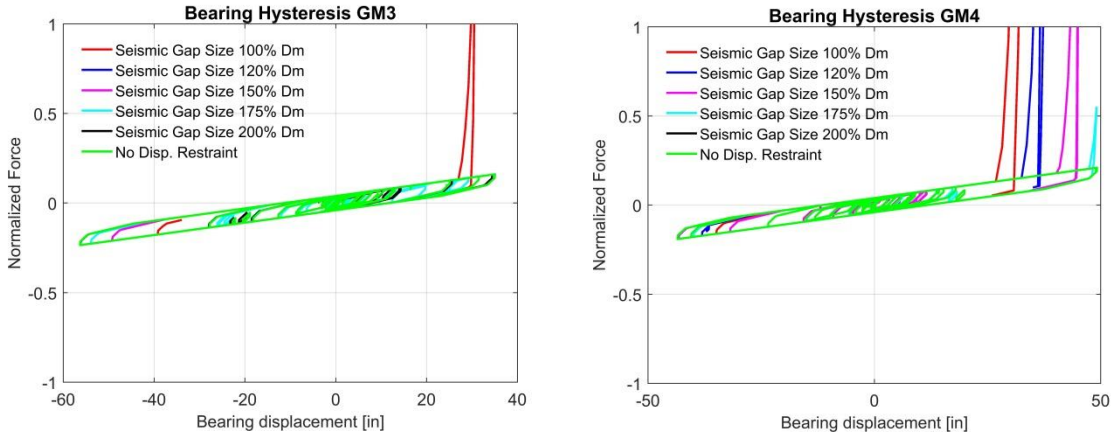

Figure. Bearing hysteresis and impact responses for use of moat wall with different seismic gap sizes. (a) GM3 (b) GM4

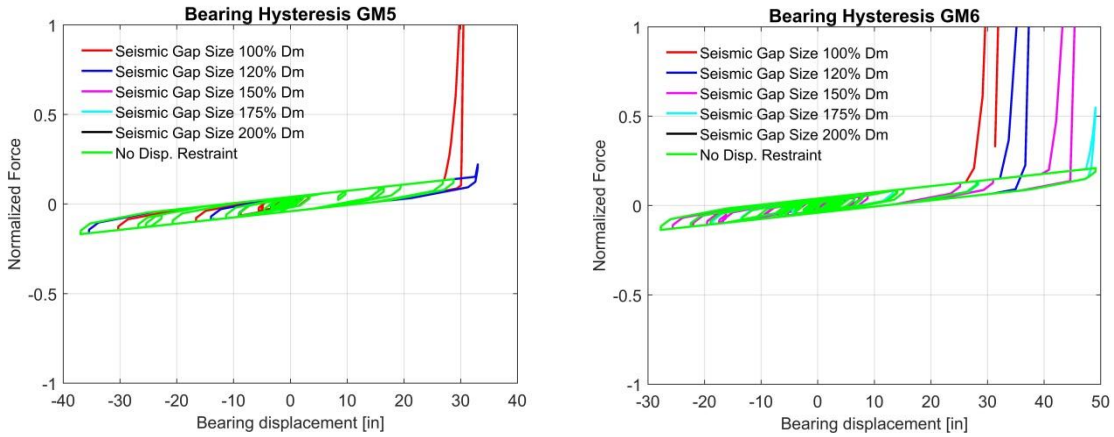

Figure Bearing hysteresis and impact responses for use of moat wall with different seismic gap sizes. (a) GM5 (b) GM6

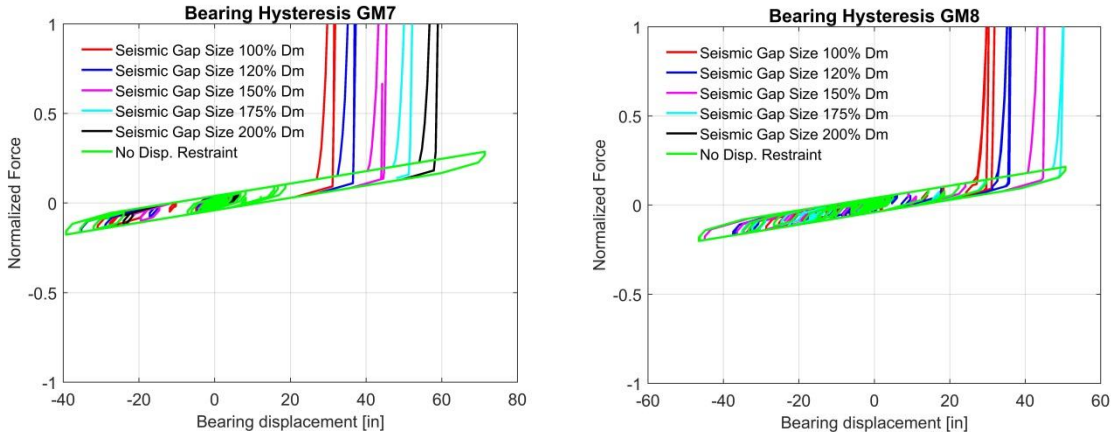

Figure. Bearing hysteresis and impact responses for use of moat wall with different seismic gap sizes. (a) GM7 (b) GM8

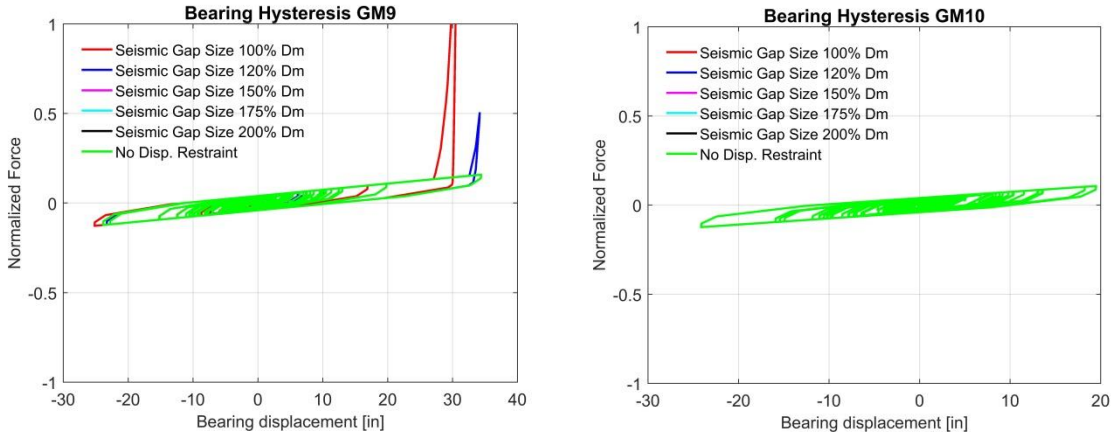

Figure. Bearing hysteresis and impact responses for use of moat wall with different seismic gap sizes. (a) GM9 (b) GM10

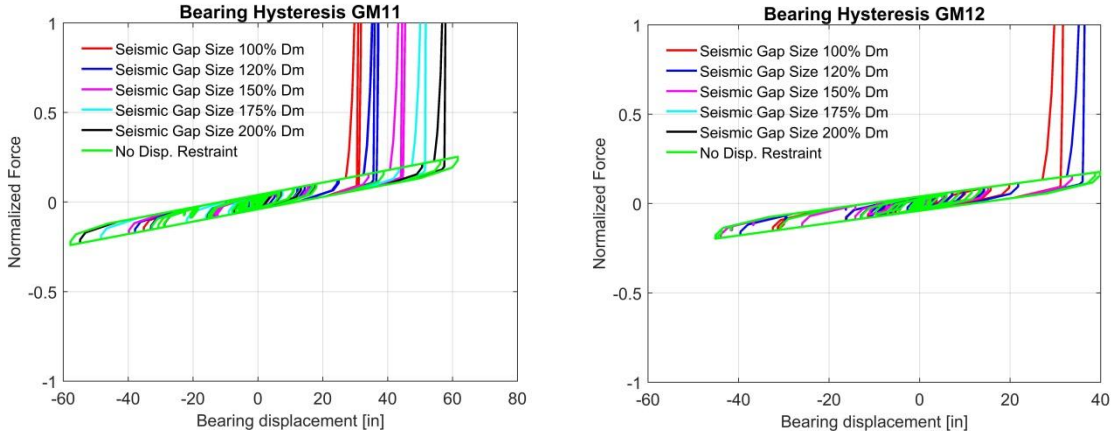

Figure. Bearing hysteresis and impact responses for use of moat wall with different seismic gap sizes. (a) GM11 (b) GM12

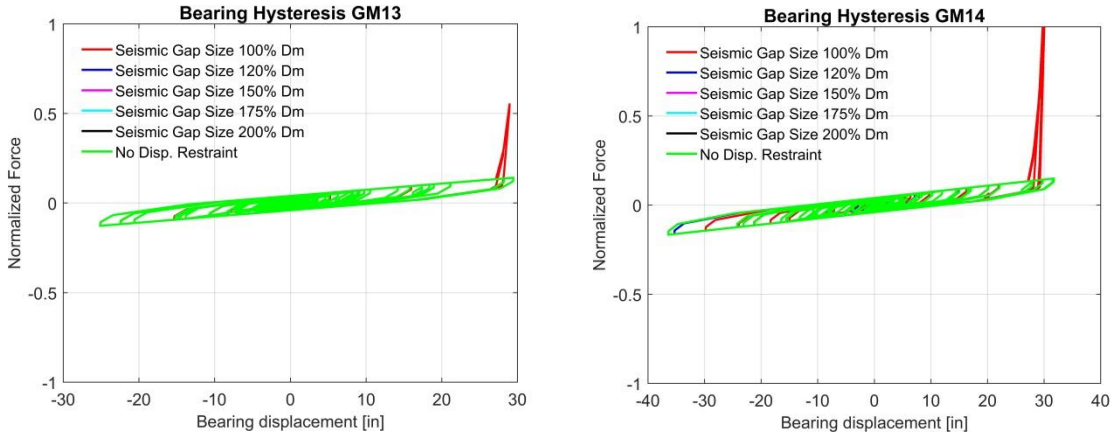

Figure. Bearing hysteresis and impact responses for use of moat wall with different seismic gap sizes. (a) GM13 (b) GM14

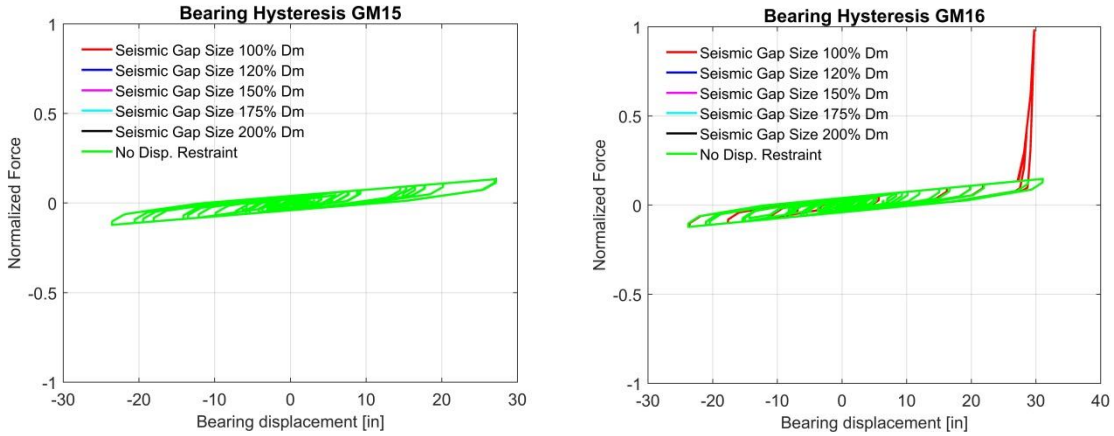

Figure. Bearing hysteresis and impact responses for use of moat wall with different seismic gap sizes. (a) GM15 (b) GM16

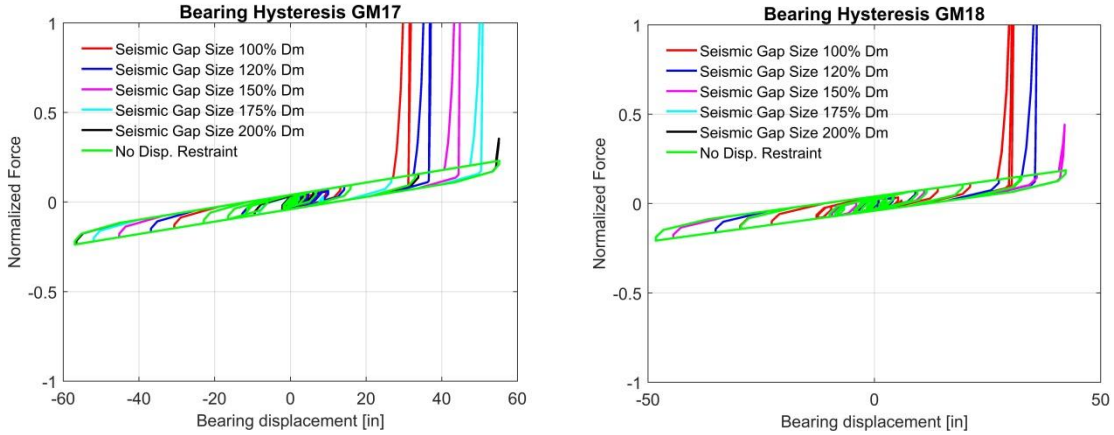

Figure. Bearing hysteresis and impact responses for use of moat wall with different seismic gap sizes. (a) GM17 (b) GM18

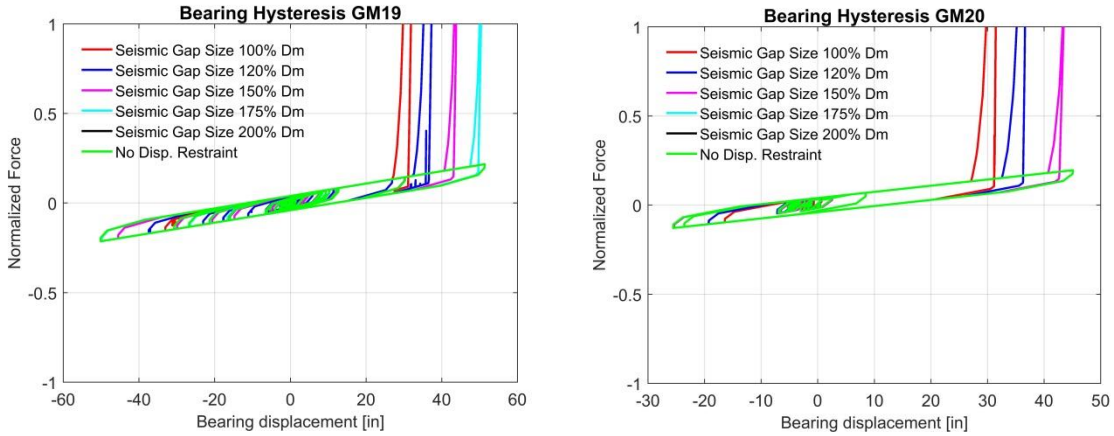

Figure. Bearing hysteresis and impact responses for use of moat wall with different seismic gap sizes. (a) GM19 (b) GM20

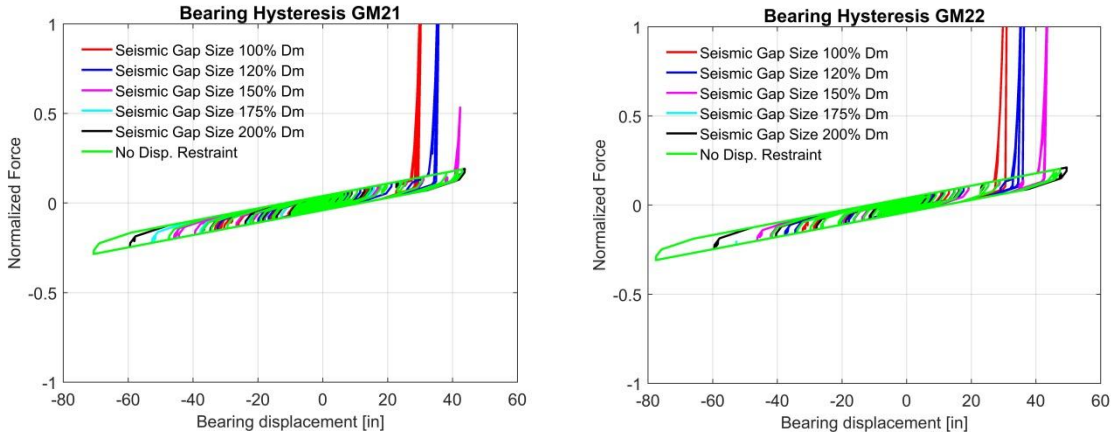

Figure. Bearing hysteresis and impact responses for use of moat wall with different seismic gap sizes. (a) GM21 (b) GM22

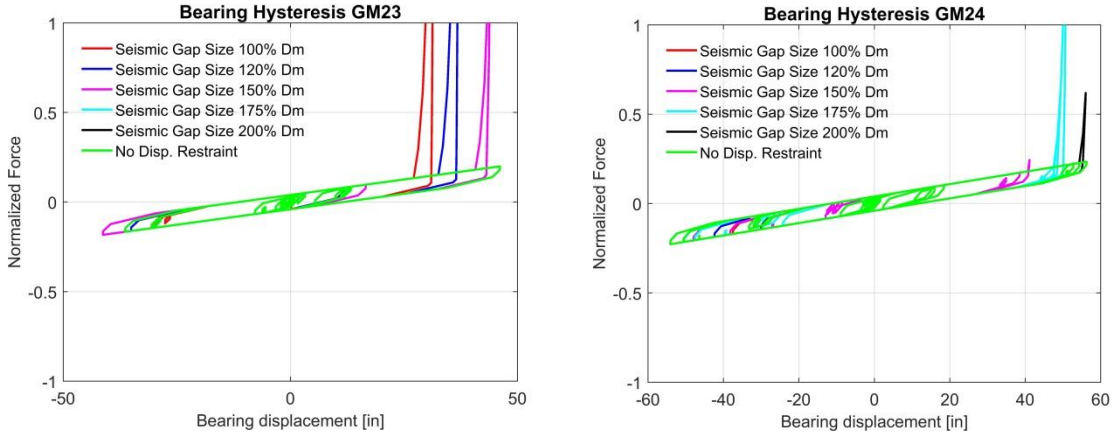

Figure. Bearing hysteresis and impact responses for use of moat wall with different seismic gap sizes. (a) GM23 (b) GM24

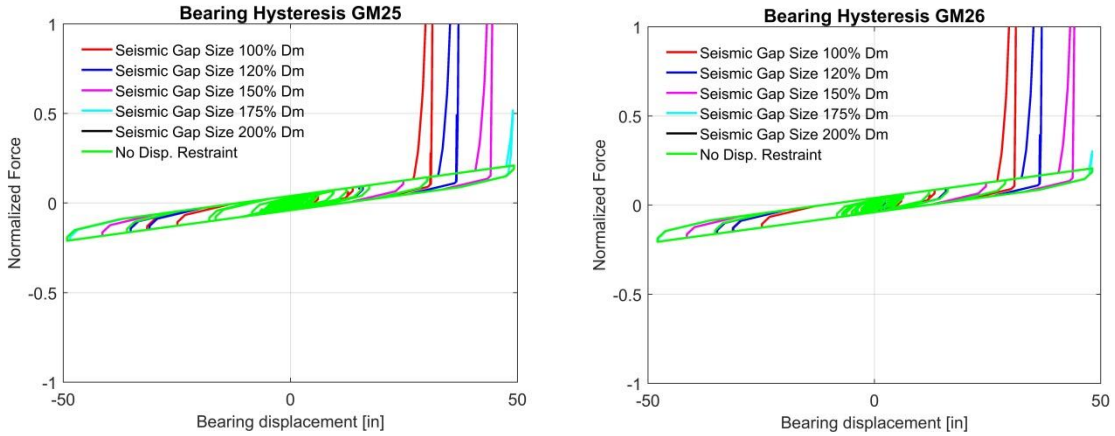

Figure. Bearing hysteresis and impact responses for use of moat wall with different seismic gap sizes. (a) GM25 (b) GM26

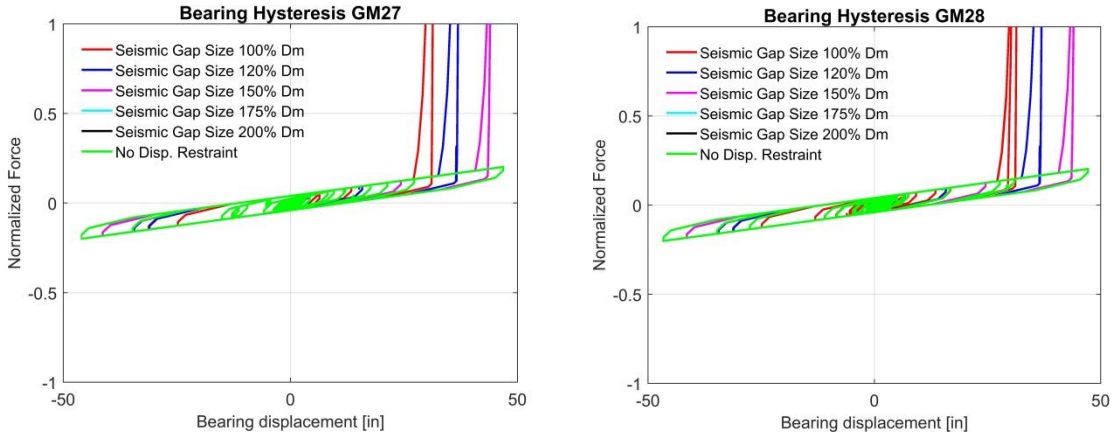

Figure. Bearing hysteresis and impact responses for use of moat wall with different seismic gap sizes. (a) GM27 (b) GM28

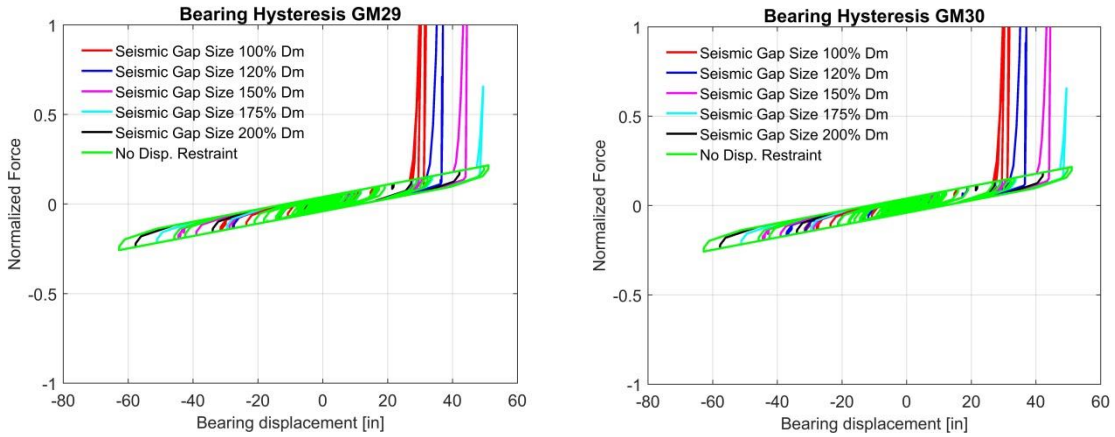

Figure. Bearing hysteresis and impact responses for use of moat wall with different seismic gap sizes. (a) GM29 (b) GM30

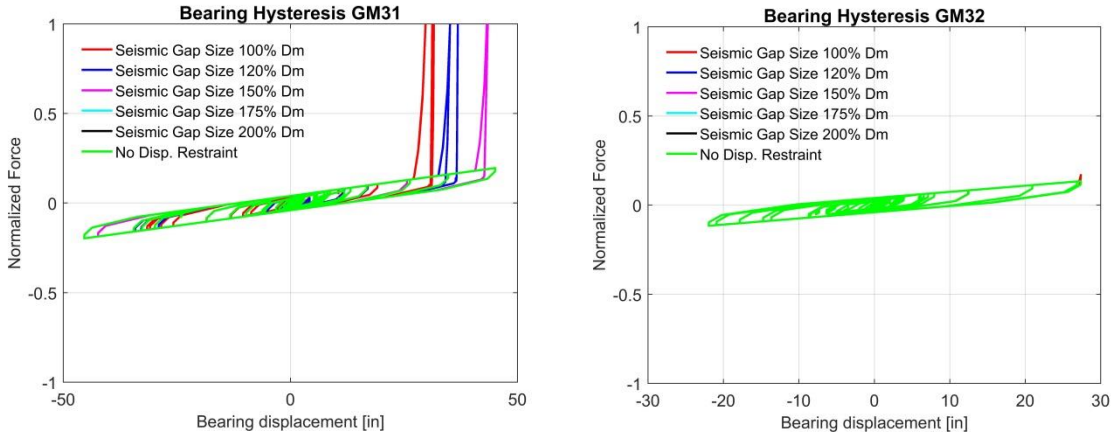

Figure. Bearing hysteresis and impact responses for use of moat wall with different seismic gap sizes. (a) GM31 (b) GM32

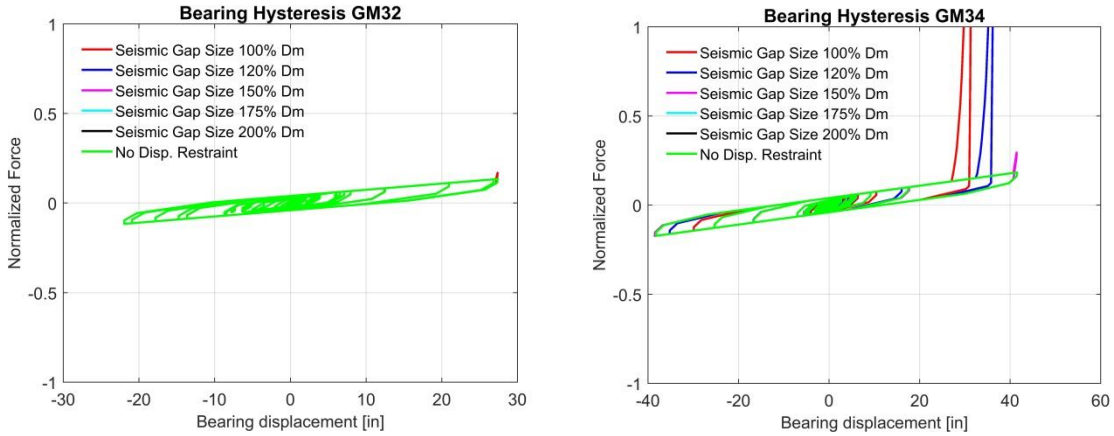

Figure. Bearing hysteresis and impact responses for use of moat wall with different seismic gap sizes. (a) GM33 (b) GM34

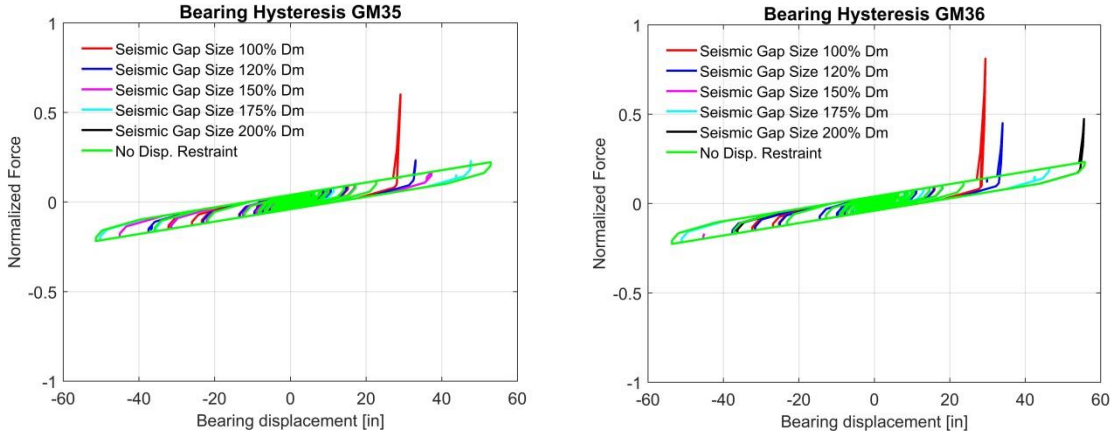

Figure. Bearing hysteresis and impact responses for use of moat wall with different seismic gap sizes. (a) GM35 (b) GM36

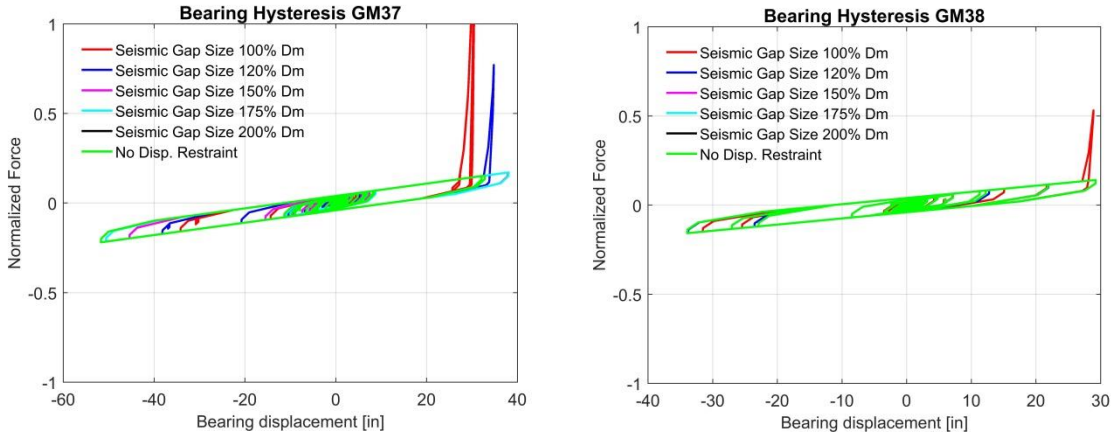

Figure. Bearing hysteresis and impact responses for use of moat wall with different seismic gap sizes. (a) GM37 (b) GM38

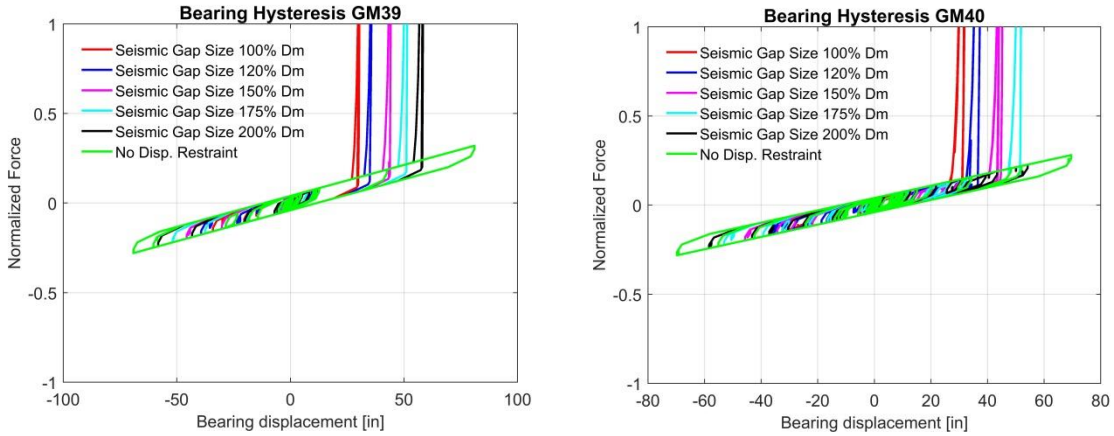

Figure. Bearing hysteresis and impact responses for use of moat wall with different seismic gap sizes. (a) GM39 (b) GM40

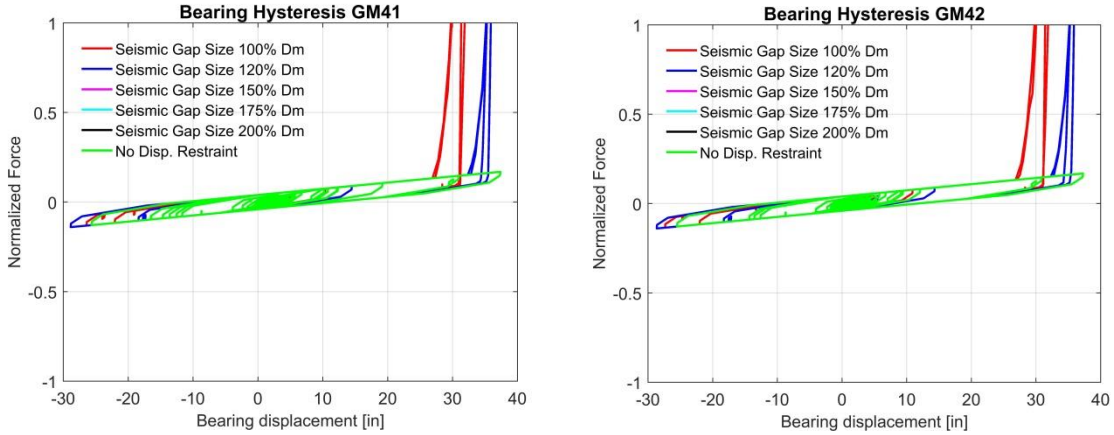

Figure. Bearing hysteresis and impact responses for use of moat wall with different seismic gap sizes. (a) GM41 (b) GM42

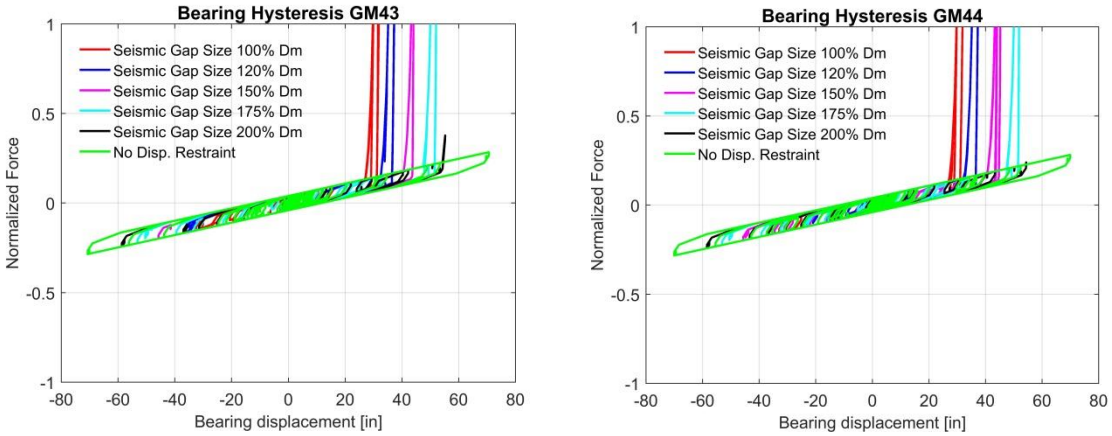

Figure. Bearing hysteresis and impact responses for use of moat wall with different seismic gap sizes. (a) GM43 (b) GM44

UPPER STRUCTURE DRIFT RESPONSE HISTORY

In this section, base story drift ratio response histories are shown and compared for the three design strategies: Using bearing without displacement restraint, using bearing with physical displacement restraint and using stiffening bearing. A representative isolator design case is shown for comparison.

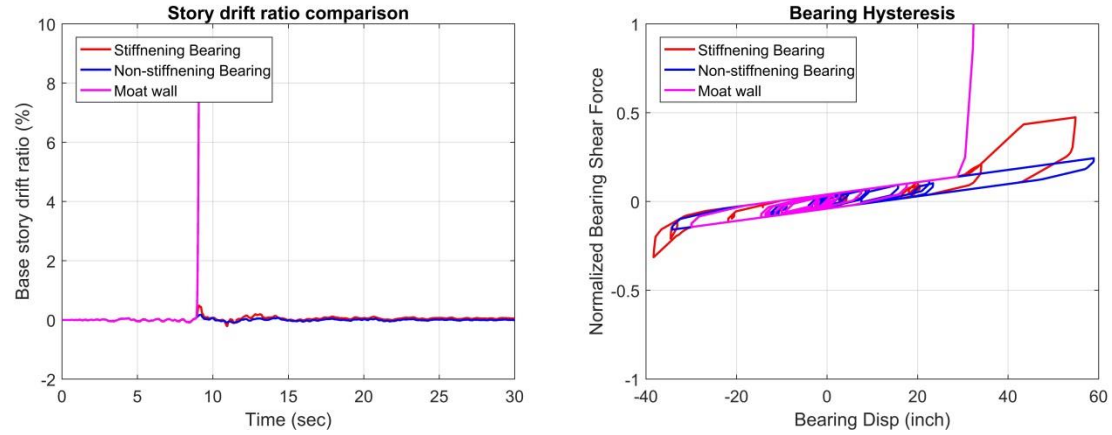

Figure. Base story drift response and bearing hysteresis responses comparison for stiffening bearing, non-stiffening bearing and moat wall case for GM 1.

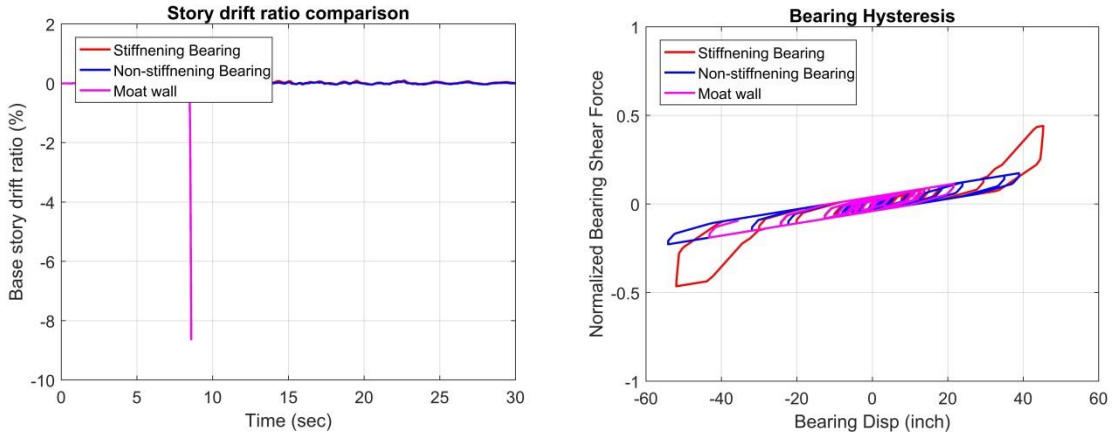

Figure. Base story drift response and bearing hysteresis responses comparison for stiffening bearing, non-stiffening bearing and moat wall case for GM2.

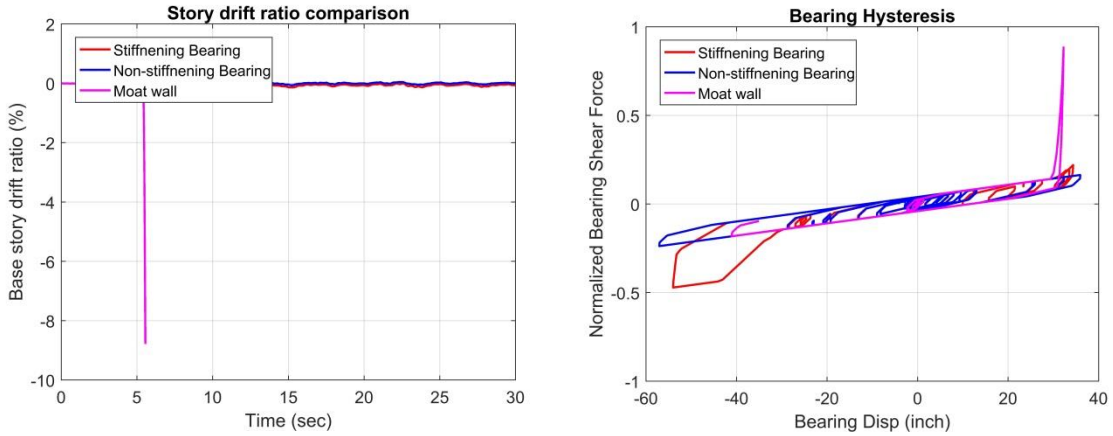

Figure. Base story drift response and bearing hysteresis responses comparison for stiffening bearing, non-stiffening bearing and moat wall case for GM 3.

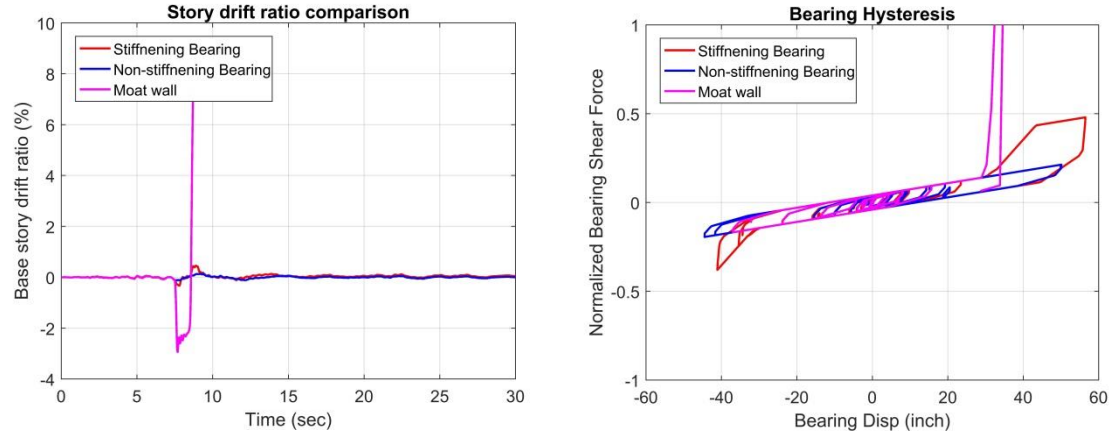

Figure. Base story drift response and bearing hysteresis responses comparison for stiffening bearing, non-stiffening bearing and moat wall case for GM 4.

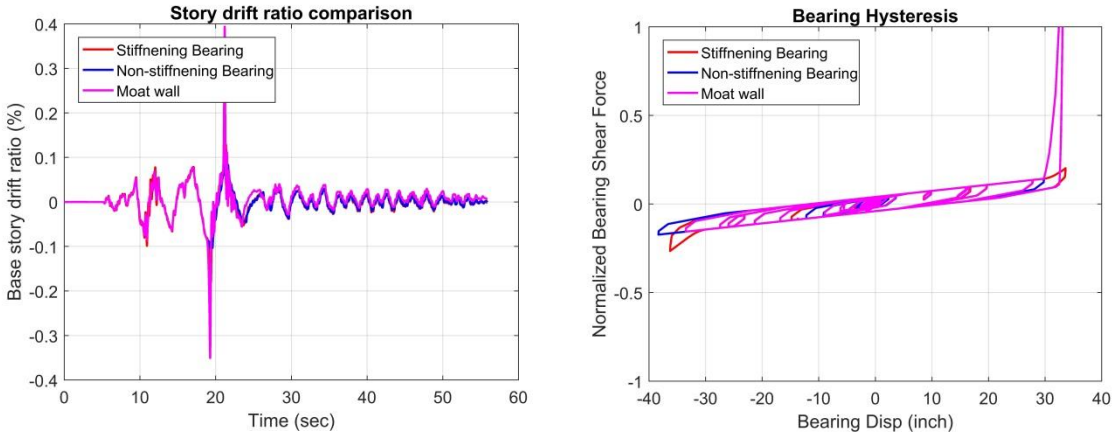

Figure. Base story drift response and bearing hysteresis responses comparison for stiffening bearing, non-stiffening bearing and moat wall case for GM 5.

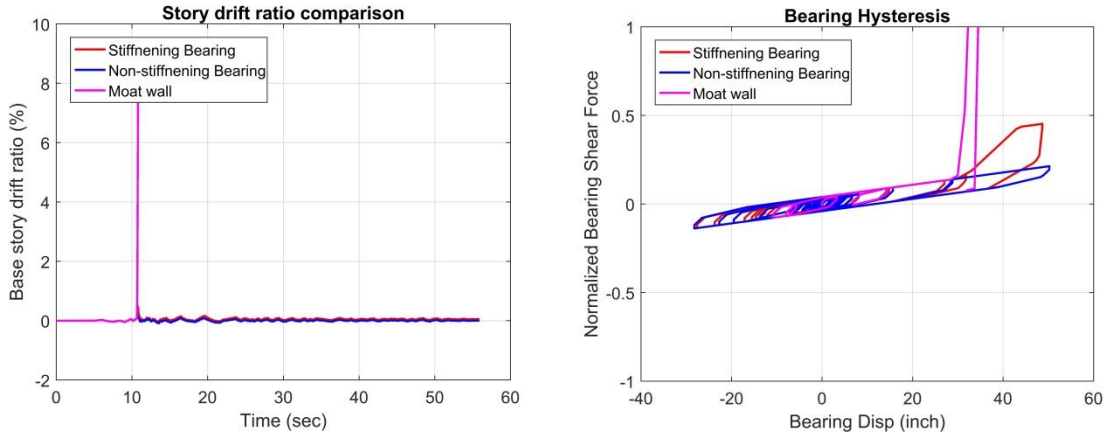

Figure. Base story drift response and bearing hysteresis responses comparison for stiffening bearing, non-stiffening bearing and moat wall case for GM 6.

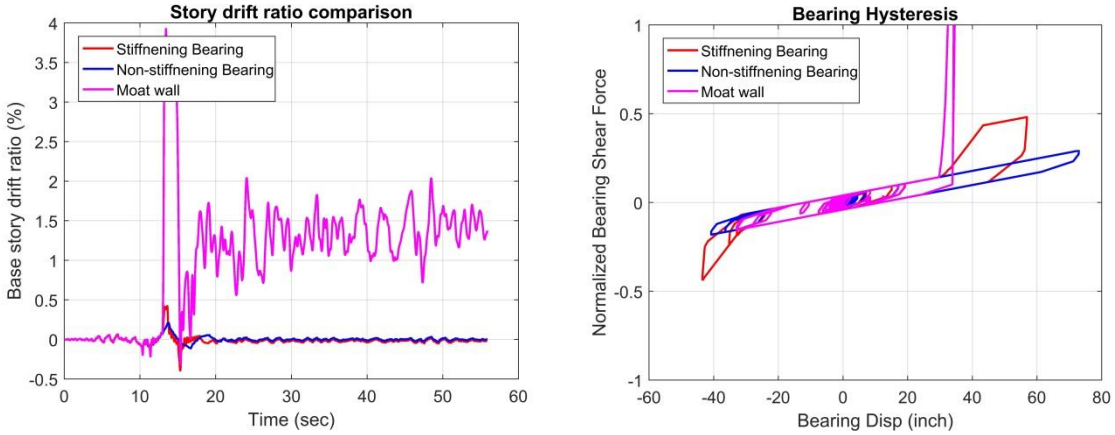

Figure. Base story drift response and bearing hysteresis responses comparison for stiffening bearing, non-stiffening bearing and moat wall case for GM 7.

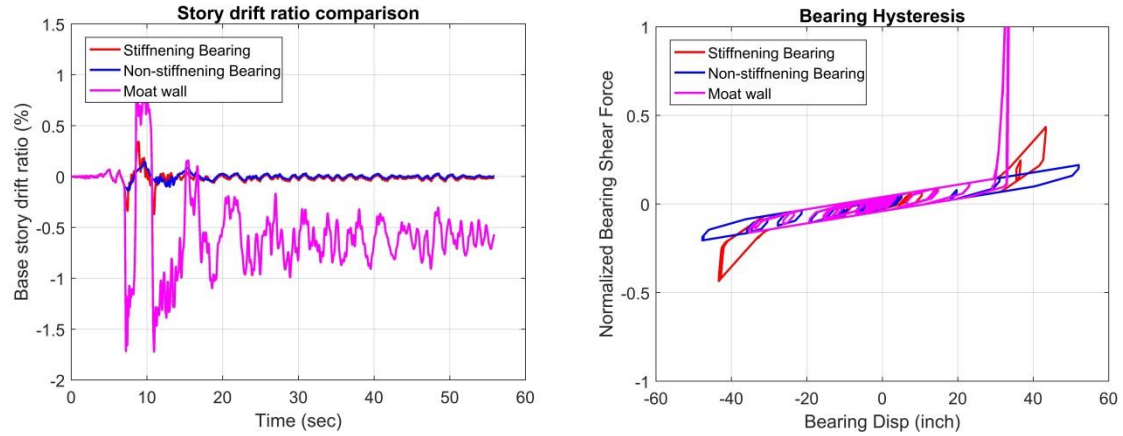

Figure. Base story drift response and bearing hysteresis responses comparison for stiffening bearing, non-stiffening bearing and moat wall case for GM 8.

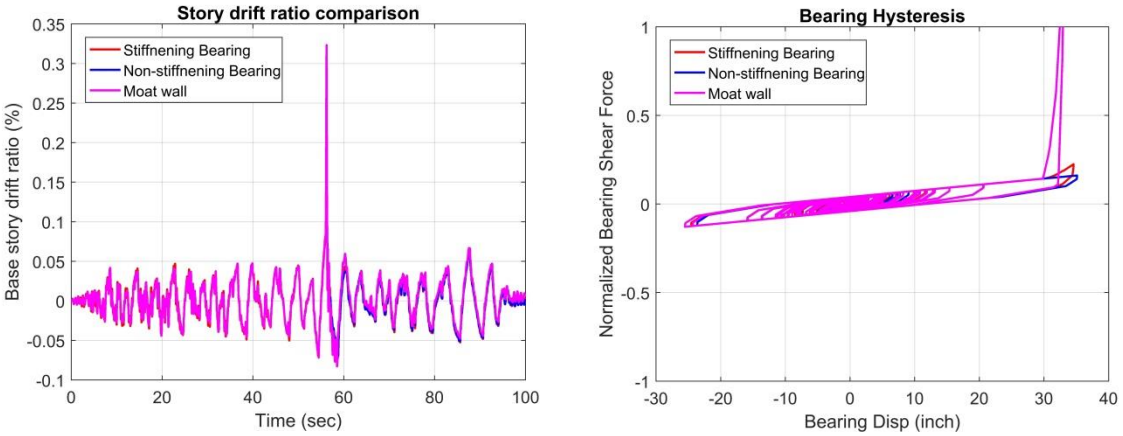

Figure. Base story drift response and bearing hysteresis responses comparison for stiffening bearing, non-stiffening bearing and moat wall case for GM 9.

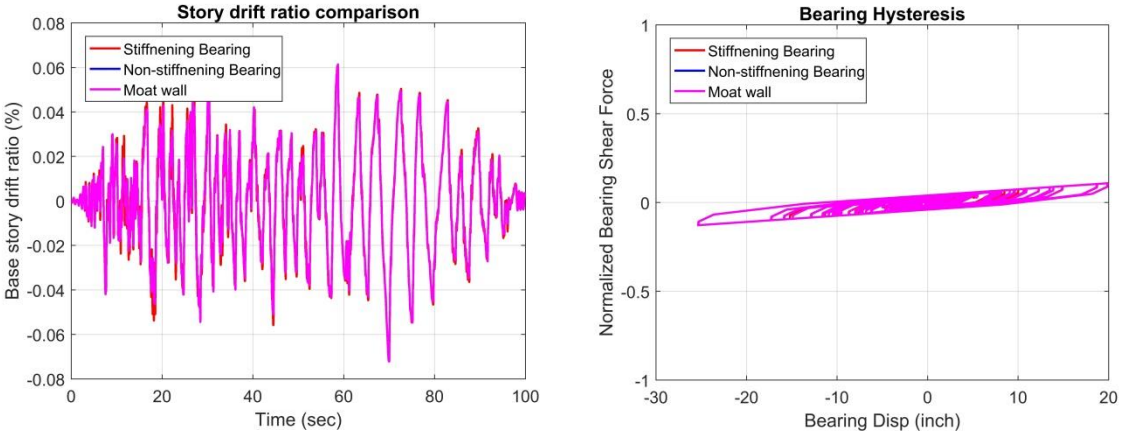

Figure. Base story drift response and bearing hysteresis responses comparison for stiffening bearing, non-stiffening bearing and moat wall case for GM 10.

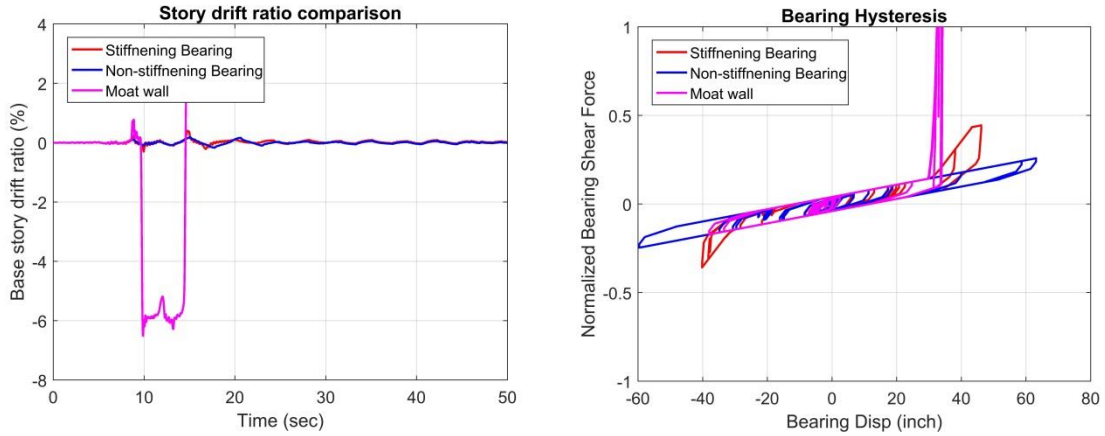

Figure. Base story drift response and bearing hysteresis responses comparison for stiffening bearing, non-stiffening bearing and moat wall case for GM 11.

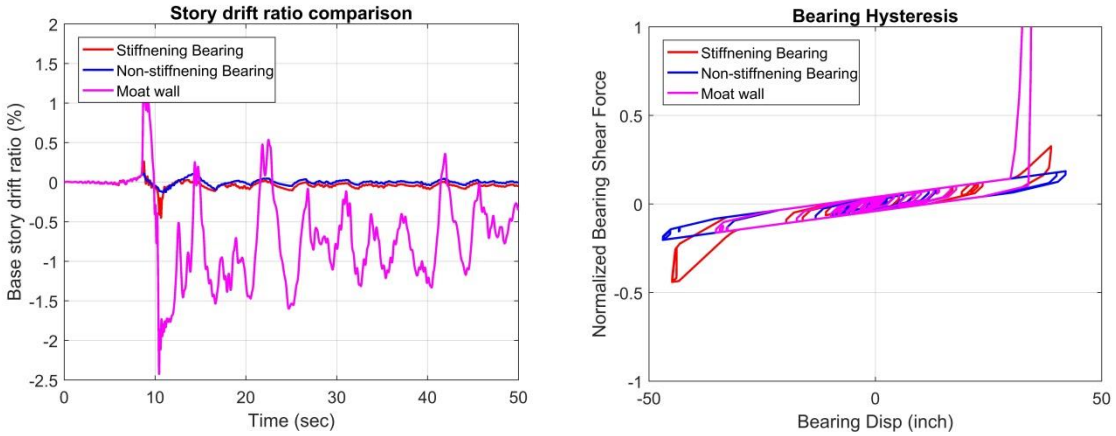

Figure. Base story drift response and bearing hysteresis responses comparison for stiffening bearing, non-stiffening bearing and moat wall case for GM 12.

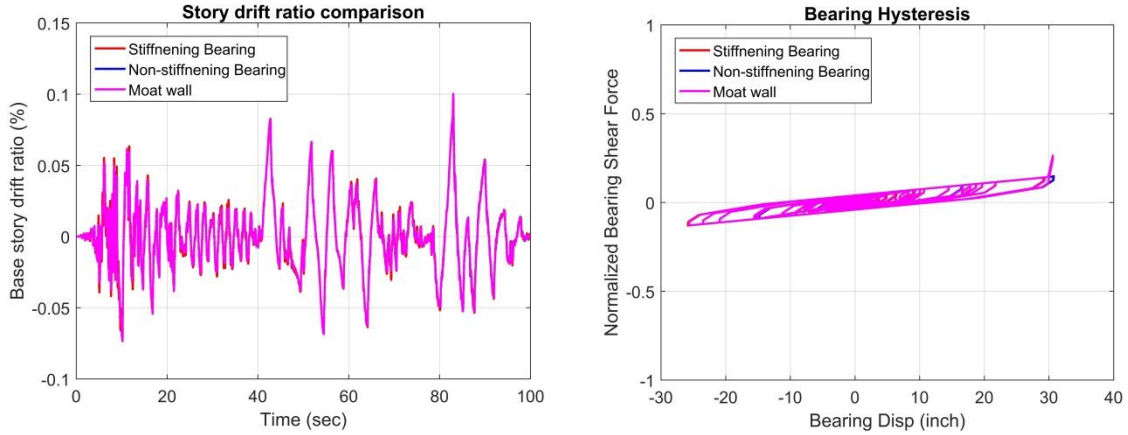

Figure. Base story drift response and bearing hysteresis responses comparison for stiffening bearing, non-stiffening bearing and moat wall case for GM 13.

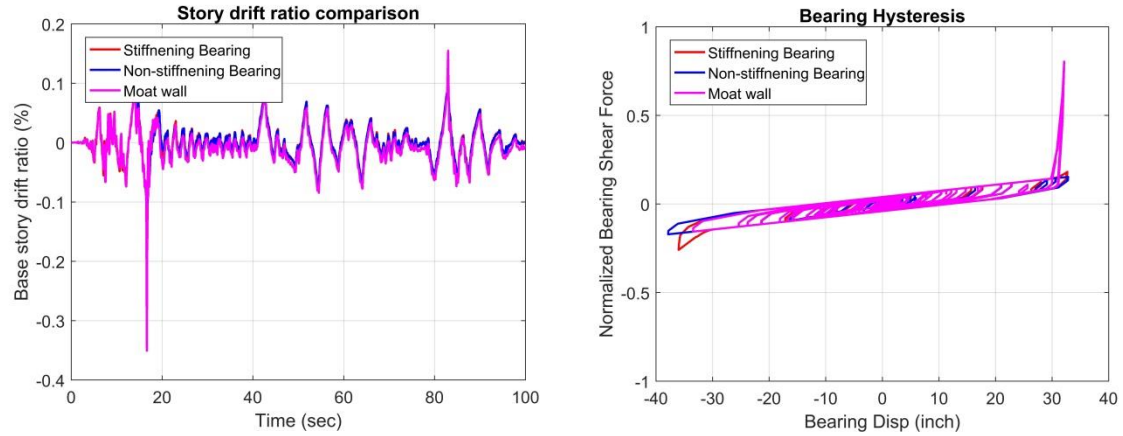

Figure. Base story drift response and bearing hysteresis responses comparison for stiffening bearing, non-stiffening bearing and moat wall case for GM 14.

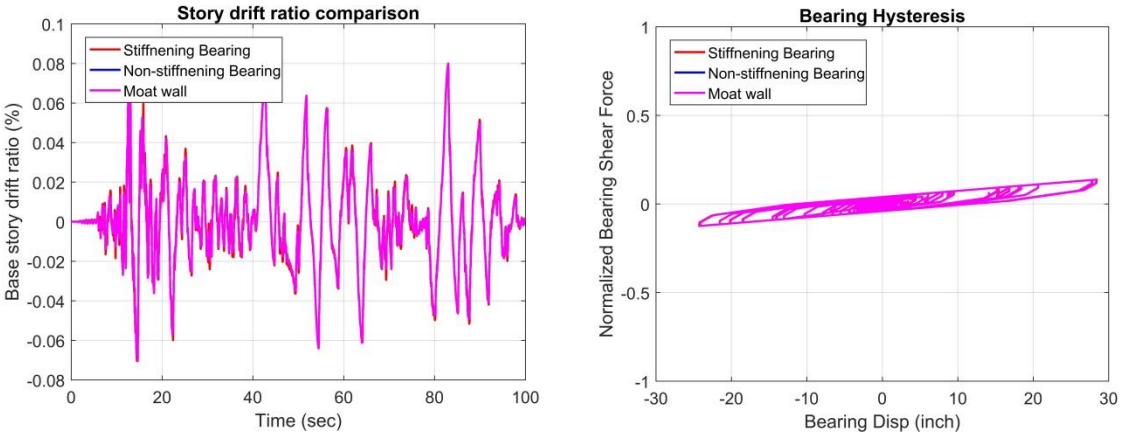

Figure. Base story drift response and bearing hysteresis responses comparison for stiffening bearing, non-stiffening bearing and moat wall case for GM 15.

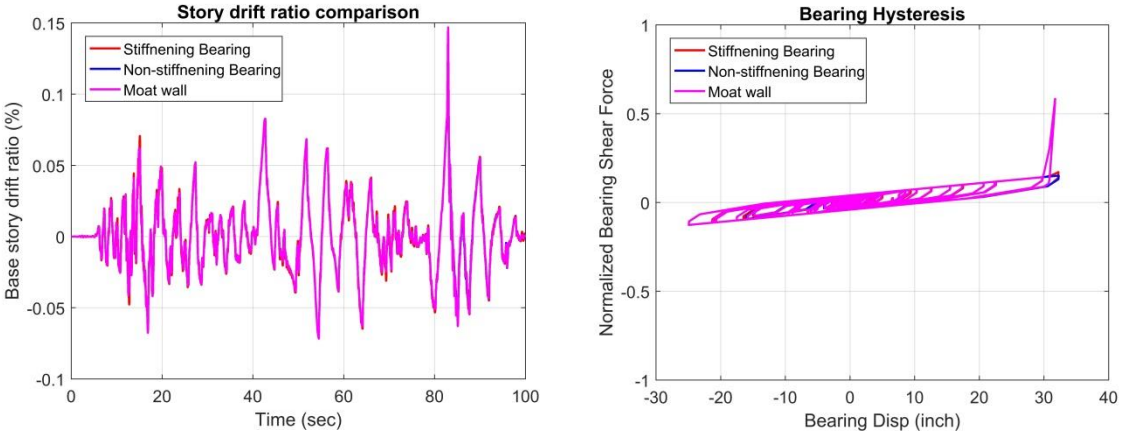

Figure. Base story drift response and bearing hysteresis responses comparison for stiffening bearing, non-stiffening bearing and moat wall case for GM 16.

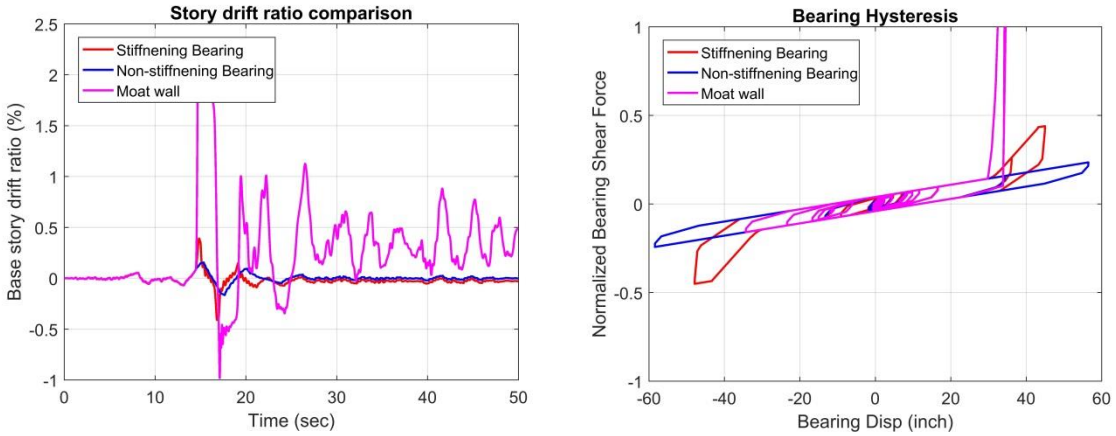

Figure. Base story drift response and bearing hysteresis responses comparison for stiffening bearing, non-stiffening bearing and moat wall case for GM 17.

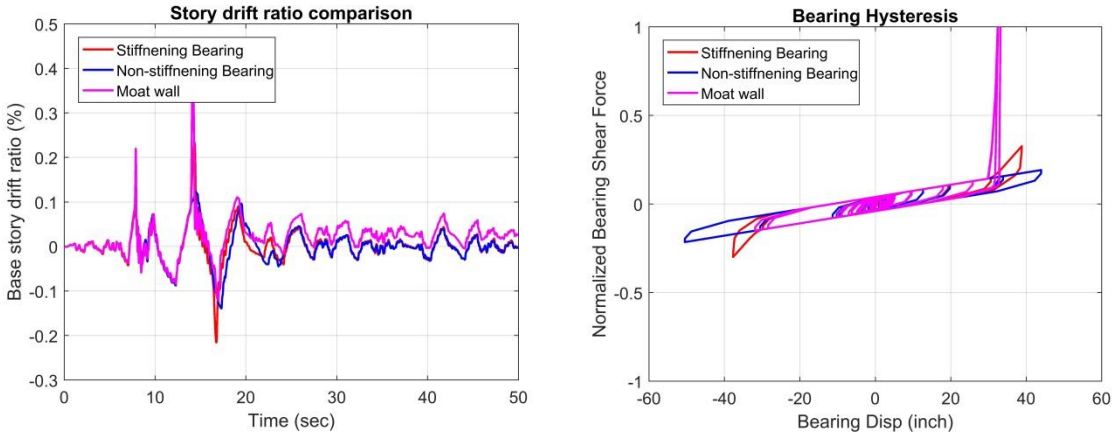

Figure. Base story drift response and bearing hysteresis responses comparison for stiffening bearing, non-stiffening bearing and moat wall case for GM 18.

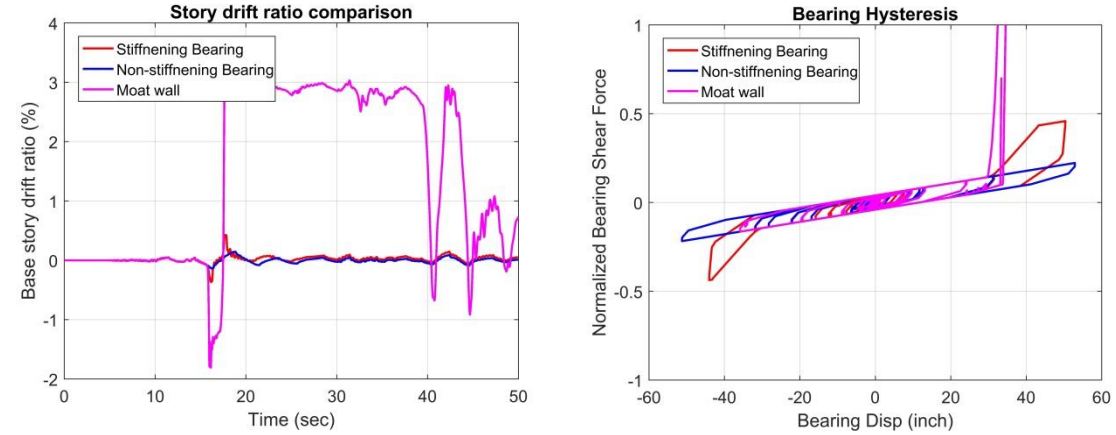

Figure. Base story drift response and bearing hysteresis responses comparison for stiffening bearing, non-stiffening bearing and moat wall case for GM 19.

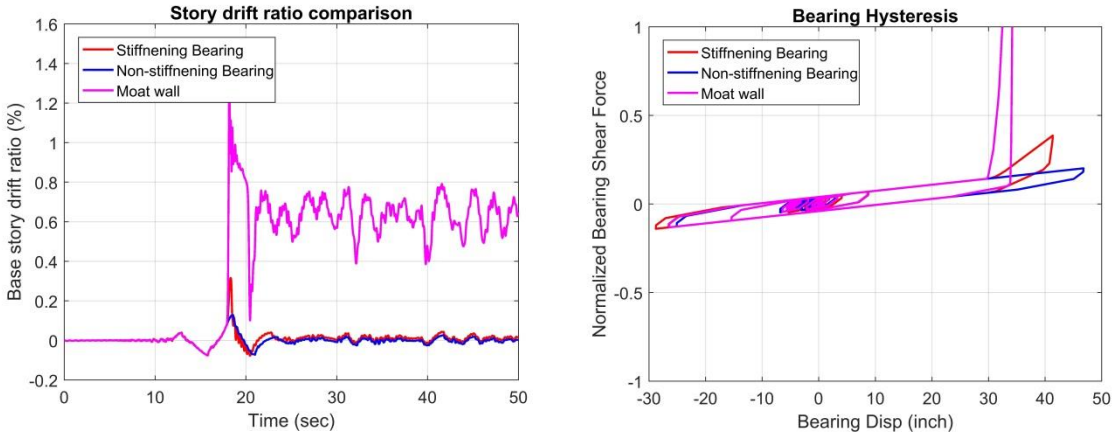

Figure. Base story drift response and bearing hysteresis responses comparison for stiffening bearing, non-stiffening bearing and moat wall case for GM 20.

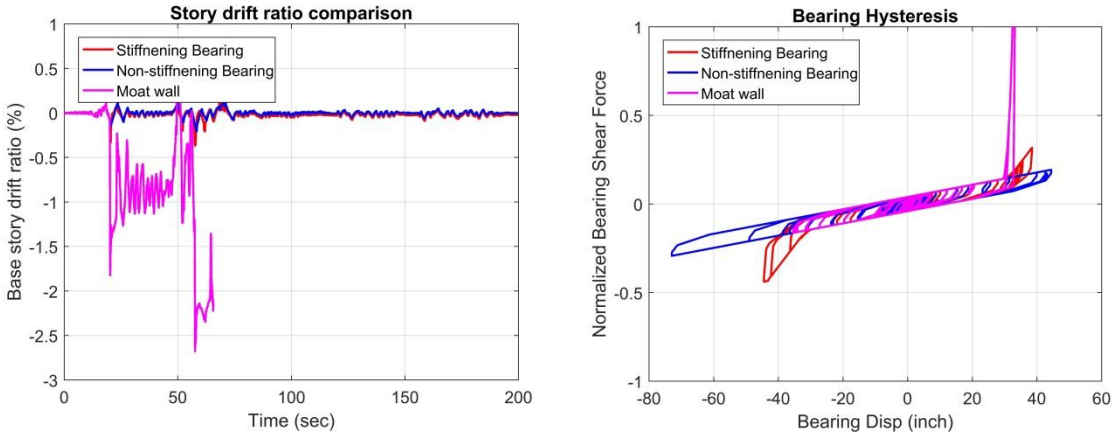

Figure. Base story drift response and bearing hysteresis responses comparison for stiffening bearing, non-stiffening bearing and moat wall case for GM 21.

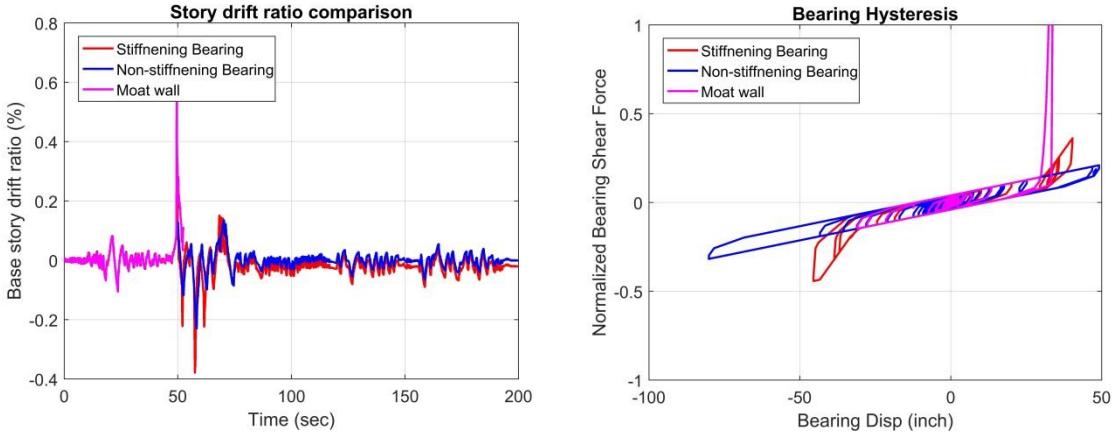

Figure. Base story drift response and bearing hysteresis responses comparison for stiffening bearing, non-stiffening bearing and moat wall case for GM 22.

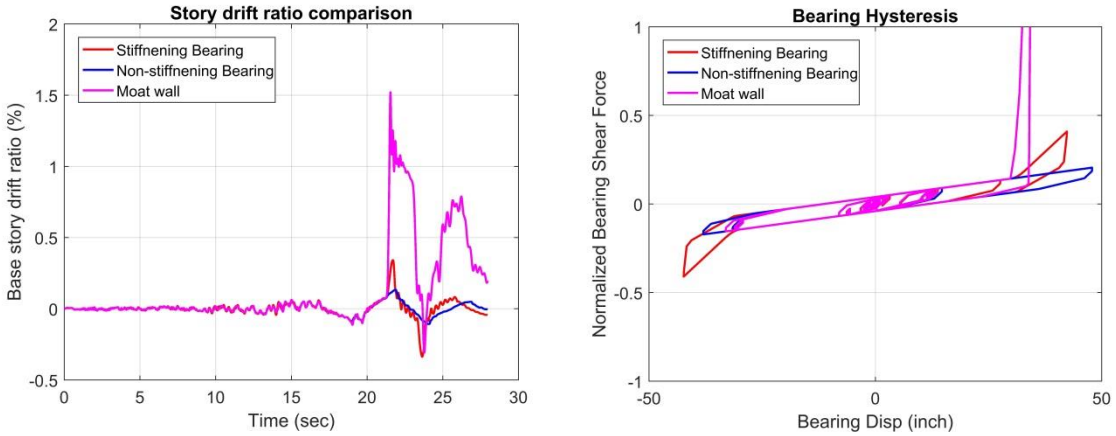

Figure. Base story drift response and bearing hysteresis responses comparison for stiffening bearing, non-stiffening bearing and moat wall case for GM 23.

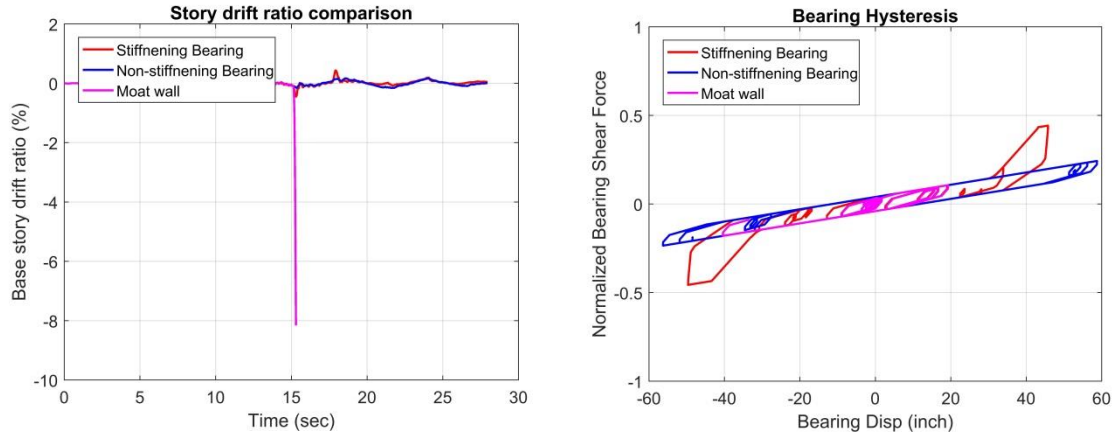

Figure. Base story drift response and bearing hysteresis responses comparison for stiffening bearing, non-stiffening bearing and moat wall case for GM 24

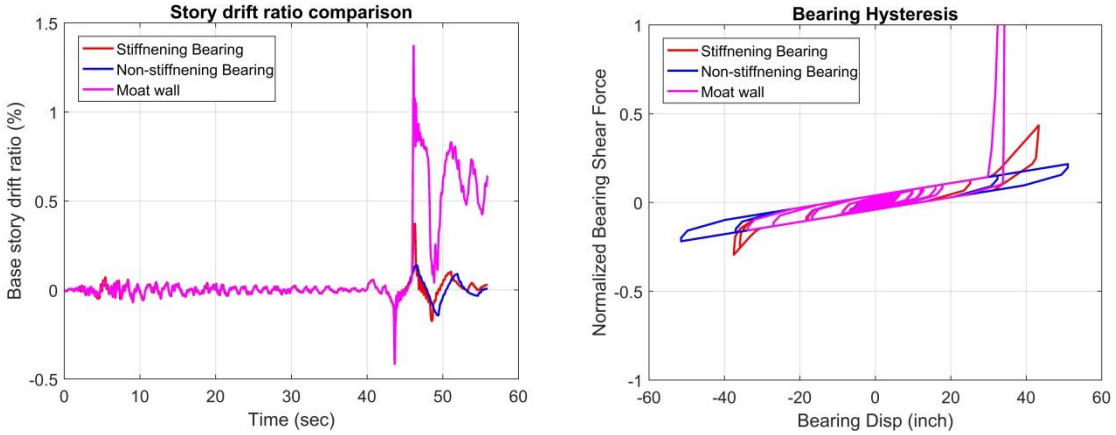

Figure. Base story drift response and bearing hysteresis responses comparison for stiffening bearing, non-stiffening bearing and moat wall case for GM 25.

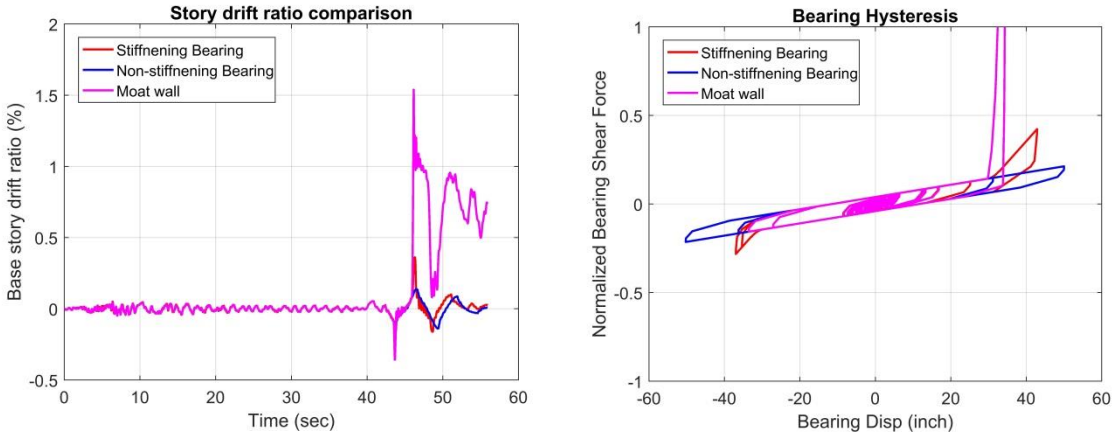

Figure. Base story drift response and bearing hysteresis responses comparison for stiffening bearing, non-stiffening bearing and moat wall case for GM 26.

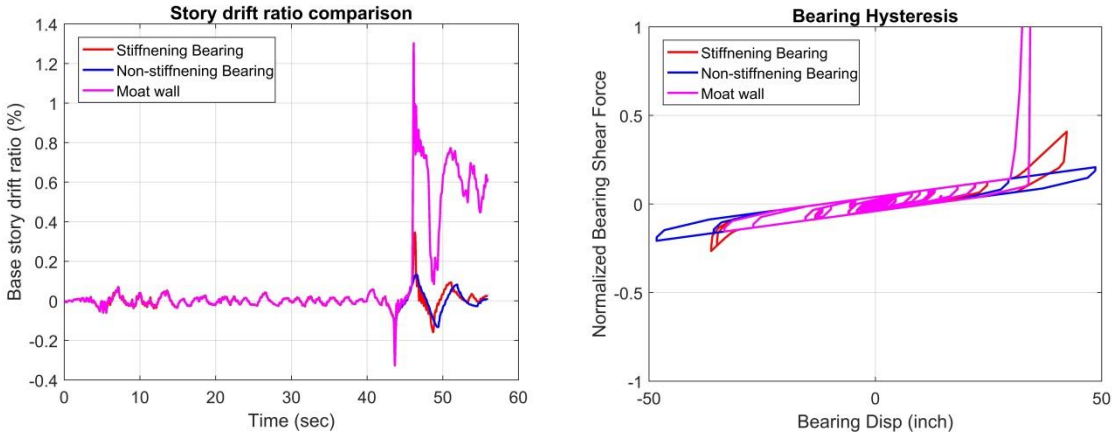

Figure. Base story drift response and bearing hysteresis responses comparison for stiffening bearing, non-stiffening bearing and moat wall case for GM 27.

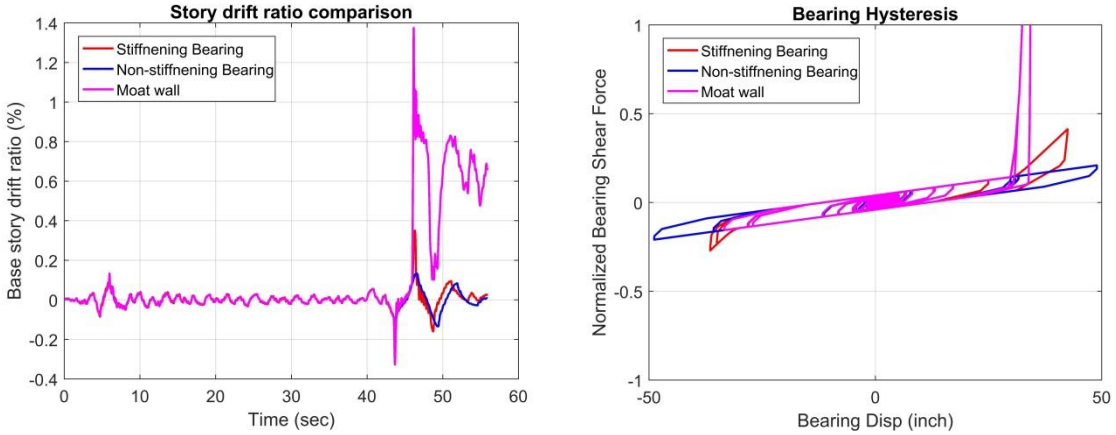

Figure. Base story drift response and bearing hysteresis responses comparison for stiffening bearing, non-stiffening bearing and moat wall case for GM 28.

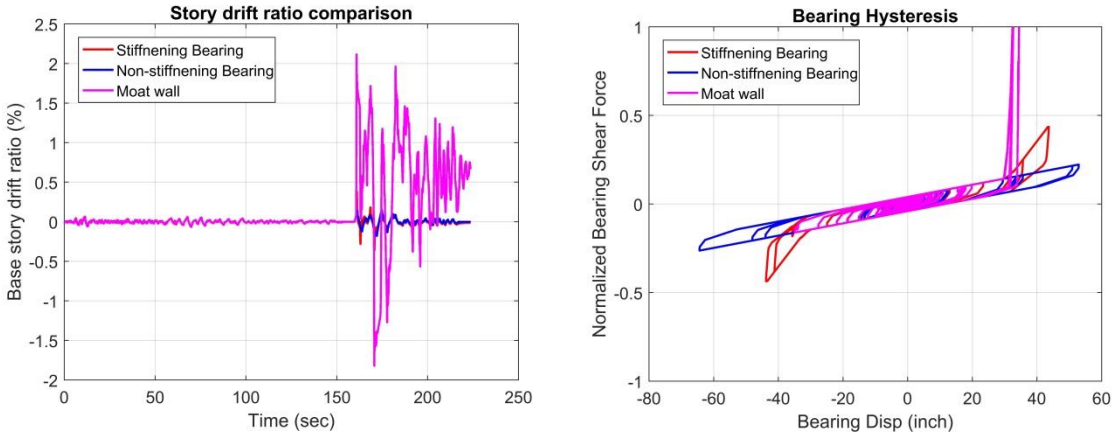

Figure. Base story drift response and bearing hysteresis responses comparison for stiffening bearing, non-stiffening bearing and moat wall case for GM 29.

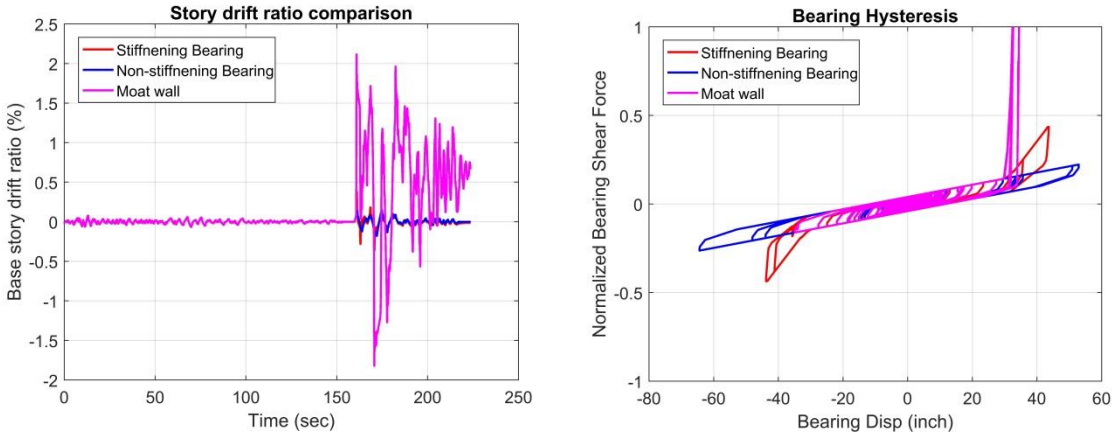

Figure. Base story drift response and bearing hysteresis responses comparison for stiffening bearing, non-stiffening bearing and moat wall case for GM 30.

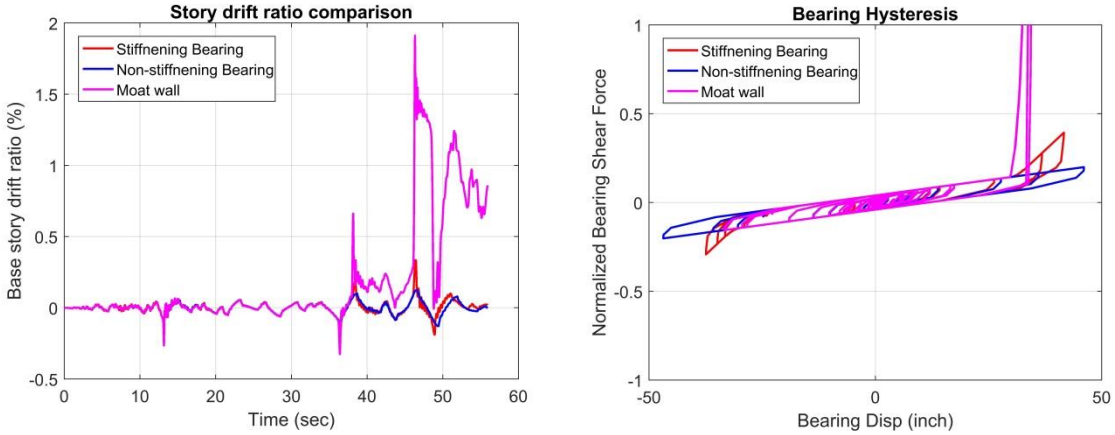

Figure. Base story drift response and bearing hysteresis responses comparison for stiffening bearing, non-stiffening bearing and moat wall case for GM 31.

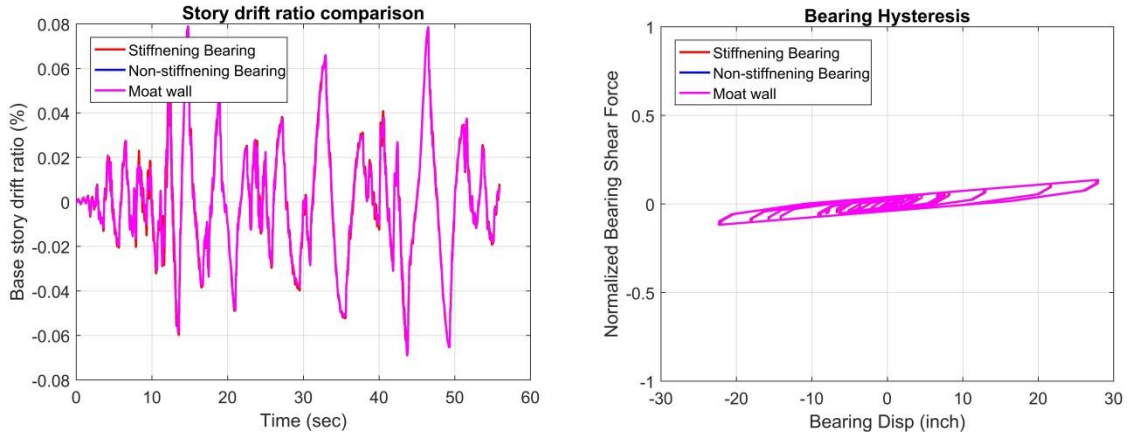

Figure. Base story drift response and bearing hysteresis responses comparison for stiffening bearing, non-stiffening bearing and moat wall case for GM 32.

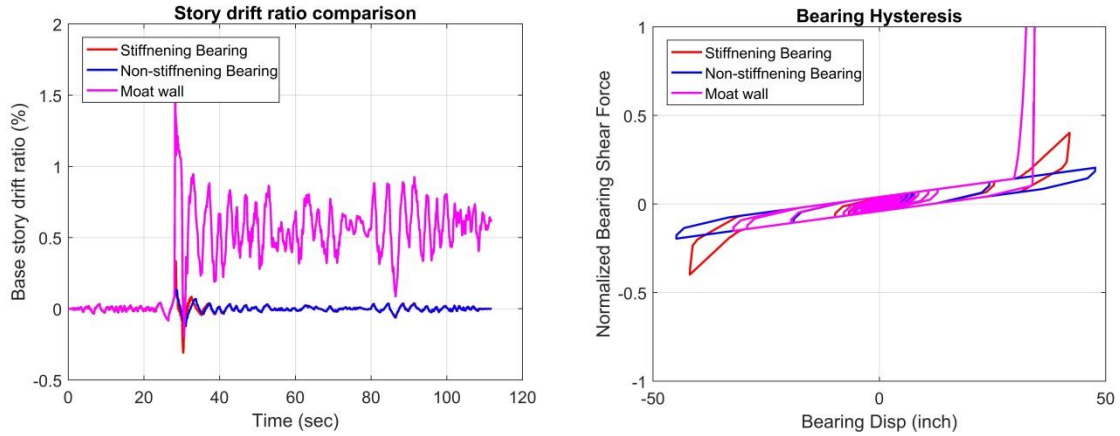

Figure. Base story drift response and bearing hysteresis responses comparison for stiffening bearing, non-stiffening bearing and moat wall case for GM 33.

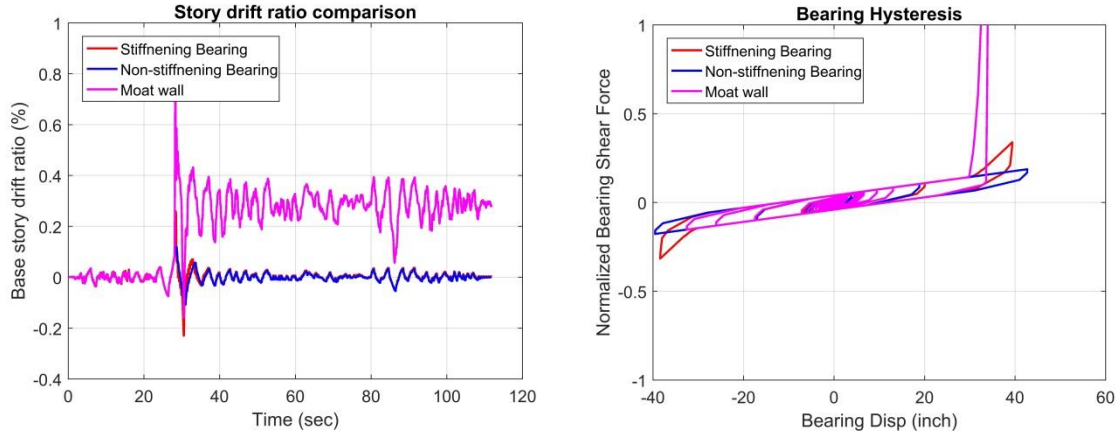

Figure. Base story drift response and bearing hysteresis responses comparison for stiffening bearing, non-stiffening bearing and moat wall case for GM 34.

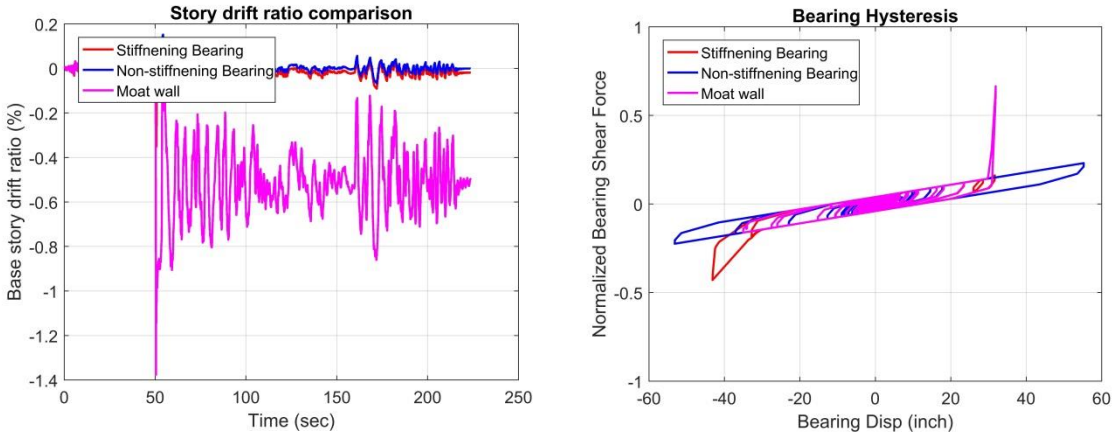

Figure. Base story drift response and bearing hysteresis responses comparison for stiffening bearing, non-stiffening bearing and moat wall case for GM 35.

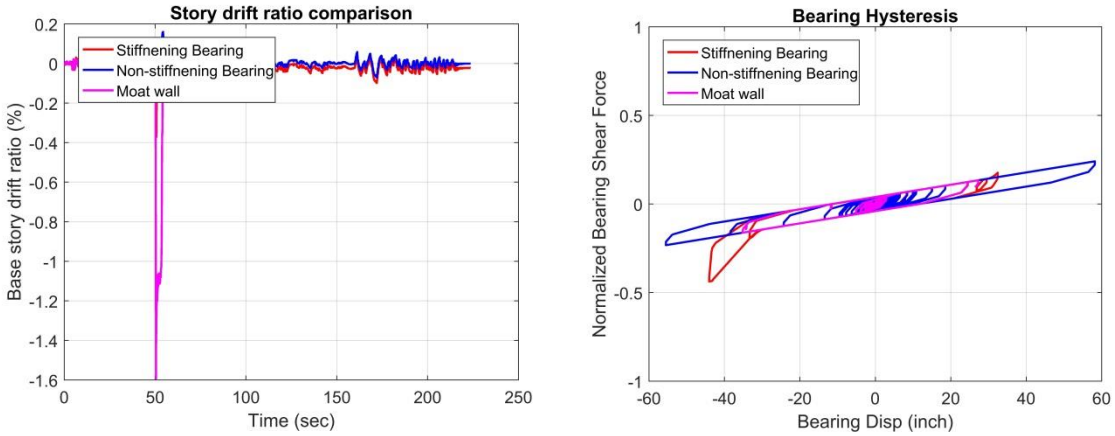

Figure. Base story drift response and bearing hysteresis responses comparison for stiffening bearing, non-stiffening bearing and moat wall case for GM 36.

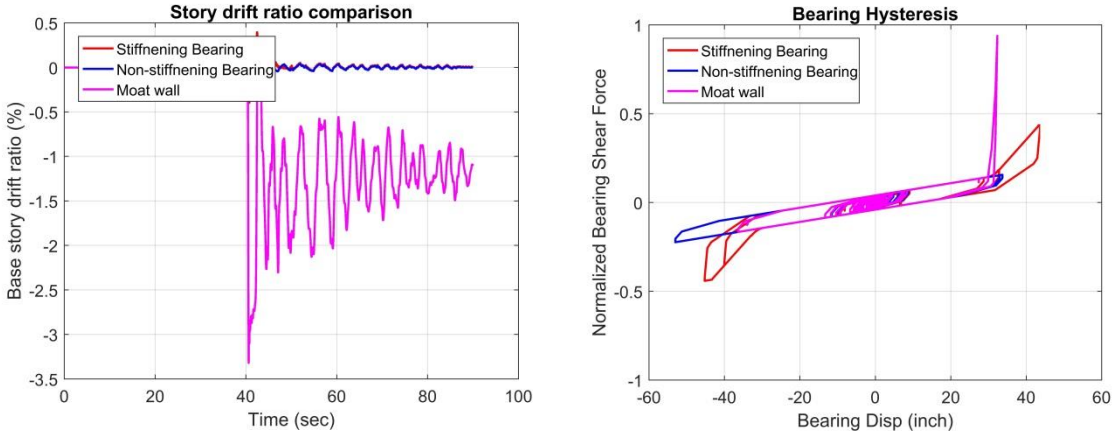

Figure. Base story drift response and bearing hysteresis responses comparison for stiffening bearing, non-stiffening bearing and moat wall case for GM 37.

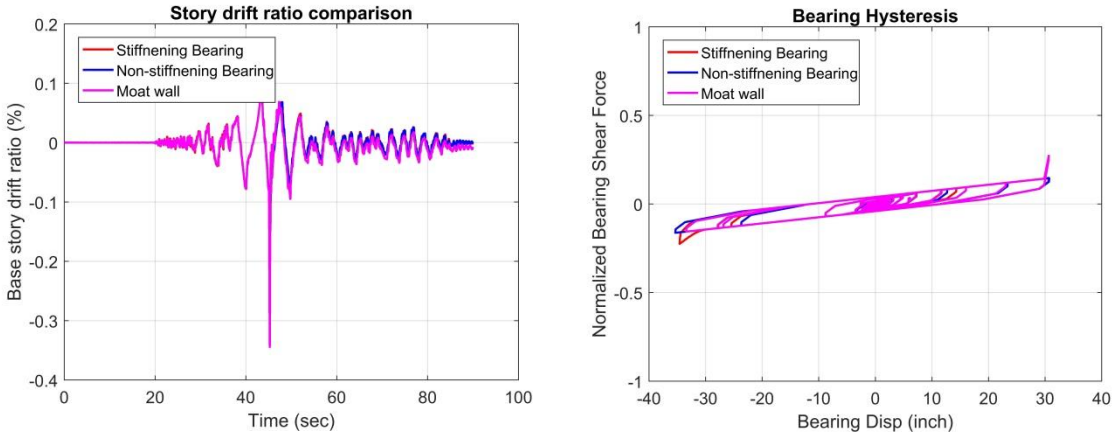

Figure. Base story drift response and bearing hysteresis responses comparison for stiffening bearing, non-stiffening bearing and moat wall case for GM 38.

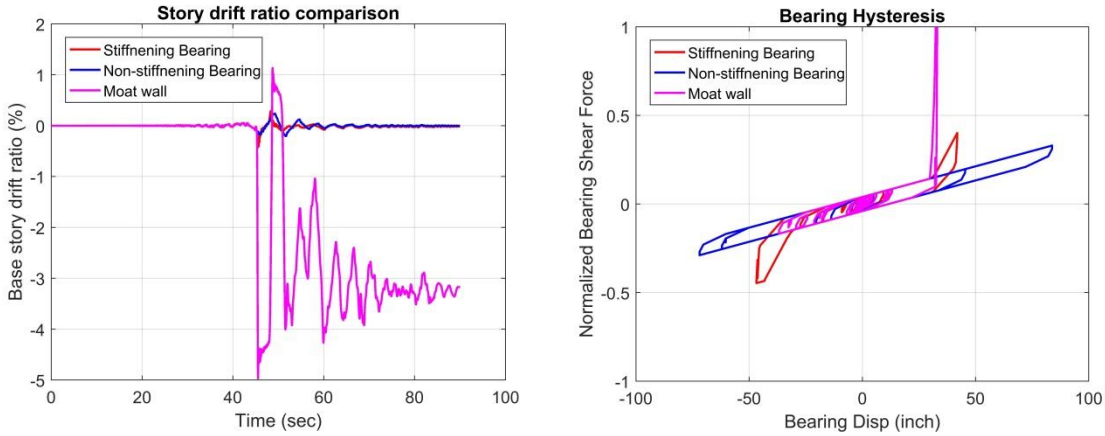

Figure. Base story drift response and bearing hysteresis responses comparison for stiffening bearing, non-stiffening bearing and moat wall case for GM 39.

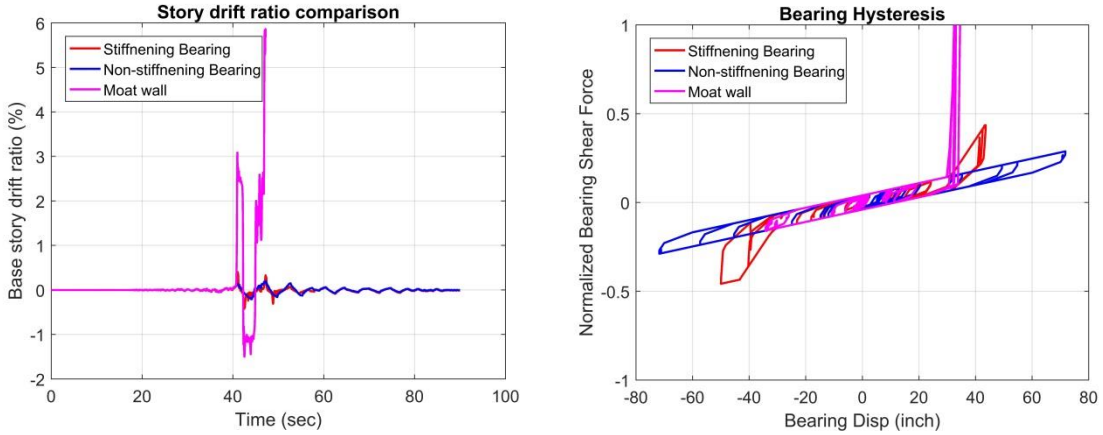

Figure. Base story drift response and bearing hysteresis responses comparison for stiffening bearing, non-stiffening bearing and moat wall case for GM 40.

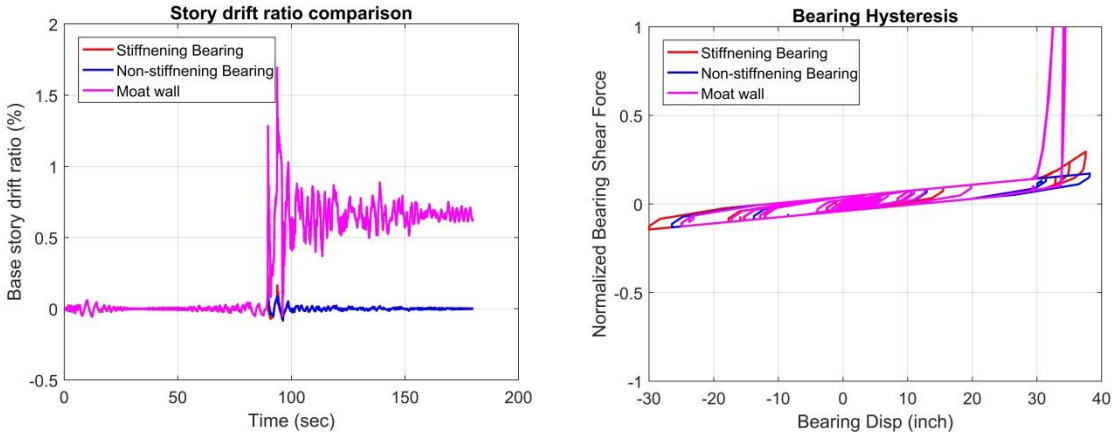

Figure. Base story drift response and bearing hysteresis responses comparison for stiffening bearing, non-stiffening bearing and moat wall case for GM 41.

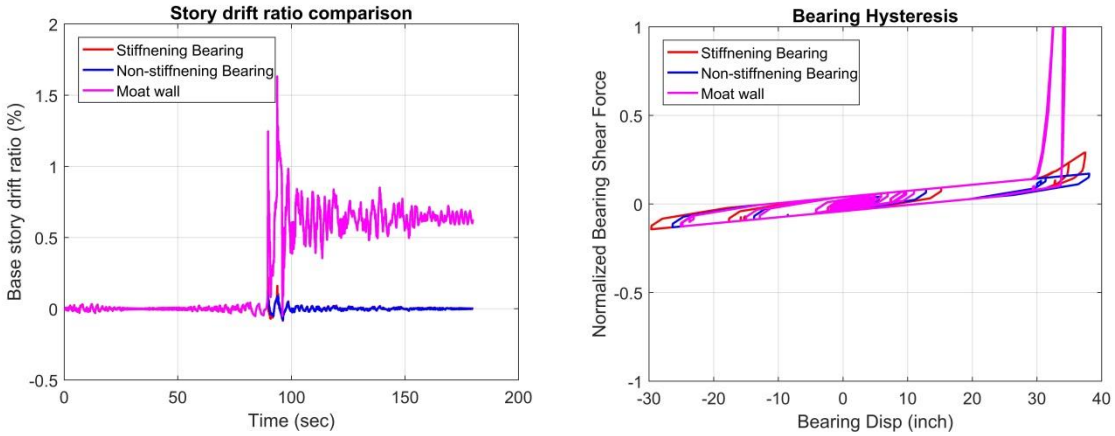

Figure. Base story drift response and bearing hysteresis responses comparison for stiffening bearing, non-stiffening bearing and moat wall case for GM 42.

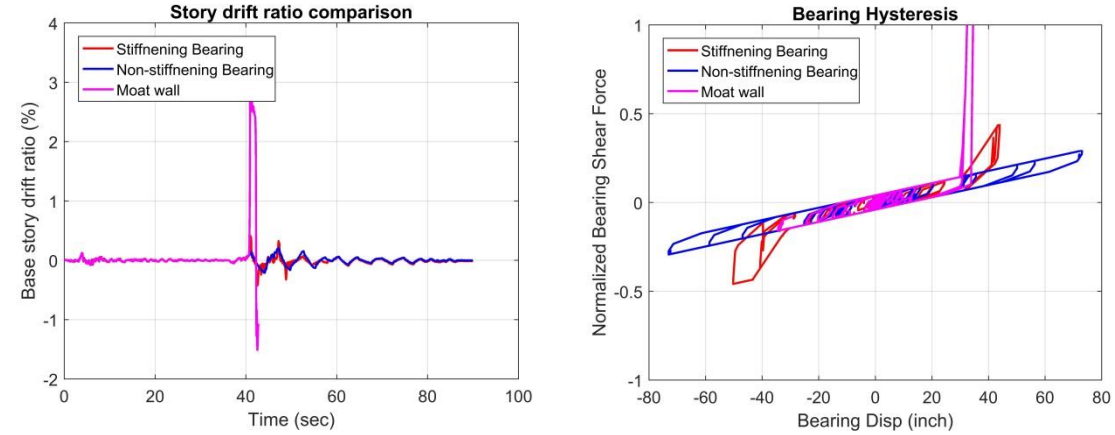

Figure. Base story drift response and bearing hysteresis responses comparison for stiffening bearing, non-stiffening bearing and moat wall case for GM 43.

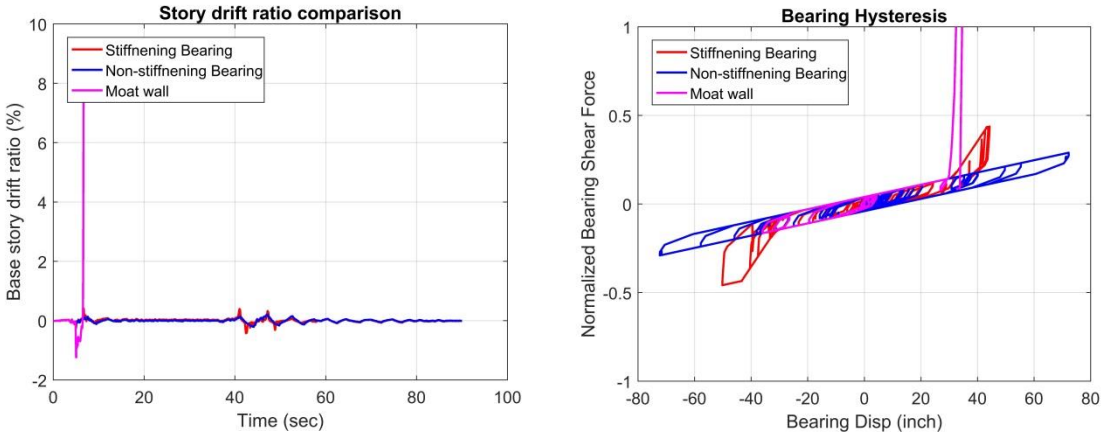

Figure. Base story drift response and bearing hysteresis responses comparison for stiffening bearing, non-stiffening bearing and moat wall case for GM 44.